AD NUMBER

AD860478

LIMITATION CHANGES

TO:

Approved for public release; distribution is unlimited.

FROM:

Distribution authorized to U.S. Gov't. agencies and their contractors; Critical Technology; OCT 1969. Other requests shall be referred to National Aeronautics and Space Administration-Manned Spacecraft Center, Attn: NASA-MSC, Houston, TX 77058. This document contains export-controlled technical data.

AUTHORITY

USAEDC ltr, 27 Jun 1973

AEDC-TR-69-144

SUMMARY OF FIVE YEARS OF ALTITUDE TESTING OF THE APOLLO SERVICE MODULE ENGINE IN ALTITUDE TEST CELL (J-3)

G. H. Schulz
ARO, Inc.

October 1969

ROCKET TEST FACILITY
ARNOLD ENGINEERING DEVELOPMENT CENTER
AIR FORCE SYSTEMS COMMAND
ARNOLD AIR FORCE STATION, TENNESSEE

NOTICES

When U. S. Government drawings specifications, or other data are used for any purpose other than a definitely related Government procurement operation, the Government thereby incurs no responsibility nor any obligation whatsoever, and the fact that the Government may have formulated, furnished, or in any way supplied the said drawings, specifications, or other data, is not to be regarded by implication or otherwise, or in any manner licensing the holder or any other person or corporation, or conveying any rights or permission to manufacture, use, or sell any patented invention that may in any way be related thereto.

Qualified users may obtain copies of this report from the Defense Documentation Center.

References to named commercial products in this report are not to be considered in any sense as an endorsement of the product by the United States Air Force or the Government.

SUMMARY OF FIVE YEARS OF ALTITUDE TESTING OF THE APOLLO SERVICE MODULE ENGINE IN ALTITUDE TEST CELL (J-3)

G. H. Schulz
ARO, Inc.

FOREWORD

This report is a summary of the salient results of altitude development and qualification testing programs on the Aerojet-General Corporation (AGC) AJ10-137 liquid-propellant rocket engine for the Apollo Service Propulsion System. These programs were sponsored by the National Aeronautics and Space Administration-Manned Spacecraft Center (NASA-MSC). Technical liaison was provided by AGC which was a subcontractor of North American Aviation-Space and Information Division (NAA-S&ID), prime contractor to NASA for the complete Apollo Service Module vehicle.

The test programs were requested to support the Apollo project under Program Area 921E, Project 9281. Testing was conducted by ARO, Inc. (a subsidiary of Sverdrup & Parcel and Associates, Inc.), contract operator of the Arnold Engineering Development Center (AEDC), Air Force Systems Command (AFSC), Arnold Air Force Station, Tennessee. The results reported in this document were obtained in the Propulsion Engine Test Cell (J-3) of the Rocket Test Facility (RTF) during the period from May 1963 through August 1968 under ARO Project Numbers RM1306, RM1356, RM1413, RM1607, RM1630, and RM1731. The manuscript was submitted for publication on May 29, 1969.

Information in this report is embargoed under the Department of State International Traffic in Arms Regulations. This report may be released to foreign governments by departments or agencies of the U. S. Government subject to approval of the National Aeronautics and Space Administration-Manned Spacecraft Center, or higher authority. Private individuals or firms require a Department of State export license.

This report was produced by the J-3 Projects Section, RTF, viz., R. L. Barebo, A. L. Berg, K. L. Farrow, M. W. McIlveen, J. M. Pelton, C. E. Robinson, and G. H. Schulz.

This technical report has been reviewed and is approved.

Donald W. Ellison	Roy R. Croy, Jr.
Lt Colonel, USAF	Colonel, USAF
AF Representative, RTF	Director of Test
Directorate of Test	

ABSTRACT

The primary results of the development and qualification testing of the Aerojet-General Corporation AJ10-137 rocket engine for the Apollo Service Module conducted at the Arnold Engineering Development Center (AEDC) are summarized. Testing of the AJ10-137, a 20,000-lb_f nominal thrust liquid-propellant engine, was conducted at combustion chamber pressures of from 77 to 133 psia and at mixture ratios of the two hypergolic propellants, nitrogen tetroxide and Aerozine-50®, from 1.4 to 2.4. Both Block I and Block II engines were tested to determine engine performance and to establish durability and reliability of the basic engine design and subsequent modifications. As a result of these tests, the Block II engine performance was established, and the engine was qualified for the lunar mission. This testing indicated and permitted solution of inadequate durability of the ablative combustion chamber at low-pressure/altitude conditions. The chamber had appeared reliable in sea-level testing conditions. Engine ignition, shutdown, and short-duration firing transient operation characteristics and performance were documented in a propulsion system configuration which included full-scale models of the spacecraft propellant tanks and lines. Satisfactory engine operation and durability were demonstrated in various simulated mission situations, such as extended-duration firings up to 635 sec, multiple firings of fractional-second durations with various coast intervals, and various propellant temperatures from 30 to 130°F.

CONTENTS

ILLUSTRATIONS

TABLES

SECTION I
INTRODUCTION

In this report are summarized the salient results of development and qualification tests of the Apollo Service Propulsion System (SPS) engine (Fig. 1) at the Arnold Engineering Development Center during the period from June 1963 to August 1968. The Apollo SPS engine is a liquid-propellant rocket engine designed for a spaceflight operation thrust level of about 20,000 lb_f with such novel features as relatively low pressure combustion, ablation-cooled combustion chamber, and

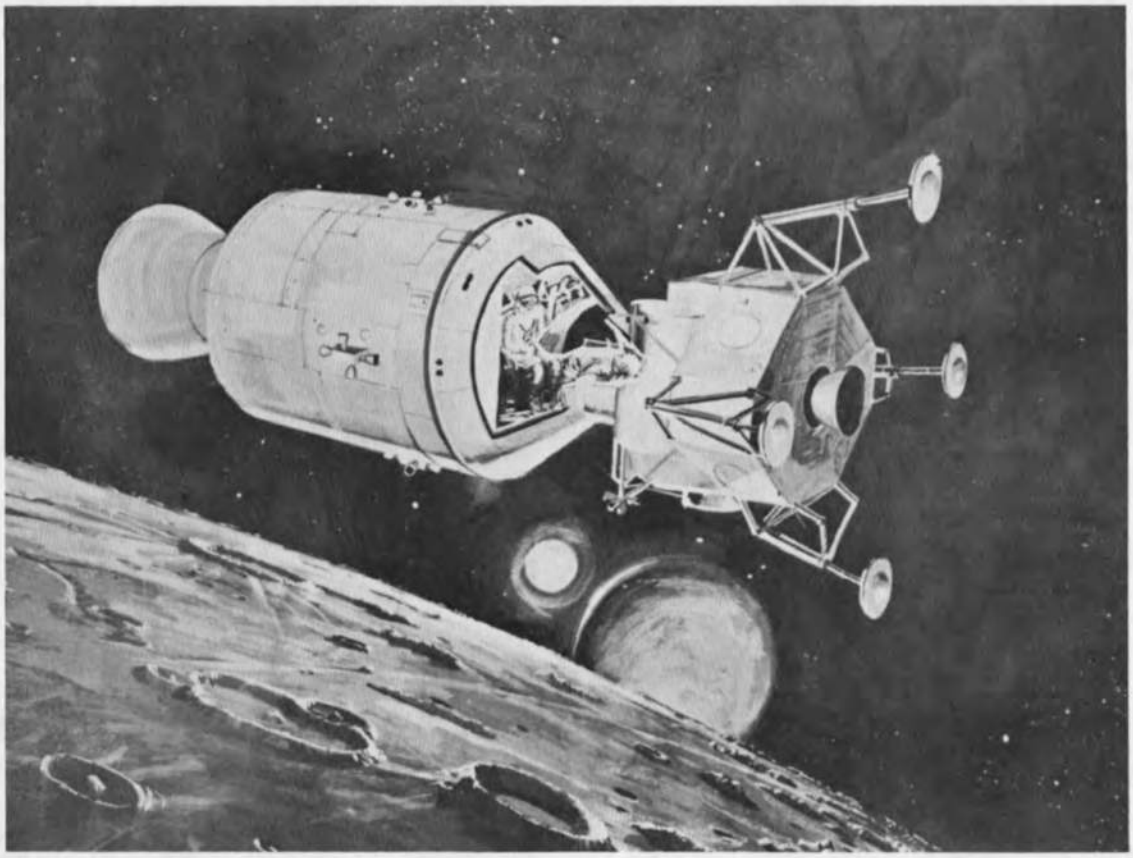

Fig. 1 The Apollo Spacecraft Service, Command, and Lunar Modules

lightweight radiation-cooled exhaust nozzle with a large area ratio (62.5:1) (Fig. 2). The engine, manufactured with the designation AJ10-137 by the Aerojet-General Corporation, provided the main propulsion of the Apollo Service and Command Modules for the cislunar and lunar orbit portions of the Apollo lunar missions. The Apollo SPS engine program at AEDC was conducted in Propulsion Engine Test Cell (J-3) (Fig. 3) of the Rocket Test Facility (RTF). It was originally planned to test eleven engine assemblies in two phases, development (Fig. 4) and qualification, to have been completed in about nine months.

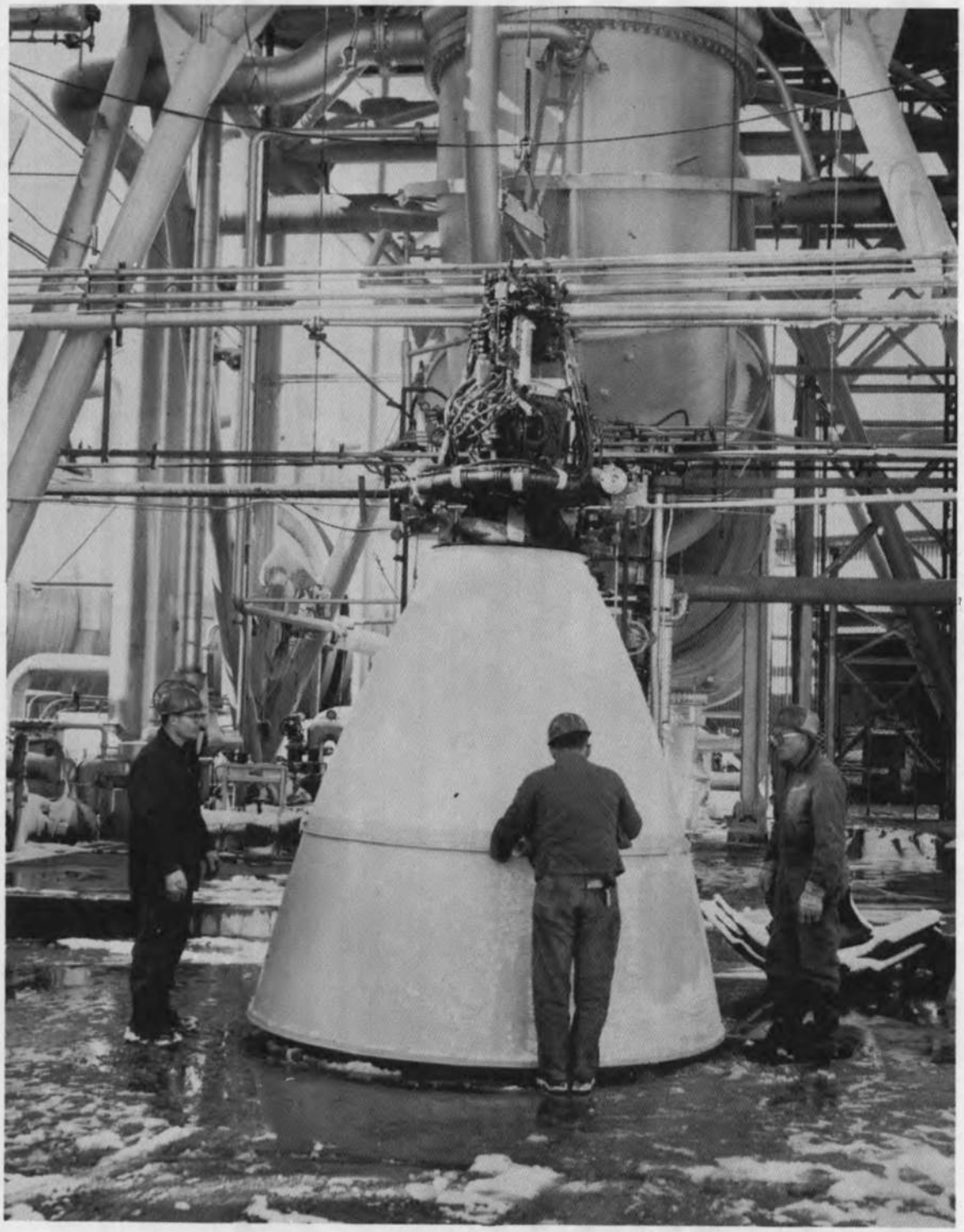

Fig. 2 Service Propulsion System Block II Engine

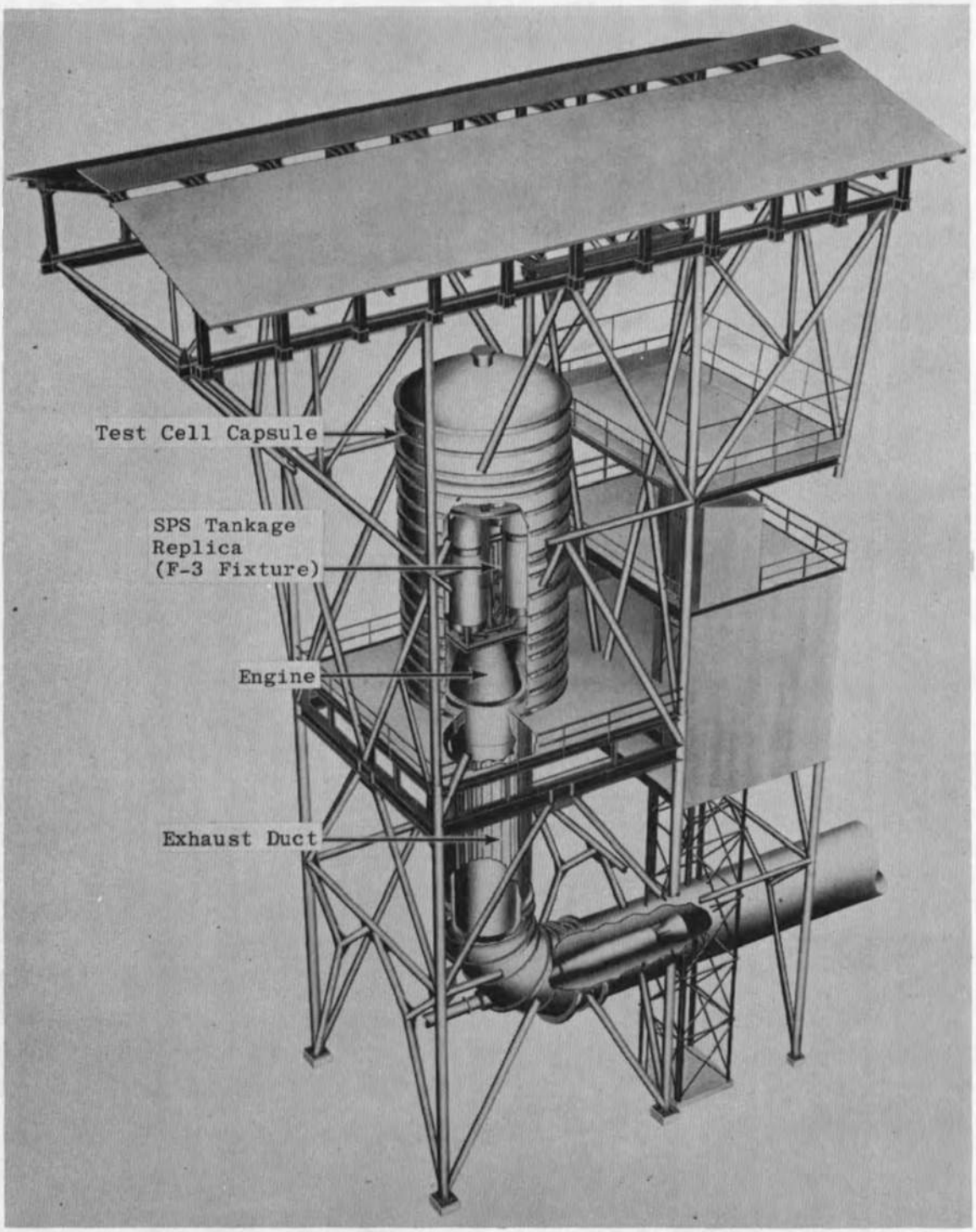

Fig. 3 Drawing of Full-Scale SPS Replica (F-3) in Test Cell J-3

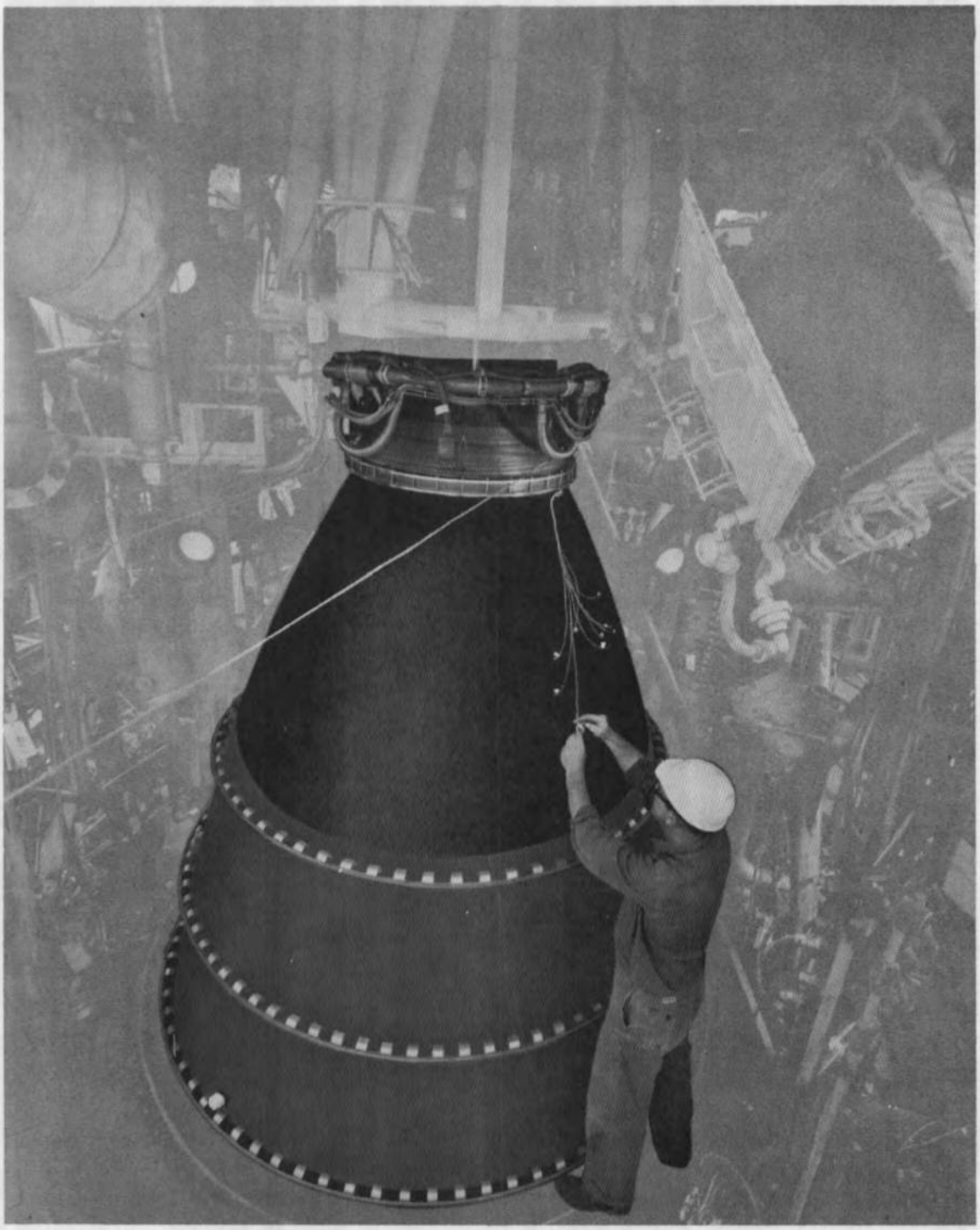

Fig. 4 Phase I Test Installation in Test Cell J-3

It was planned to select an exhaust nozzle extension from a few candidate designs, document engine durability and performance at various operating conditions in the test cell vacuum environment (cell pressure below 0.15 psia), and proceed with formal qualification. However, unexpected vacuum environment effects on engine durability and performance prolonged the initial development and resulted in qualification of an interim compromise engine (Block I) in April 1966. Ensuing development tests produced a Block II engine with improved performance and good durability. The Block II engine design was qualified in February 1967, except for the bipropellant valve which was qualified in August 1968. The chronology of the Apollo SPS engine program at AEDC was:

		No. of Firings	Engine Assemblies	Inclusive Dates
Phase I	Development	77	12	5/63 to 4/64
Phase II	Development/ Prequalification	192	9	8/64 to 10/65
Phase III	Qualification (Block I)	104	7	11/65 to 4/66
Phase IV	Development (Block II)	261	9	4/66 to 10/66
Phase V	Qualification (Block II)	180	6	11/66 to 2/67
Phase VI	Qualification and R&D (Block II)	222	5	2/68 to 9/68
		1036	48	

During these tests, design modifications were indicated and proved for the exit nozzle extension, combustion chamber, injector, and bipropellant valve. Also, during Phases II through V, gimbal operations and dynamics were demonstrated and documented for manufacturer analysis, combustion stability was proved with explosive pulse charges, and engine operation transients were recorded with propellant system dynamics duplicated by a full-scale boilerplate replica of SPS propellant tanks and lines, designated the F-3 test fixture. Apollo SPS propellant pressurization system and propellant utilization system[1] were not used because a variety of off-design tank pressures were required during nearly all test periods and the SPS pressurization regulators were not

[1]The propellant utilization system senses remaining propellant quantities and shifts oxidizer flow rate with a throttling valve for balanced propellant consumption to minimize residual propellant weight.

readily adaptable to the wide pressure range, the SPS pressurization system was not designed for remotely controlled operation, and a utilization system was not available for AEDC tests. The AEDC pressure regulators were used, and a fixed orifice was substituted in the oxidizer line for the utilization valve. Results of the individual test phases or portions thereof are detailed in Refs. 1 through 16.

Table I is an outline of the SPS engine component variations that were evaluated in this program and are discussed in this report. The development history is given for the simulated altitude tests that resulted in satisfactory operation and durability of the metallic exit nozzle extension, the fiber glass/phenolic combustion chamber, the propellant injector, and the engine-mounted bipropellant valve (TCV). The F-3 fixture was changed from Block I to Block II configuration propellant lines and tank arrangement between test periods DC and DD of Phase IV (Parts I and II). The change was deferred from the start of Phase IV to permit early evaluations of the Block II engine performance and durability while the F-3 design modification kit was being fabricated. Engine ballistic performance and operating characteristics are summarized for the altitude tests from early engine evaluations through the Block II engine qualification, the influences of propellant mixture ratio (MR) and temperatures and of combustion pressures on specific impulse (I_{sp}) are indicated, and the engine ignition (FS1), shutdown (FS2), and short-duration (impulse bit) firing characteristics are exemplified.

SECTION II
ENGINE COMPONENT DEVELOPMENT

2.1 NOZZLE EXTENSION

A nozzle development program involving eight designs was conducted as part of the development of the SPS engine at AEDC (Phase I). The eight nozzle extension designs tested at AEDC are shown in Fig. 5. The nozzle extension was attached to the chamber at an expansion area ratio (A/A*) of 6:1, providing an overall expansion ratio of 62.5:1 at the nozzle exit. The nozzle extension was radiation cooled and was constructed of columbium and titanium alloys.

TABLE I
ENGINE COMPONENT VARIATIONS

Test No.	Engine S/N	Combustion Chamber S/N	Combustion Chamber Type[1]	Nozzle Extension S/N	Nozzle Extension Type[2]	Injector S/N	Injector Type	Bipropellant Valve S/N	Bipropellant Valve Type
Phase I Development									
A-01 to -02	1*	1*	8:1,I	A-4	All Ti	AF-30	Long Impingement Triplet	WF-1	Preprototype, Fuel Actuated
A-01 to -03	2*	2*	↓	A-11	All Ti	AF-28	Doublet	CF-3	↓
B-01	3*	3*		A-2	All Ti, Reinforced	AFF-4	Quadlet	CF-4	
B-02	4*	3*		A-1	Cb 20:1/Ti	AFF-4	Quadlet	CF-5	
C-1 to -11	5*	4*	12:1,K	ARO	Steinless Steel	AFF-24	Doublet	---	Nonflight
C-12	6*	4*	12:1,K	---	All Ti, Reinforced	AFF-24	↓	---	Nonflight
B-03	7*	5*	8:1,J	---	Cb 20:1/Ti, 3 Rings	AFF-37		CF-5	Preprototype, Fuel Actuated
C-13, -14	8*	AEDC-1	12:1,K	ARO	Stainless Steel	AFF-24		---	Nonflight
A-03, -04	9*	AEDC-1	↓	A-2	All Ti, Reinforced	AFF-24		---	Nonflight
C-01	10*	---		A-2	All Ti, Reinforced	AFF-23		16	Prototype, Fuel Actuated
B-04, -05	11*	2*	8:1,J	21	Cb/Ti, Reinforced	AFF-37		17	↓
C-02	12*	AEDC-3	12:1,K	---	All Ti, Reinforced	AFF-23		17	
A-05	13*	A-9	8:1,J	1	Cb/Ti, Reinforced	AFF-24		22	
C-03	14*	3*	8:1,I	22	↓	AFF-23		17	
A-06	15*	A-1	8:1,I	22		BF-18	8-Baffle, Doublet	CF-3	Preprototype, Fuel Actuated
C-04	16*	---	8:1,Mod. J; Lightweight	7	↓	AFF-23	Doublet	17	Prototype, Fuel Actuated
Phase II Development and Prequalification									
A, C	9	A-11	8:1;J	1	Cb/Ti	AFF-78	Doublet	20	Block 1, Fuel Actuated
D, F	9-1	50	8.1,Mod. J	39	Cb 40.1/Ti	AFF-78	Doublet	20	↓
G, K	11	47	↓	26	↓	AFF-46	Baffled; Doublet	32	
L	6A	77		27		47	↓	36	
M, N	11A	75		26		91		32	
P, Q	9B	74		25		47		101	Pneumatically Actuated
R, S	11B	155		26		46		↓	↓
T, U	11C	208		27		64			
V, W	11D	211	↓	26	↓	64	↓	↓	↓
Phase III Qualification									
CA	23	214	8:1,Mod. J	42	Cb 40.1/Ti	65	Baffled, Doublet	108	Pneumatically Actuated
CB	23A	213	↓	42	↓	65	↓	↓	↓
CC	23B	219		45		82			
CD	23C	222		↓		↓			
CE, CF	23D	223							
CG, CH	22	220		42		64		104	
CI	21	212	↓	29	↓	71	↓	105	↓
Phase IV Block II Development Part I									
DA	22D	260	6.1,Mod. J	28	Cb 40:1/Ti	87	Baffled;Doublet;Block 1	104	Pneumatically Actuated
DB	22E	261	↓	↓	↓	73	Added Fuel Holes	↓	↓
DC	22F	263				73	Added Fuel Holes		
Phase IV Part II									
DD	21A	263	6:1, A-1**	27	Cb 40:1/Ti	110	B,D,5-4-2***	102	Pneumatically Actuated
DE	21B	299	↓	27	↓	110	B,D,5-4-2	↓	↓
DF	21C	303		41		83	B;D, Blk 1, 5-4-4		
DG	21D	305		41		93	B;D, Blk 1, 5-4-4		
DH	21E	306		42		105	B,D,5-4-4,Counterbored		
DI	21F	310	↓	42	↓	105	B,D,5-4-4,Counterbored	↓	↓
Phase V Block II Qualification									
EA	54	311	8:1, A-1	52	Cb 40.1/Ti	104	(Baffled, Doublet, 5-4-4; Counterbored)	122	Pneumatically Actuated
EB	54A	315	↓	52	↓	104	↓	122	↓
EC	54B	313		54		115		128	
ED	54C	320		54		115		128	
EE	55	318		53		103		122	
EF	55A	324	↓	54	↓	103	↓	122	↓
Phase VI Block II Qualification and R&D									
FA	54D	351	8:1, A-2**	54	Cb 40:1/Ti	104	5-4-4 Baffled; Doublet, Counterbored	128	Mod I-C (All Pneumatic)
FB	↓	↓	↓	↓	↓	↓	↓	↓	↓
FC									
FD	54E								
FE	54F					84		DV-2	
FF	↓					↓		↓	
FG									
FH									
FJ									
FK	54G	352		52				122	Mod I-D (All Pneumatic)
FL	54G	352		52				122	↓
FM	55	1	(Steinless Steel; 8:1)	54		98		DV-4	
FN	↓	↓	↓	↓		↓		↓	
FO									
FP	54H	352	6:1, A-2**	52		94		126	Mod I-E (All Pneumatic)
FQ	54H	352	8.1, A-2**	52		94		126	Mod I-E (All Pneumatic)

*Arbitrary number assignment for ARO identification
**Also Mod. J flange, but injector seal and chamber construction changed
***Number sequence indicates baffle configuration - see Section 2.3

[1]Exit area ratio (A/A*) and nozzle flange design
[2]Area ratio (A/A*) of material change joint, material, construction feature

The steinless steel extension was built by ARO for certain development test firings

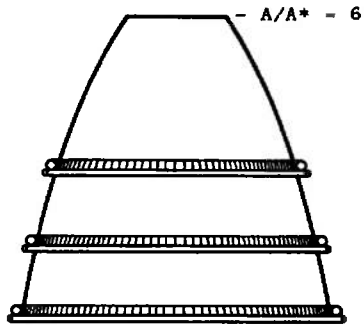

Material: Titanium
Reinforcement: Three Circumferential Stiffeners

a. Configuration I

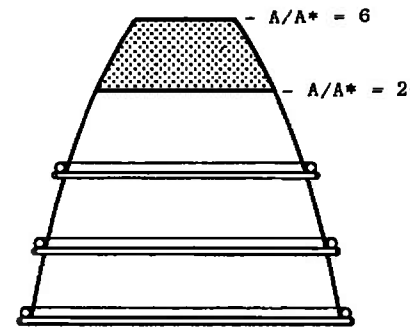

Material: Columbium, 6:1 to 20:1
Titanium, 20:1 to 62.5:1
Reinforcement: Three Circumferential Stiffeners

b. Configuration II

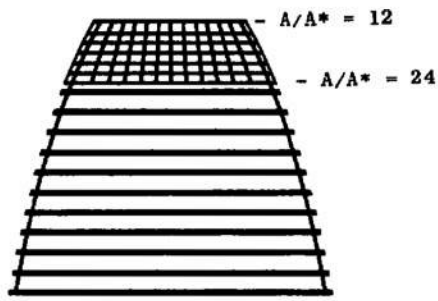

Material: Titanium
Reinforcement: 17 Circumferential and 36 Longitudinal Stiffeners

c. Configuration III

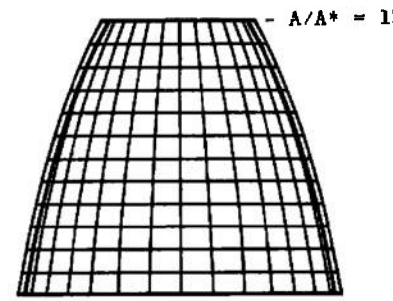

Material: Titanium
Reinforcement: 12 Circumferential and 36 Longitudinal Stiffeners

d. Configuration IV

Fig. 5 Exit Nozzle Extension Configurations

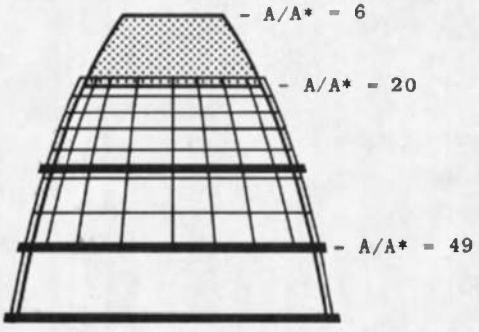

Material: Columbium, 6:1 to 20:1
Titanium, 20:1 to 62.5:1
Reinforcement: 10 Circumferential and 16 Longitudinal Stiffeners

e. Configuration V

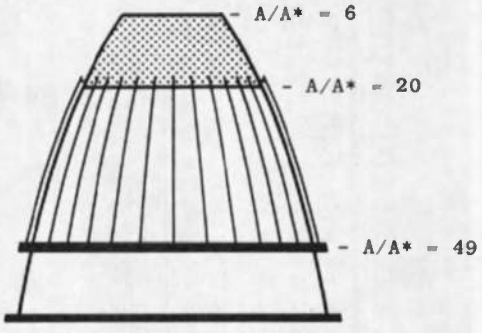

Material: Columbium, 6:1 to 20:1
Titanium, 20:1 to 62.5:1
Reinforcement: 2 Circumferential and 32 Longitudinal Stiffeners

f. Configuration VI

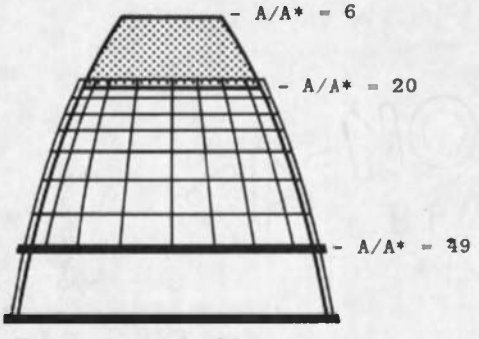

Material: Columbium, 6:1 to 20:1
Titanium, 20:1 to 62.5:1
Reinforcement: 9 Circumferential and 16 Longitudinal Stiffeners

g. Configuration VII

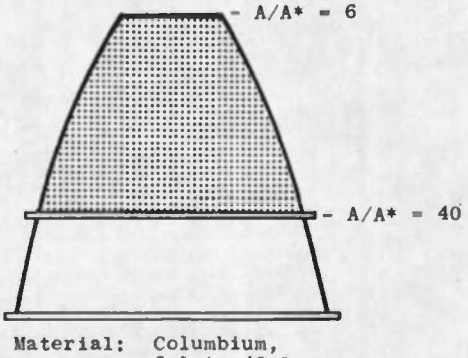

Material: Columbium, 6:1 to 40:1
Titanium, 40:1 to 62.5:1
Reinforcement: Two Circumferential Stiffeners

h. Configuration VIII

Fig. 5 Concluded

Configuration I (Fig. 5a) was used to start testing although previous subscale tests indicated all-titanium construction would not withstand long firing durations. This nozzle extension was constructed of a titanium alloy consisting of 5-percent aluminum, 2.5-percent tin, and 92.5-percent titanium. The nozzle extension had a wall thickness of 0.025 in. and a nominal weight of 132 lb_m. Three circumferential stiffeners, located as shown in Fig. 5a, were used for structural reinforcement. Three extensions of this design were used. The first failed because of facility exhaust diffuser operational difficulties; the second failed because of an engine injector failure which produced severe oscillatory side forces. Both of these failures were within the first 6 sec of operation. The third nozzle extension failed after about 8 sec of normal engine and facility operation because of circumferential buckling at the nozzle attachment flange ($A/A^* = 6:1$) as shown in Fig. 6.

Fig. 6 Nozzle Extension Failure during Test B-2, Configuration I

As anticipated, the failure indicated insufficient structural strength of titanium at the high temperature operating conditions.

The second nozzle extension configuration (Configuration II, Fig. 5b) was constructed of columbium from the 6:1 to 20:1 area ratio and titanium alloy from the 20:1 area ratio to the nozzle exit. Three circumferential stiffeners, located in the same manner as on Configuration I, were used for structural reinforcement. The columbium section was implemented because of its higher structural strength at elevated temperatures. This nozzle was expected to be adequately durable, and the design proved to be more durable under normal operating conditions than did Configuration I; however, the new design still did not have sufficient strength to withstand normal operating temperatures. The nozzle failed in the titanium section in a similar manner as Configuration I, after about 97 sec of engine operation (Fig. 7). The circumferential failure of Configuration II occurred just aft of the columbium in the titanium at the 24:1 area ratio. This indicated that the columbium section was satisfactory but that the titanium portion was not strong enough.

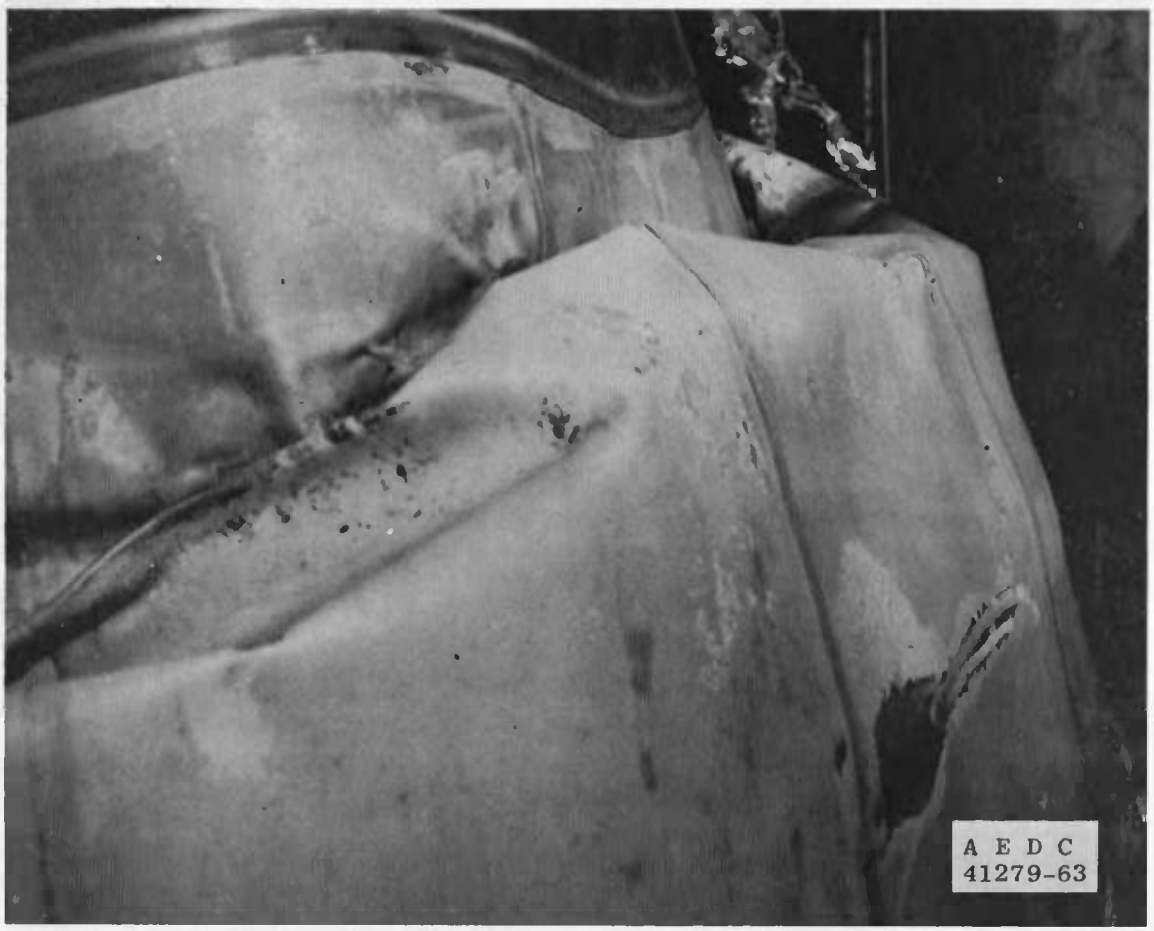

Fig. 7 Nozzle Extension Failure, Configuration II

After nozzle extension design Configuration II, several designs using all titanium and columbium-titanium combinations with various patterns of circumferential and longitudinal stiffeners (Figs. 5c, d, e, f, and g) were tested with varying degrees of success. (Two of these nozzles, Configurations III and IV, were designed to attach to the 12:1 area ratio chamber discussed later.) The persistence of facility exhaust diffuser operational difficulties, in conjunction with structurally inadequate nozzle extensions, precluded a definitive analysis of the effectiveness of the nozzle extension designs. But the nozzle designs with both longitudinal and circumferential stiffeners did have one very apparent inadequacy in common: the stiffeners remained cooler than the sheet metal skin, and wrinkles and cracks occurred because of the differential thermal expansion between the skin and stiffeners (Fig. 8).

Fig. 8 Differential Expansion Effects on Nozzle Extension, Configurations III and IV

A satisfactory nozzle design resulted from the nozzle development program (Configuration VIII). For this design, columbium was used from the 6:1 to the 40:1 area ratio station and titanium from the 40:1 to the 62.5:1 area ratio station (Figs. 2 and 5h). Configuration VIII weighed approximately 170 lb. This extension had a history of success

extending from Phase II through Phase VI. The nozzle serial numbers, the cumulative firing duration, and the number of engine ignitions on each Configuration VIII nozzle extension tested from Phase II through Phase VI are listed below:

Nozzle Serial Number	Cumulative Firing Time, sec	Number of Ignitions
25	408	27*
26	1158	57
27	2890	86
28	1088	56*
29	2710	110
39	615	15
41	1512	55
42	3281	119
45	1767	48
52	3184	111
54	3187	231

*Destroyed by Combustion Chamber Failure (Phase II)

These data indicate the relatively good durability of this nozzle configuration compared with the engine design operating life of 750 sec total burning time and 50 starts. Many of the nozzles listed above were still usable after the listed firing time.

A temperature history and a profile are presented in Figs. 9 and 10, respectively, for a typical Configuration VIII nozzle.

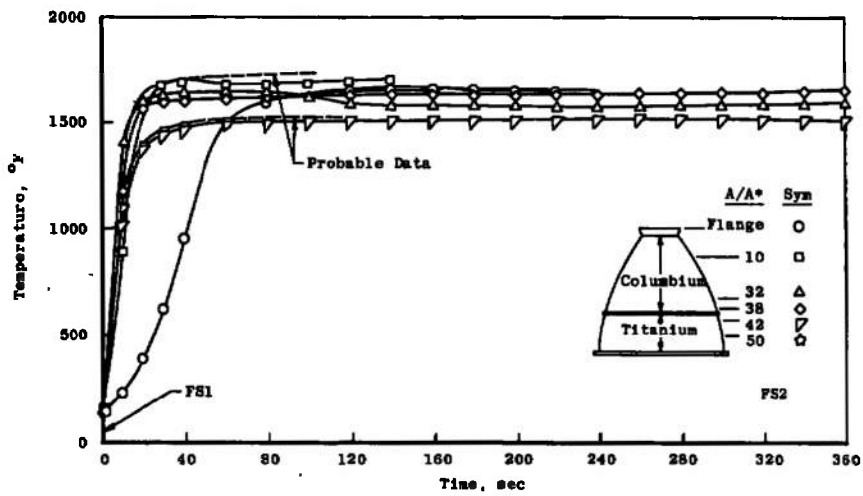

Fig. 9 Nozzle Temperature History, Configuration VIII

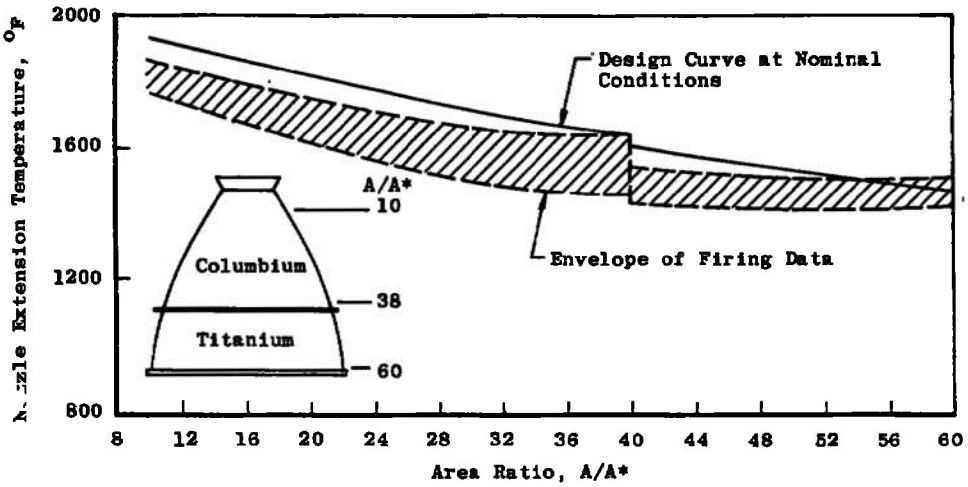

Fig. 10 Nozzle Temperature Profile, Configuration VIII

2.2 COMBUSTION CHAMBER

The combustion chamber was constructed with a silica cloth (Refrasil®) tape ablative liner bonded with phenolic resin, an asbestos insulating layer bonded with phenolic, and an outer structural wrap of glass cloth and filament rovings bonded with epoxy resin. Injector and nozzle extension mounting flanges were bonded between the insulating layer and the outer structural wrap. The ablative liner tape was oriented with an aft-running slant to provide a "shingle" effect for the combustion gas flow. Chamber construction began with the ablative liner formed on a contoured mandrel and autoclave cured. The insulation layer was added and cured. The metal attachment flanges and structural wraps were added to complete the assembly.

The basic chamber design and contour were not greatly changed during testing at AEDC (see Fig. 11a). A lightweight construction chamber was tested during Phase I, test C-04, but the thinned chamber failed upstream of the nozzle extension attachment flange after a 6.35-sec firing and an accumulated firing time of 746 sec. Subsequent tests were conducted with the heavier standard chamber construction; however, major changes were made in the attachment flanges at the injector and nozzle extension interfaces. The changes to the combustion chamber/nozzle extension flanges were made for weight reduction; the changes to the injector/combustion chamber flange were incorporated to improve gas seal reliability and to prevent delamination of the liner. Two combustion chambers, which differed from the basic 6:1 area ratio configuration shown in Fig. 11a, extended to the 12:1 area ratio station (Fig. 11b). The longer chamber proved unnecessary when columbium material provided adequate high temperature strength for the nozzle extension.

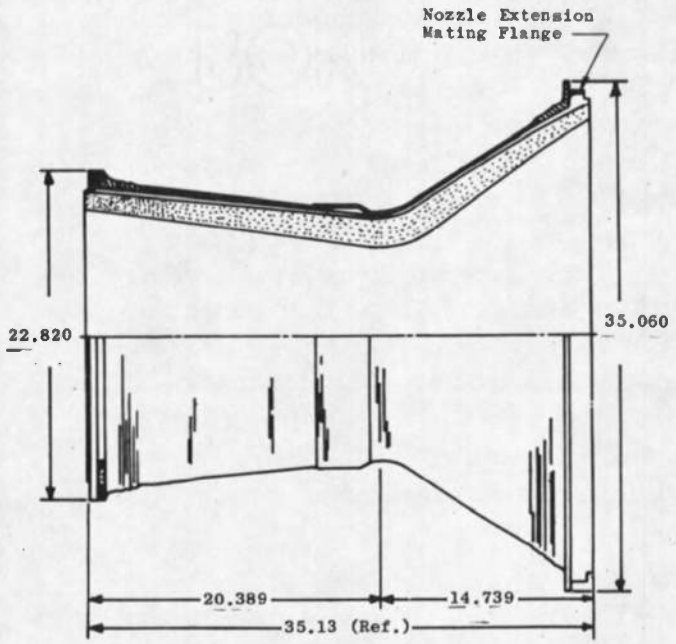

a. Dimensions of Standard 6:1 Area Ratio Chamber

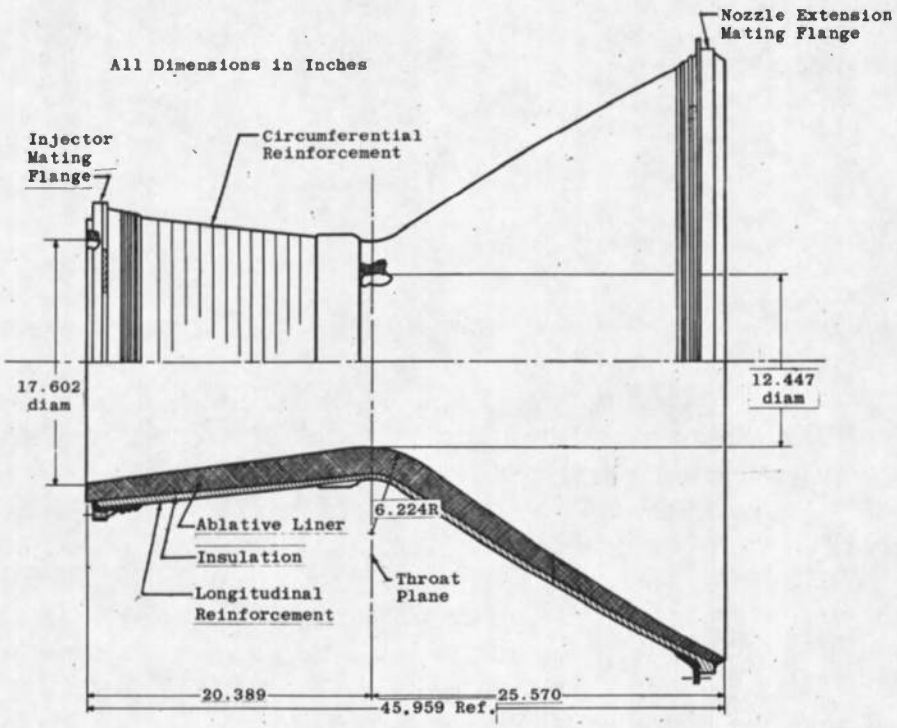

b. Dimensions of 12:1 Area Ratio Chamber

Fig. 11 Ablative Thrust Chamber Details

The changes to the combustion chamber/nozzle extension flange are shown in Fig. 12. The original flanges were designated the "I" and "K" types (Figs. 12a and b, respectively), with the former used on the 6:1 area ratio chambers and the latter on the 12:1 chambers. When the nozzle extension was modified from all titanium to the columbium/titanium type (see Section 2.1), the chamber flange design was altered and designated as the J-flange (Fig. 12c). After the nozzle construction proved satisfactory in the interface area, the design was modified to provide a lighter weight configuration, and was designated as the "modified J flange" (Fig. 12d). Additional testing confirmed the adequacy of this design, and it became the approved configuration which was used on all engines in Phases II through VI. The only other difficulty encountered with this flange design was during Phase V when a bond separation occurred at the chamber flange (Fig. 13).

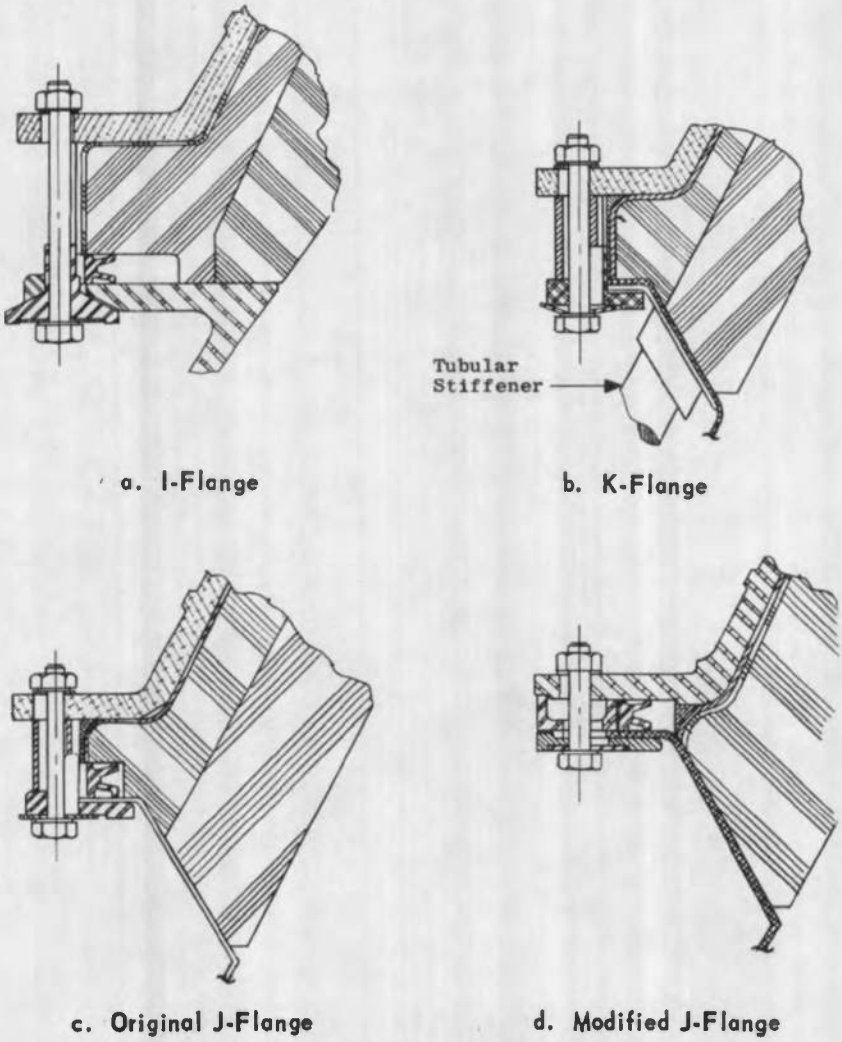

a. I-Flange

b. K-Flange

c. Original J-Flange

d. Modified J-Flange

Fig. 12 Chamber/Nozzle Extension Flange Designs

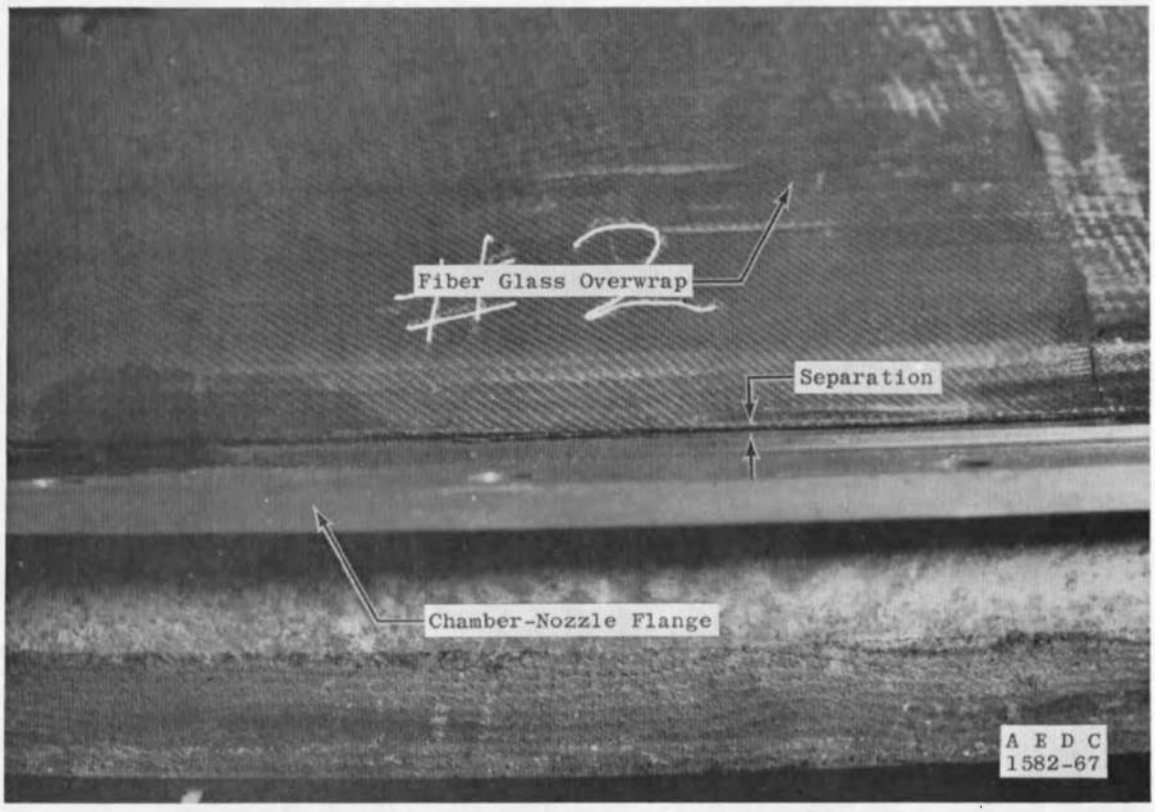

Fig. 13 Chamber Flange Separation (Phase V, S/N 324)

The various designs of chamber forward end (chamber/injector interface) which were tested are shown in Fig. 14. The original design for the injector/chamber flange (Fig. 14a) was used for all chambers in Phase I and all but the last four test periods of Phase II. About the middle of Phase II, after test period M, posttest inspection of the chamber (S/N 75) revealed delaminations of the ablative material at the injector seal area (Fig. 15).

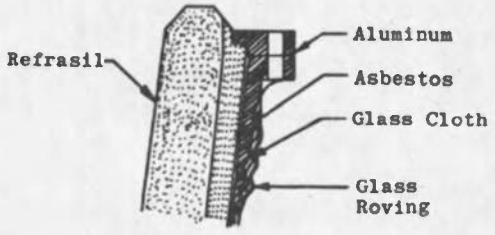

a. Chamber Flange (Used in Phase I and Part of Phase II)

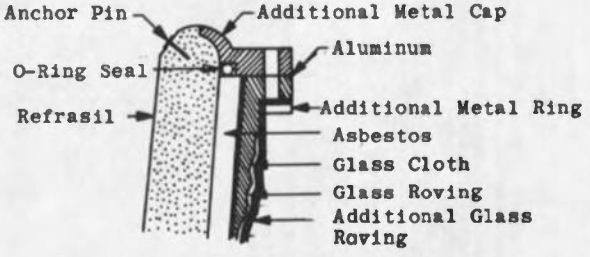

b. Modified Chamber Flange (Used without Anchor Pins for Two Test Periods of Phase II and First Two Periods of Phase III, Used with Pins for Last Two Test Periods of Phase III)

Fig. 14 Combustion Chamber Flange Designs (Injector Interface)

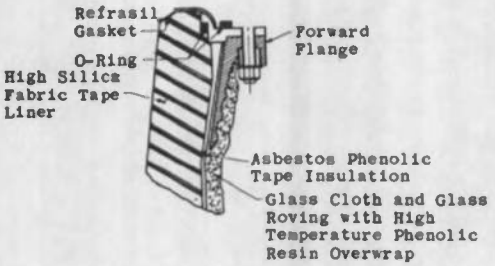

c. Modified Chamber Flange (Used during Last 7 Test Periods of Phase III)

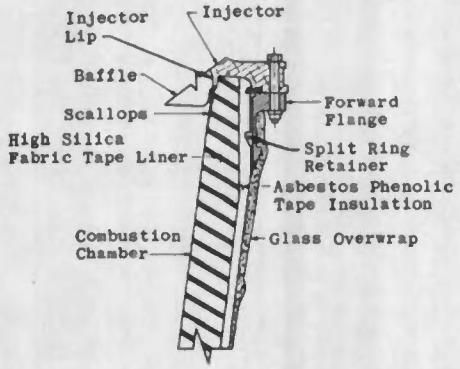

d. Modified Chamber Flange (Used during First Three Test Periods of Phase IV)

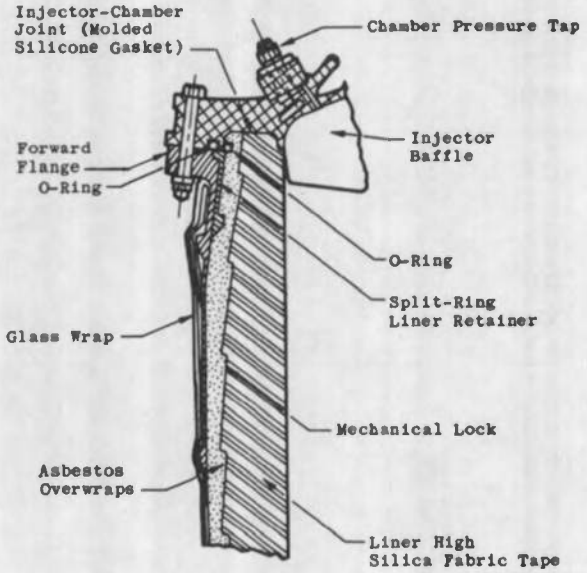

e. Modified Chamber Flange (Used during Remaining Phase IV and All Of Phase V and VI Tests)

Fig. 14 Concluded

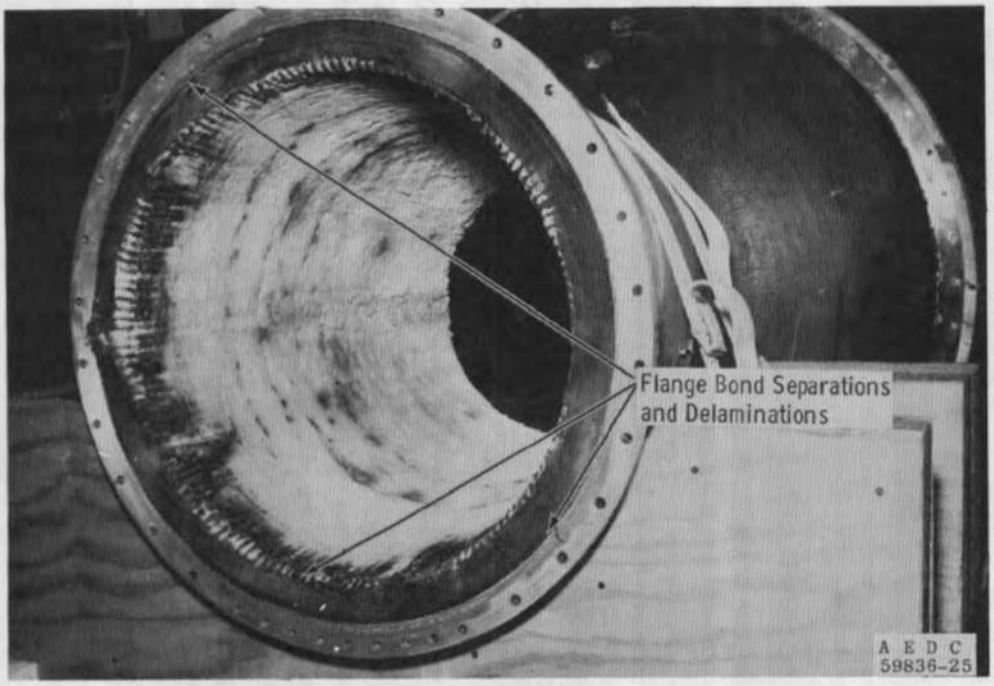

Fig. 15 Chamber S/N 75, Postfire

Test periods P, Q, R, and S, with chambers S/N 74 and 155 of the same design, revealed the severity of the problem with failures at the forward flange (Fig. 16a). These two chambers had operated for a total of 408 and 332 sec, respectively, of which 223 and 149 sec, respectively, were at the maximum chamber pressure (125 psia). Figure 16b shows chamber S/N 74 with a section removed and indicates the condition of the failure area. It was noted that the bond area was protected by virgin material in the radial direction, but the portion of the chamber that seals the joint of the injector flange was severely charred and eroded. Figure 16c is a top view of chamber S/N 155 showing the severity of erosion in the seal area. These delaminations of the ablative liner were suspected of contributing to, or perhaps even initiating, the flange-bond failures by permitting hot gas leakage behind the chamber/injector seal.

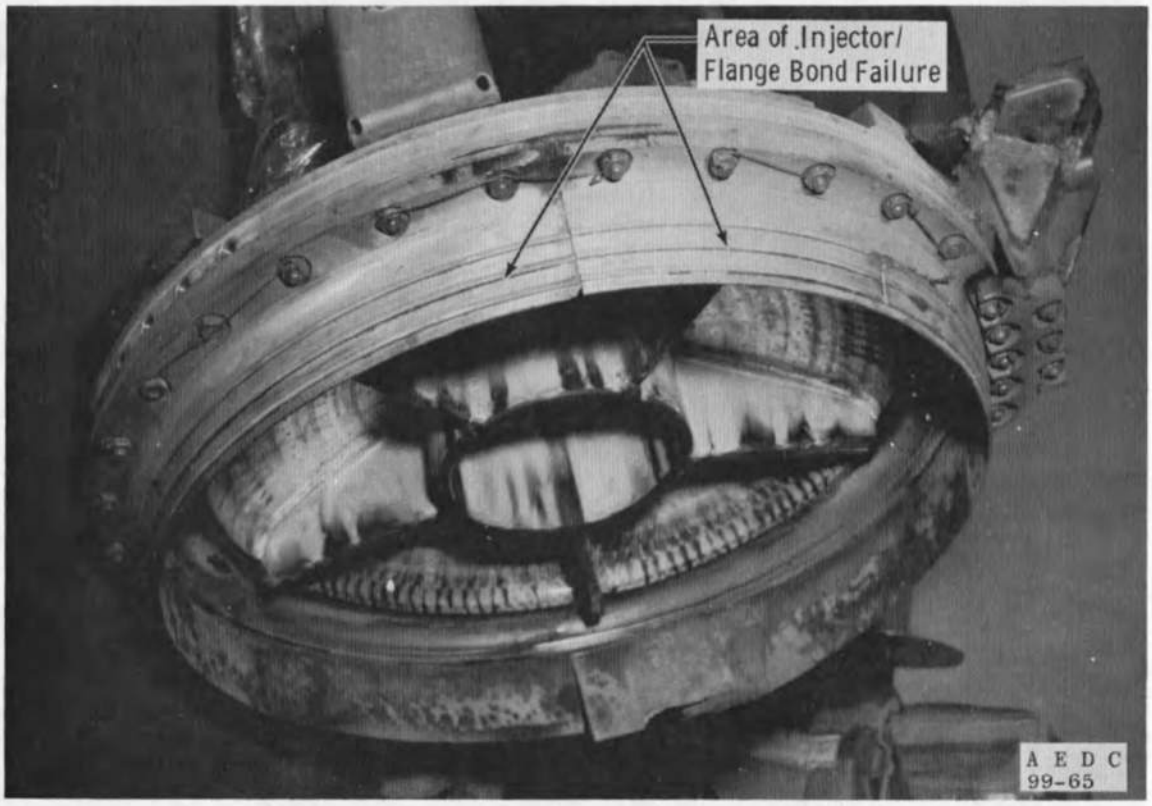

a. Engine S/N 11B Injector and Chamber Flange (S/N 155)

Fig. 16 Chamber Failures at Forward Flange Area

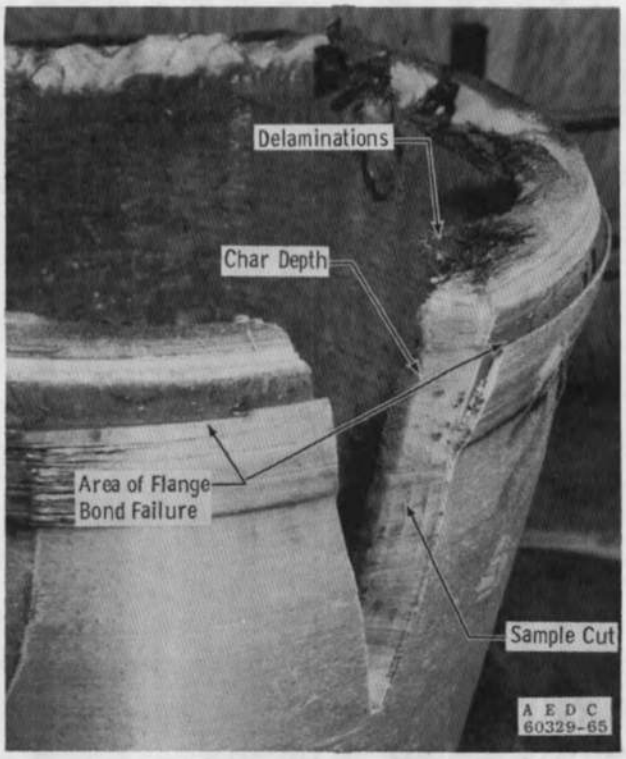

b. Chamber S/N 74

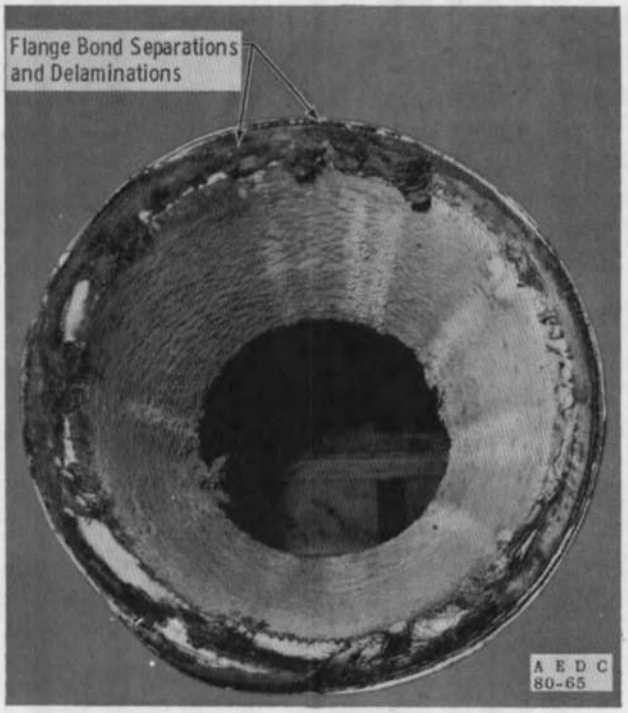

c. Chamber S/N 155

Fig. 16 Concluded

A chamber modification was made with additional glass roving to prevent flange movement, and the injector seal was redesigned to include an aluminum cap over the asbestos insulating layer and partially over the ablative liner as shown in Fig. 14b. An O-ring was added to prevent the flow of gas along the phenolic into the flange bond area. This modified chamber was tested for a total of 766 sec, of which 200 sec were at a chamber pressure of 125 psia and 355 sec at 110 psia. The chamber exhibited a notable improvement in durability over those previously tested even though posttest examination did reveal some delamination in the forward ablative liner and erosion of the metal cap (Fig. 17).

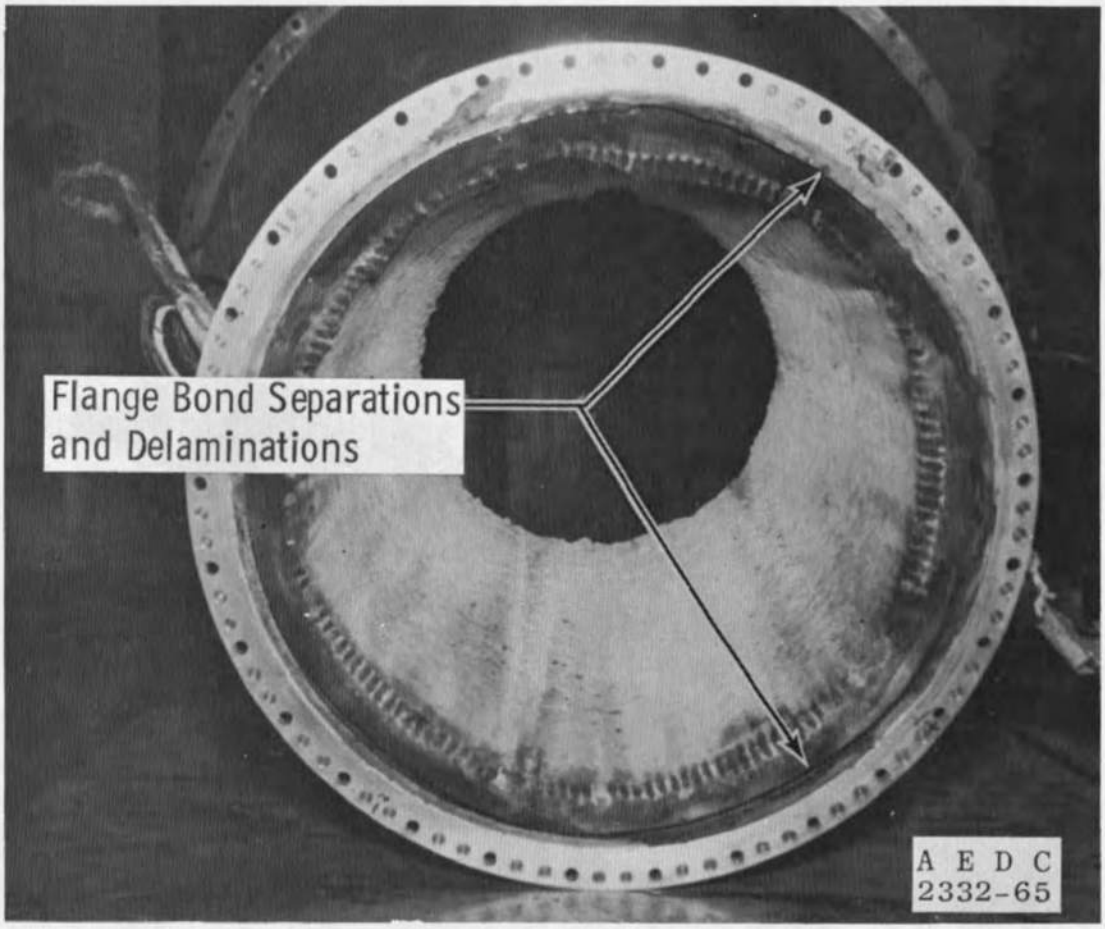

Fig. 17 Chamber S/N 208, Postfire, Injector End

To prevent delamination of the forward end, stainless steel pins were installed in the ablative liner to anchor the Refrasil material laminations (Figs. 14b and 18). Twenty-two pins were equally spaced

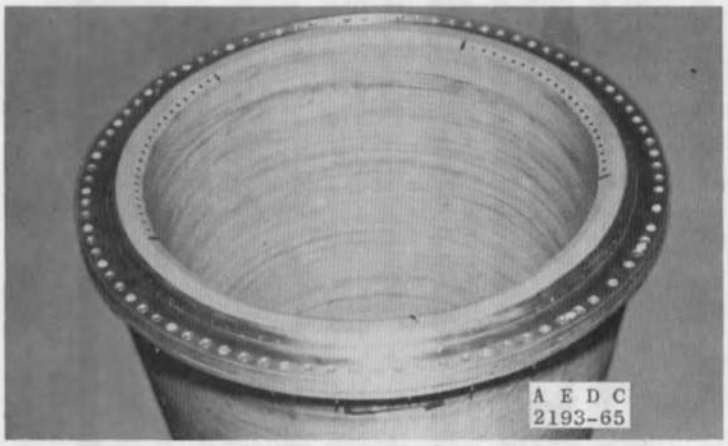

Fig. 18 Prefire, Chamber S/N 211 with Anchor Pins

in two areas. Unpinned areas were left in between for comparison to aid evaluation of any improvement in interface durability. The test period for this chamber was discontinued short of completion because of high temperatures of the injector and chamber flanges. The total firing time was 501 sec, of which the final 278 sec were at 125-psia chamber pressure. Posttest examination revealed the same forward end delamination and showed that the anchor pins had not appreciably improved chamber interface durability (Fig. 19).

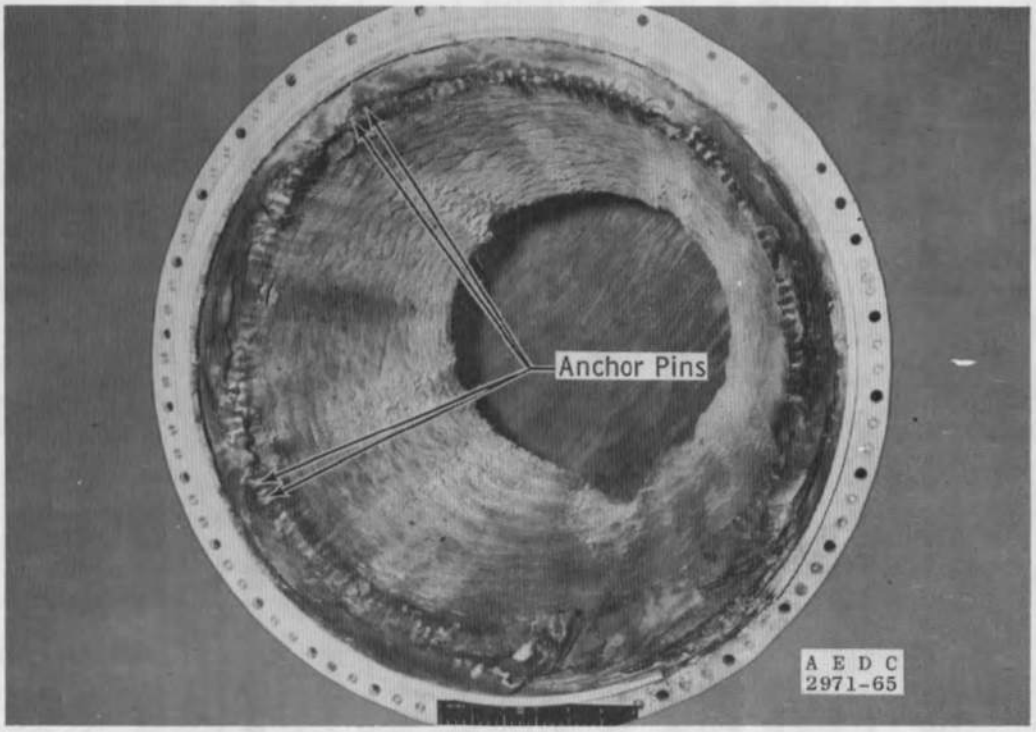

Fig. 19 Postfire Condition, Chamber S/N 211

Figures 20 and 21 are temperature histories for the chambers with and without the stainless steel pins. There was no apparent improvement in the overall temperature history from the use of the pins. The temperature histories in Fig. 21 do not indicate any differences between the areas with and without pins. Use of pins was discontinued. These tests completed Phase II testing.

The initial two chambers tested in Phase III were of the same construction as shown in Figs. 11a and 14b. These two chambers exhibited the same forward end delaminations as experienced previously. Graphs of the temperature-time history of the chamber flange and injector are shown in Figs. 22 and 23 for the second of the two chambers (S/N 213). Figure 24 is a postfire view of this chamber.

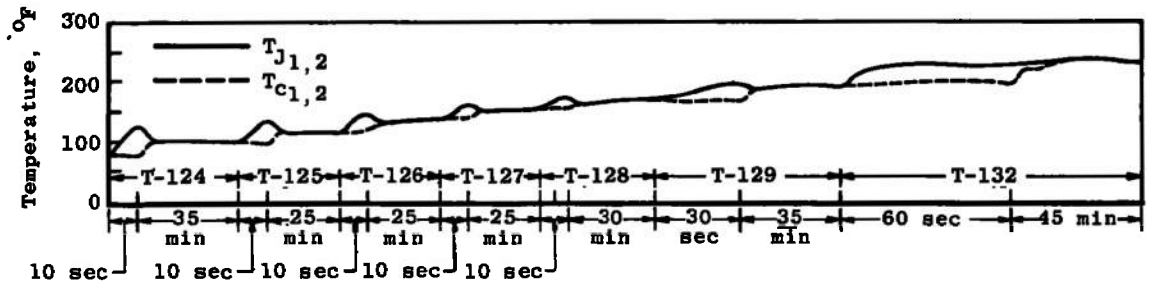

a. Initial Firings

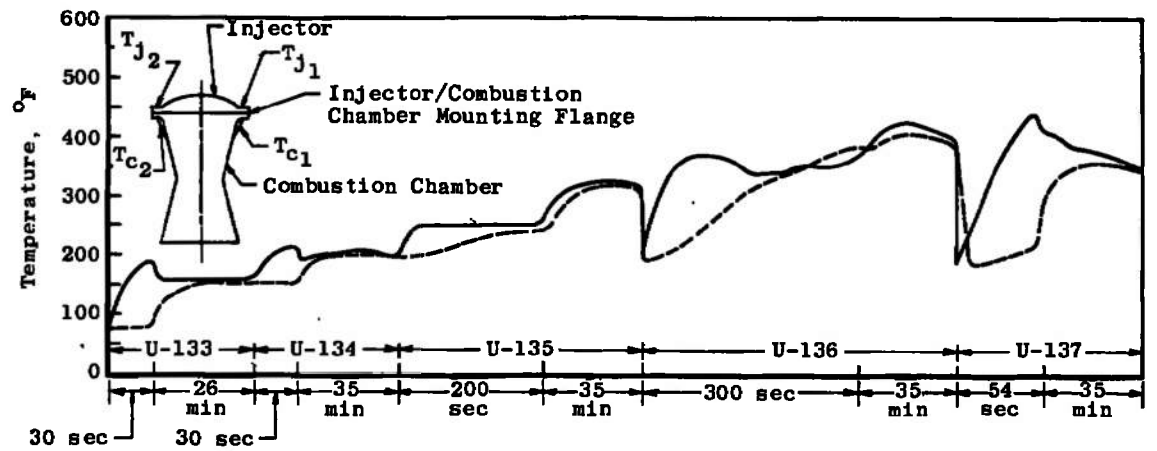

b. Final Firings

Fig. 20 Temperature History, Chamber without Anchor Pins

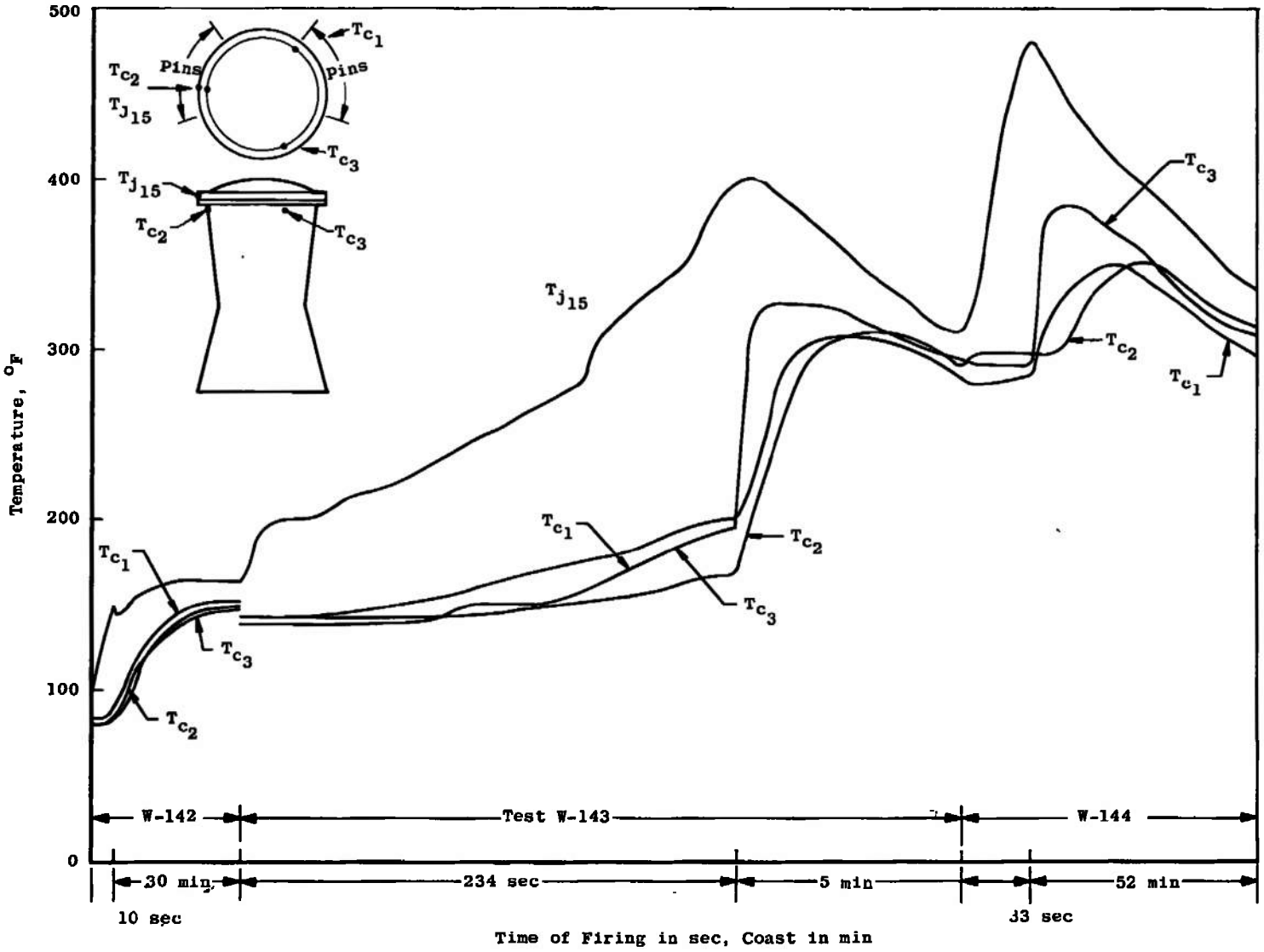

Fig. 21 Temperature History, Chamber with Anchor Pins

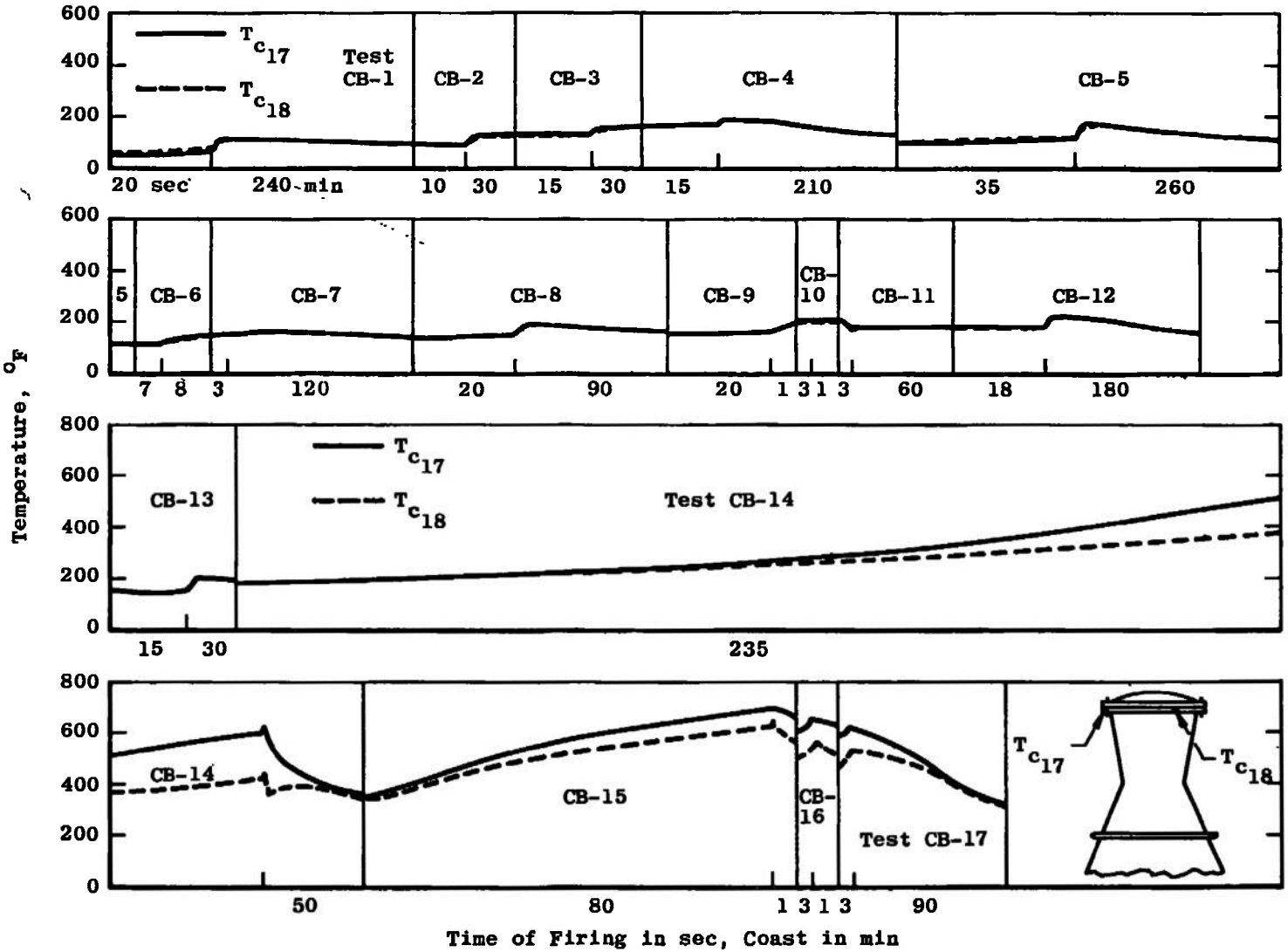

Fig. 22 Temperature History, Chamber S/N 213

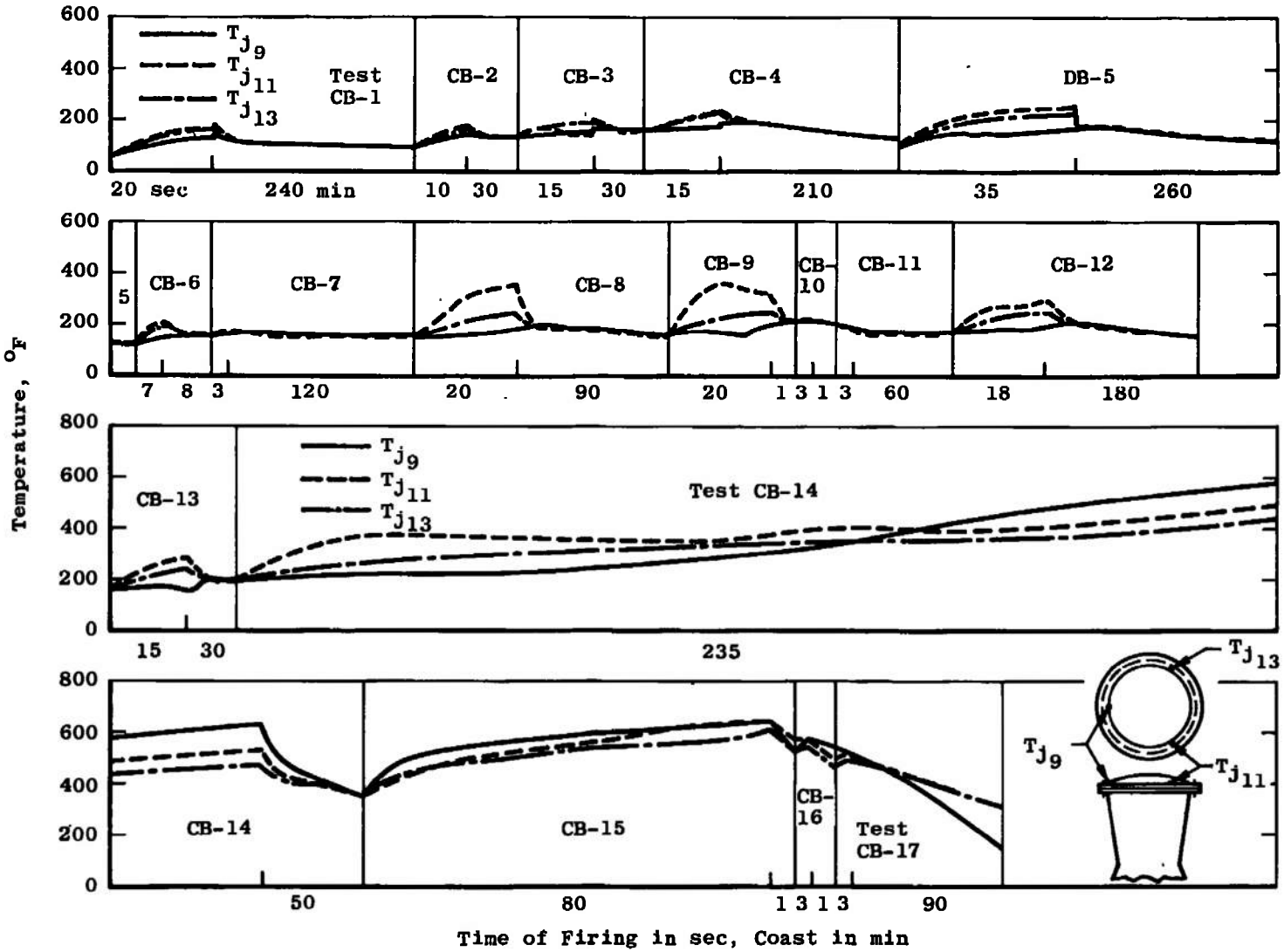

Fig. 23 Temperature History, Chamber S/N 213

Fig. 24 Postfire Condition, Chamber S/N 213

After the test of chamber S/N 213, a new injector/chamber seal was devised with Refrasil and silicone rubber gaskets and silicone O-rings to seal the outboard surfaces of the flange, as shown in Fig. 14c. This seal performed satisfactorily as can be seen by comparing Figs. 22 and 23 with Figs. 25 and 26, which show temperatures obtained using the old-type seal (S/N 213) and corresponding data graphs for the new seal (chamber S/N 222). Test durations were the same, but temperatures with the new seal were considerably lower during the long firings. Figure 27 is a postfire view of the chamber on which the new-type seal was used. This new chamber/injector seal was used on the remainder of the chambers tested in Phase III and performed satisfactorily until the final test period. The final test period of Phase III consisted of long-duration firings at high combustion chamber pressure (110 psia). Figures 28 and 29 are temperature-time graphs of the injector flange temperatures from these firings and show the increasing flange temperatures, which were indicative of incipient failure. This engine was not disassembled prior to shipment; therefore, no postfire photographs are available. This completed the testing of the Block I chamber.

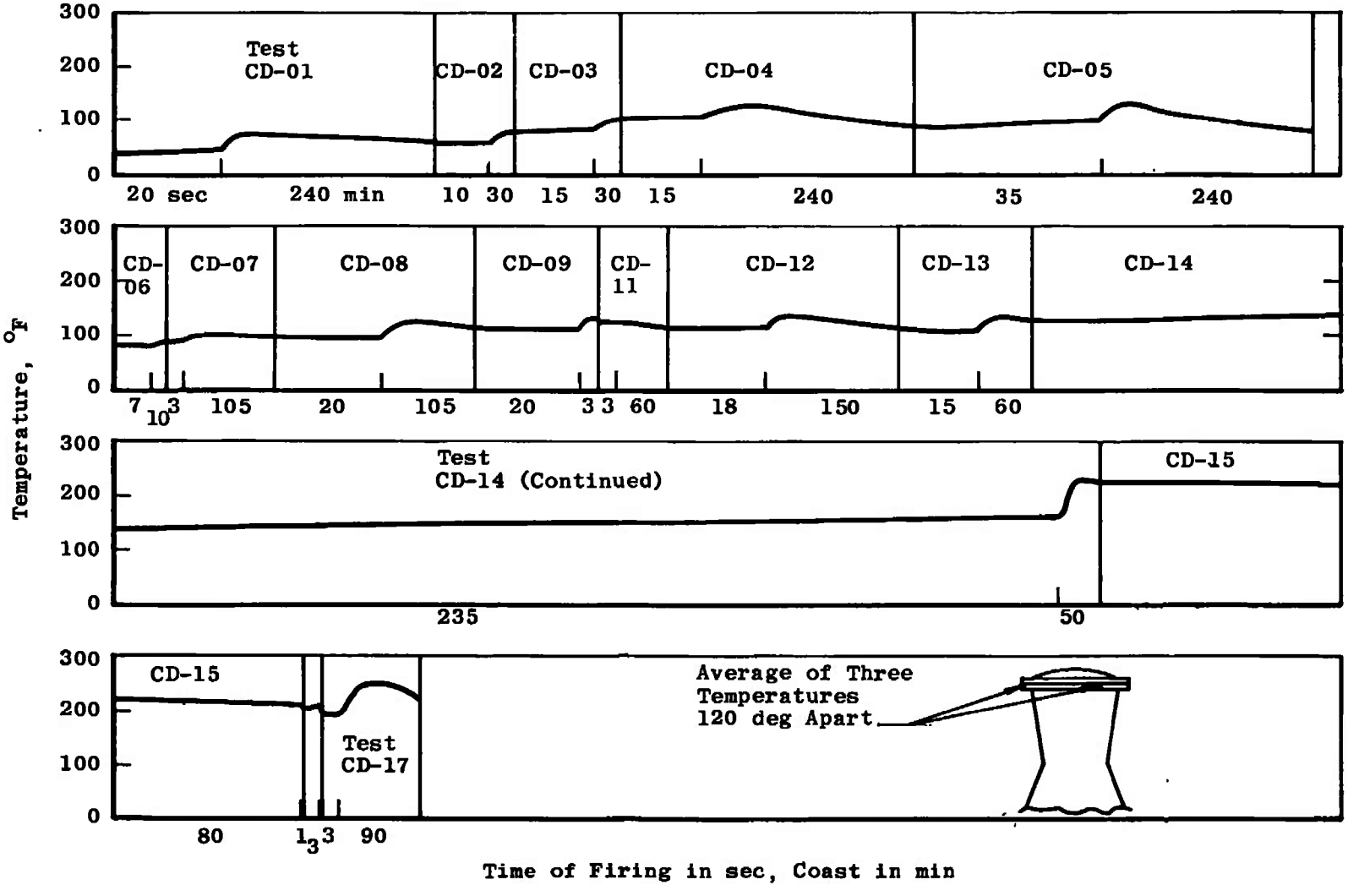

Fig. 25 Temperature History, Chamber S/N 222

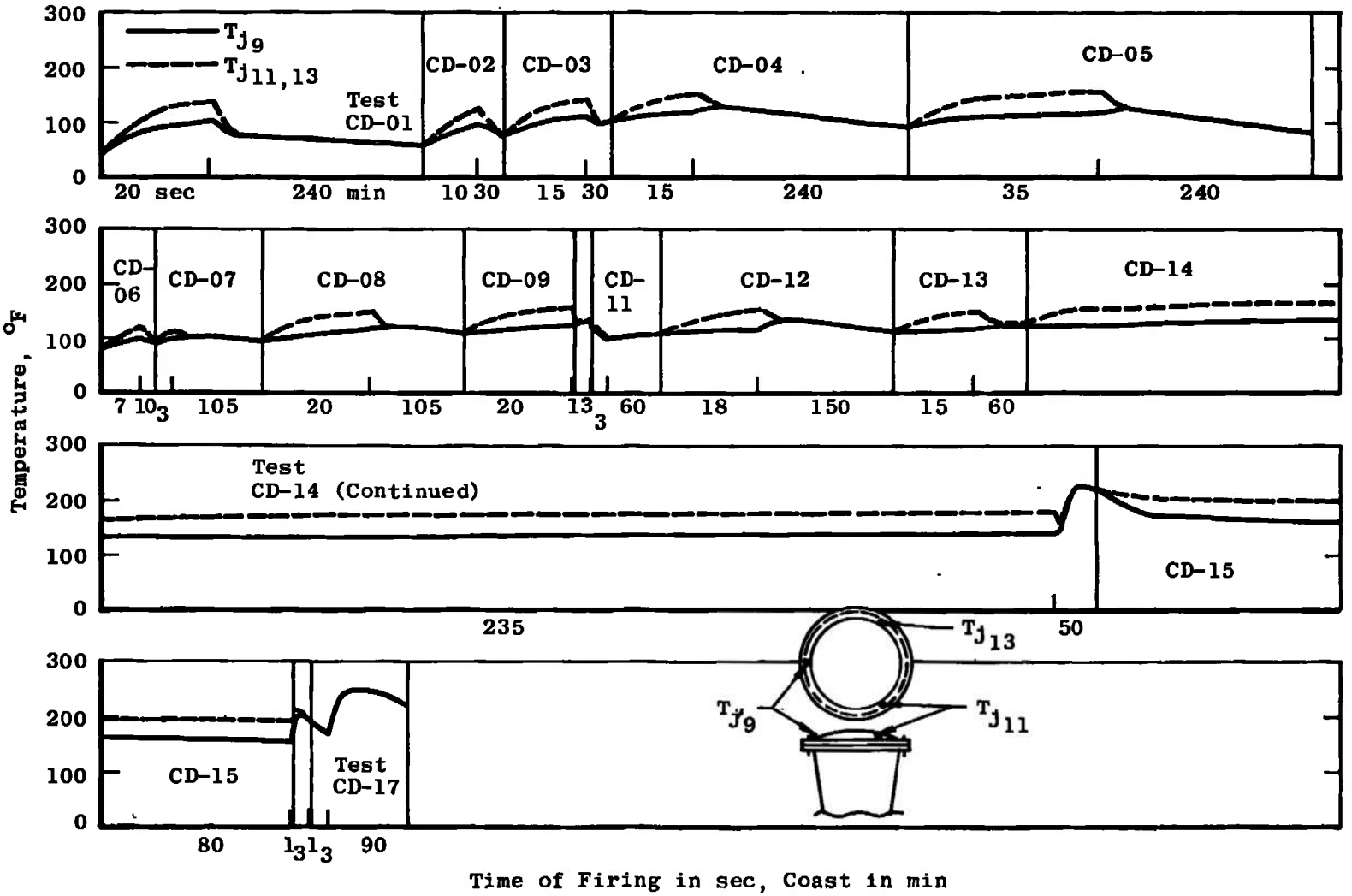

Fig. 26 Temperature History, Chamber S/N 222

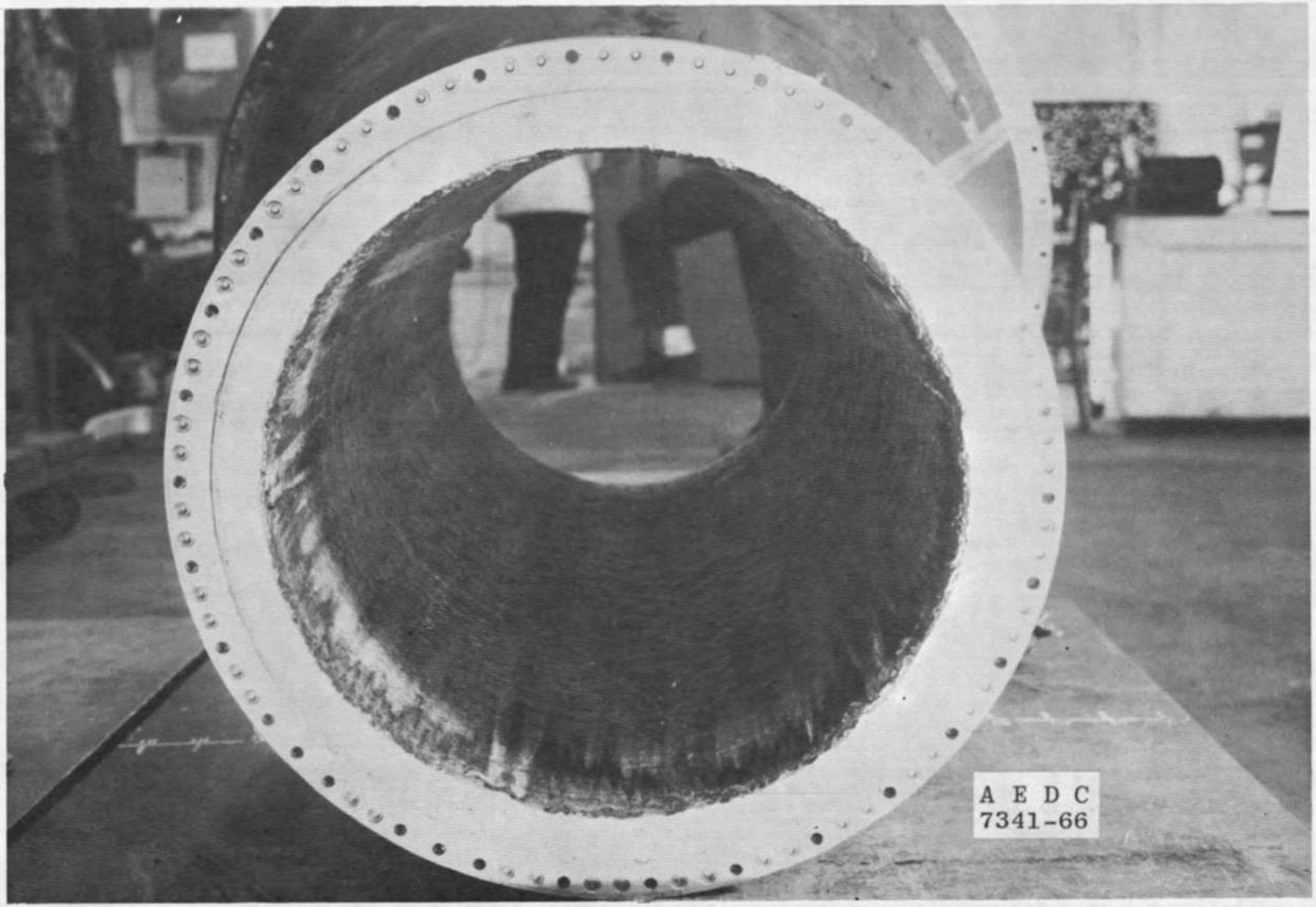

Fig. 27 Postfire Condition, Chamber S/N 222, New-Type Chamber Seal

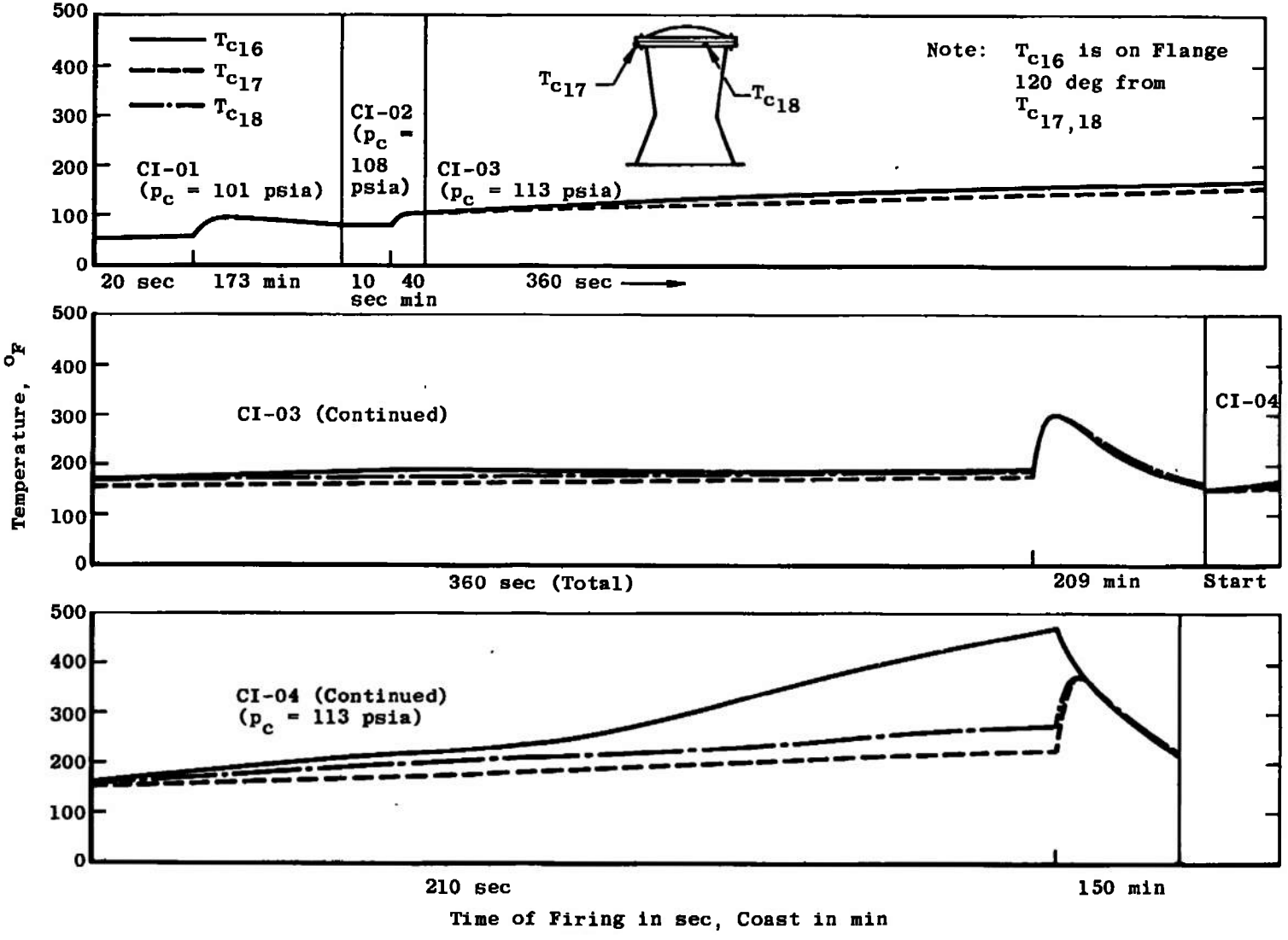

Fig. 28 Combustion Chamber Temperature History

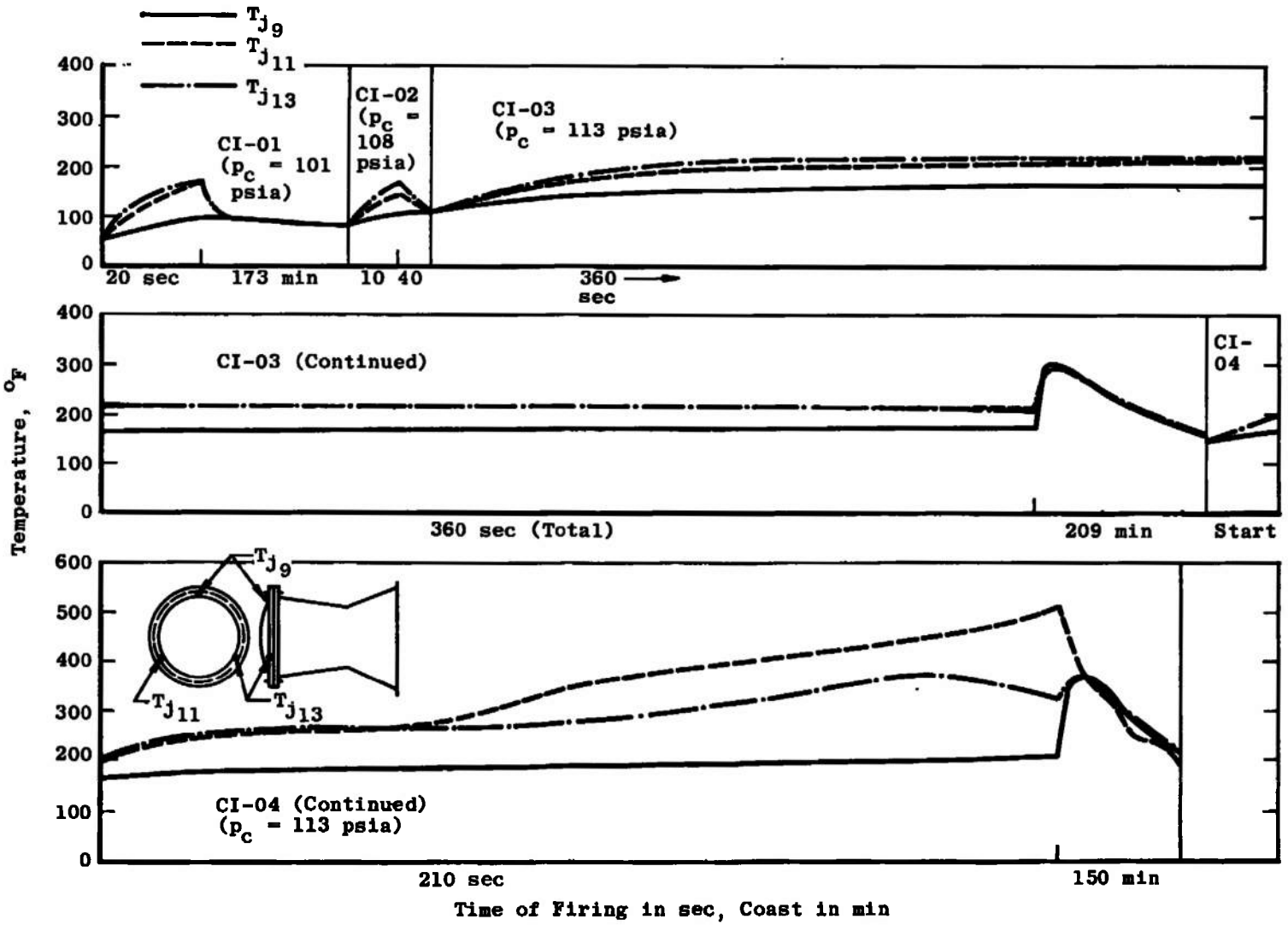

Fig. 29 Injector Flange Temperature History

Testing of the Block II chamber design (see Section I) involved evaluation of a new chamber/injector seal (Fig. 14d). This seal consisted not only of a silicone gasket and O-rings, as used previously, but also included an extension of the injector ID to form a lip over the interface area. This seal configuration performed satisfactorily. An injector/chamber compatibility problem still caused severe erosion of the chamber downstream of the seal area (Section 2.3.4).

The only other change to the chamber design, to ensure the physical integrity of the interface seal, was the addition of a mechanical lock between the insulation and the ablative liner (Fig. 14e). This lock scheme was a series of steps at the interface of the insulation and ablative liner to prevent slippage of the ablative liner away from the injector. This design was satisfactory, and no further complications were encountered during Phases IV, V, and VI.

During Phase VI test period DC, chamber S/N 263 developed two "blisters" in the ablative lining where the lining bond to the insulation layer separated locally, about halfway between the injector and throat. Several minor changes were made to the chamber fabrication and cure cycle which were not documented at AEDC because neither the type nor degree of change was made available by the manufacturer. The cure cycle changes prevented blisters, and the subsequent chamber durability was quite good.

2.3 INJECTOR

2.3.1 Phase I

Four injector designs were tested during the initial phase. These included a long impingement triplet, a quadlet impingement, and a doublet impingement; all of which were unbaffled. A doublet impingement type which had six radial baffles and one cylindrical baffle was also tested. Figures 30 and 31 show the unbaffled and baffled doublet impingement injectors. The unbaffled injectors were all similar except that the pattern of the orifices was changed. Film cooling of the injector/combustion chamber interface and chamber wall was provided by fuel flow from nonimpinging orifices in the outer fuel ring of the injector, adjacent to the mounting flange. Approximately 5 percent of the fuel flow was injected for film cooling.

The long impingement triplet injector (S/N AF-30) was tested first and was used for two firings of 4- and 6-sec duration. Combustion instability of 90-Hz frequency developed during the first test, and 1600-Hz instability developed during the second test.

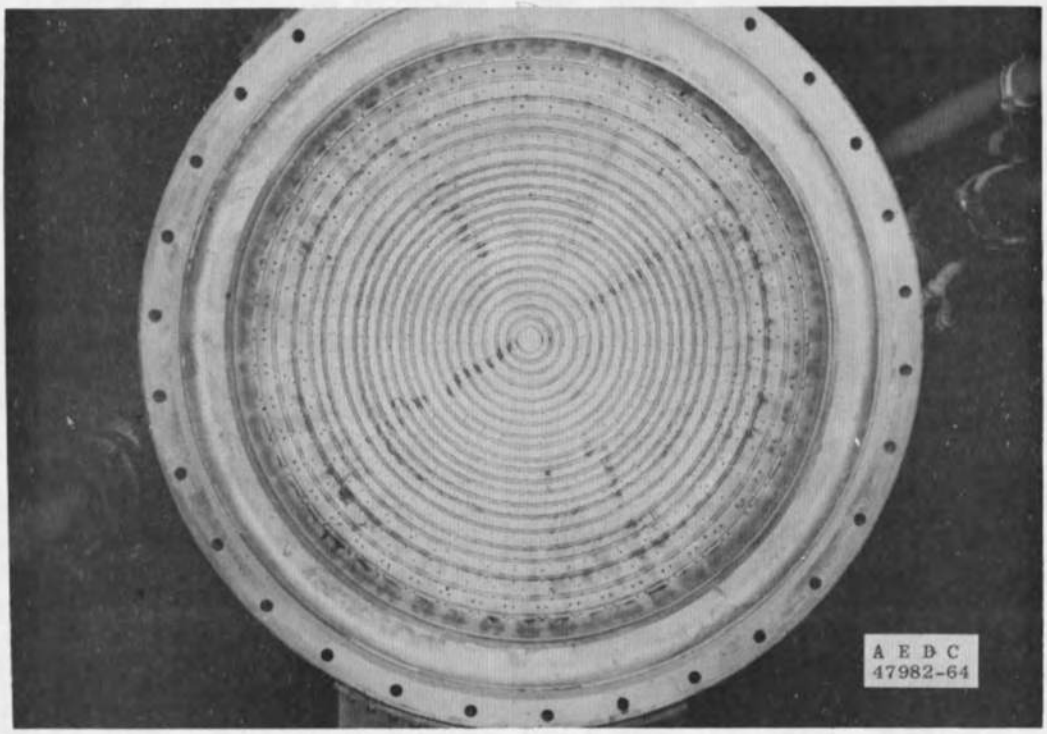

Fig. 30 Unbaffled Doublet Injector, View Looking Upstream

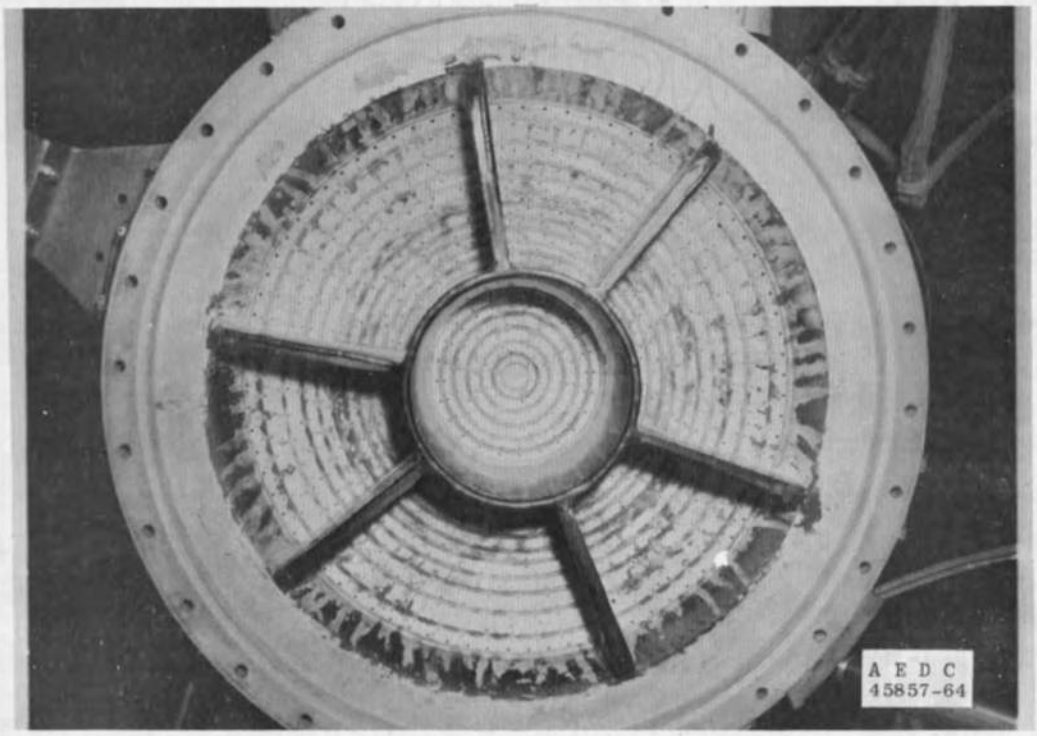

a. View Lookino Upstream

Fig. 31 Baffled Doublet Injector

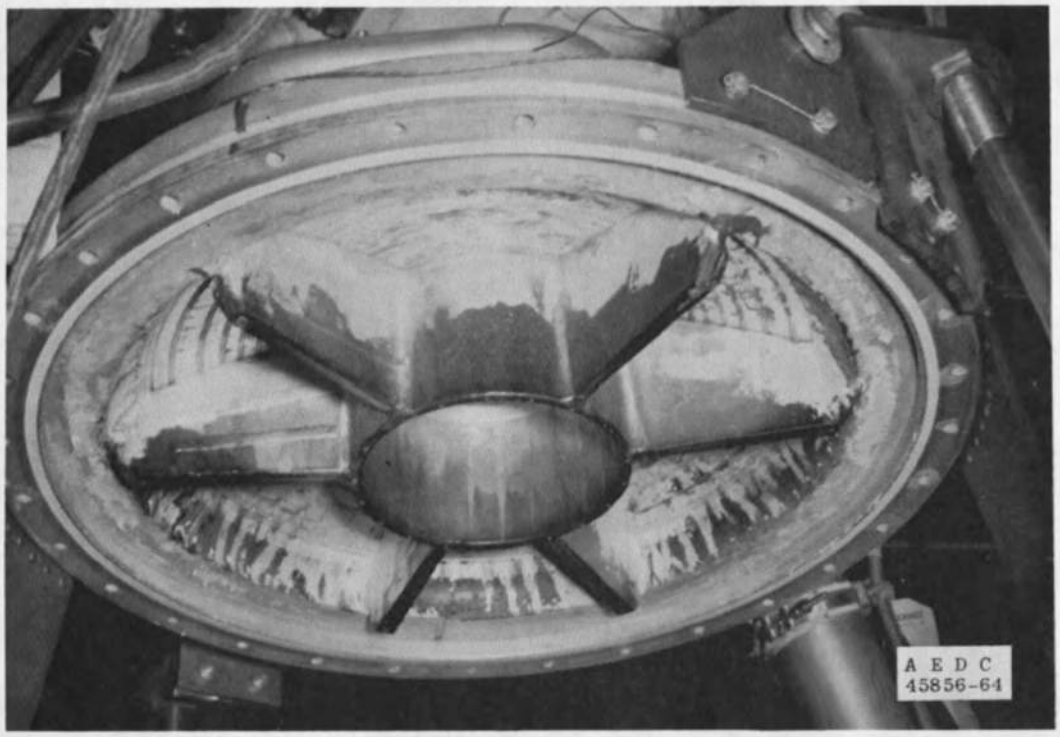

b. Three-Quarter View Looking Upstream

Fig. 31 Concluded

The second injector tested had a quadlet configuration with two oxidizer and two fuel orifices impinging. Three separate tests of 5, 8, and 15 sec were conducted with this injector; the last two were terminated early because of nozzle extension failures (see Section 2.1).

Four different injectors of the third configuration were tested as shown below:

Injector S/N	Test (Phase I)	Total Firing Time, sec
AF-29	A1-01, -02, -03	14
AFF-24	C-1 to C-14 A-03, -04, -05	1319
AFF-37	B-03, -04, -05	202
AFF-23	C-01, -02, -03, -04	1787

Injector S/N AF-29 failed during the last 4 sec of testing when a 120-deg segment of the outer oxidizer ring failed. Injector S/N AFF-24 performed satisfactorily during facility checkout firings (C-01 to C-14) and two engine development tests (A-03, -04). The last firing of test A-05 was terminated automatically by the combustion stability monitor (CSM) when a check valve burst in the thrust chamber valve actuator dump line. The injector had performed satisfactorily. Injector S/N AFF-37 performed satisfactorily during tests B-04 and B-05-1, -2, and -7, but during test B-05-3, combustion instability developed and the fuel header developed a crack before the test was terminated (Fig. 32). Extreme chamber ablation had resulted from the instability (Fig. 33). The CSM had not terminated the test because it has been set for ±150 g's and a minimum of 1000 Hz, whereas the instability conditions were 150 g's at a frequency of 760 Hz. The CSM was reset for subsequent tests to terminate when the vibration conditions exceeded ±60 g's and 600 Hz for over 0.040 sec.

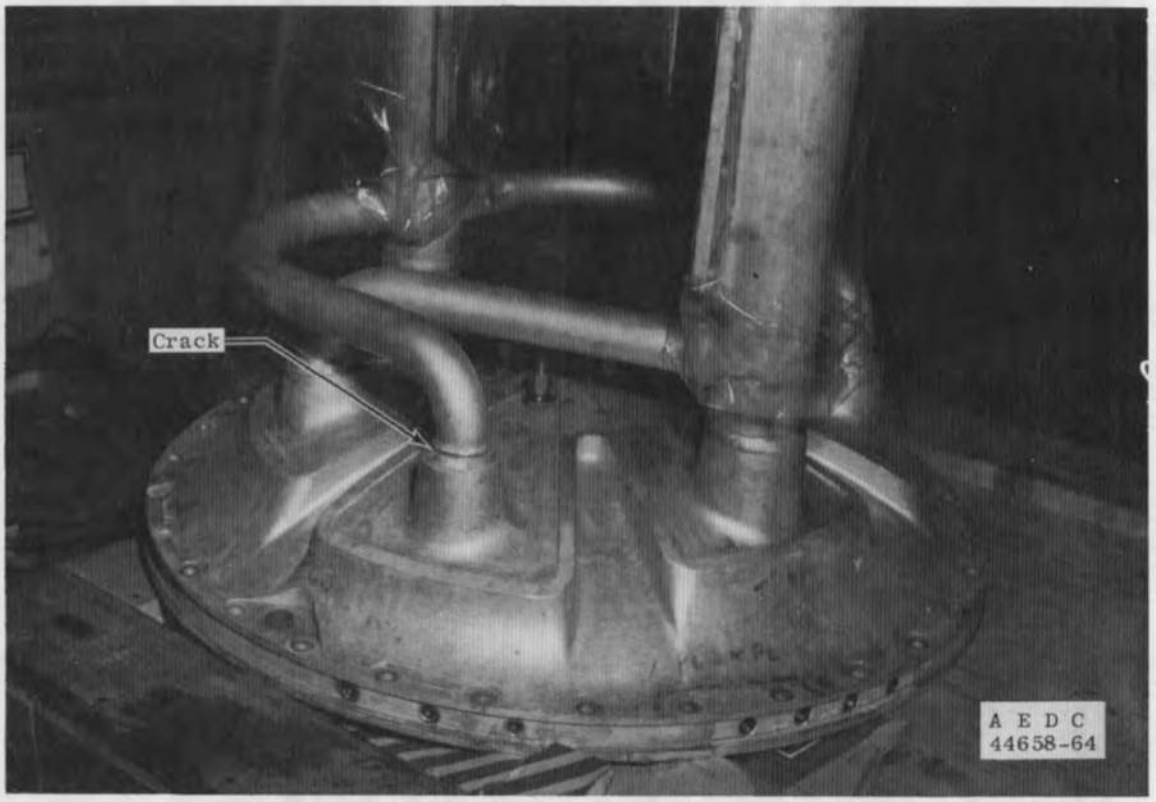

Fig. 32 Injector Fuel Header Failure, S/N AFF-37

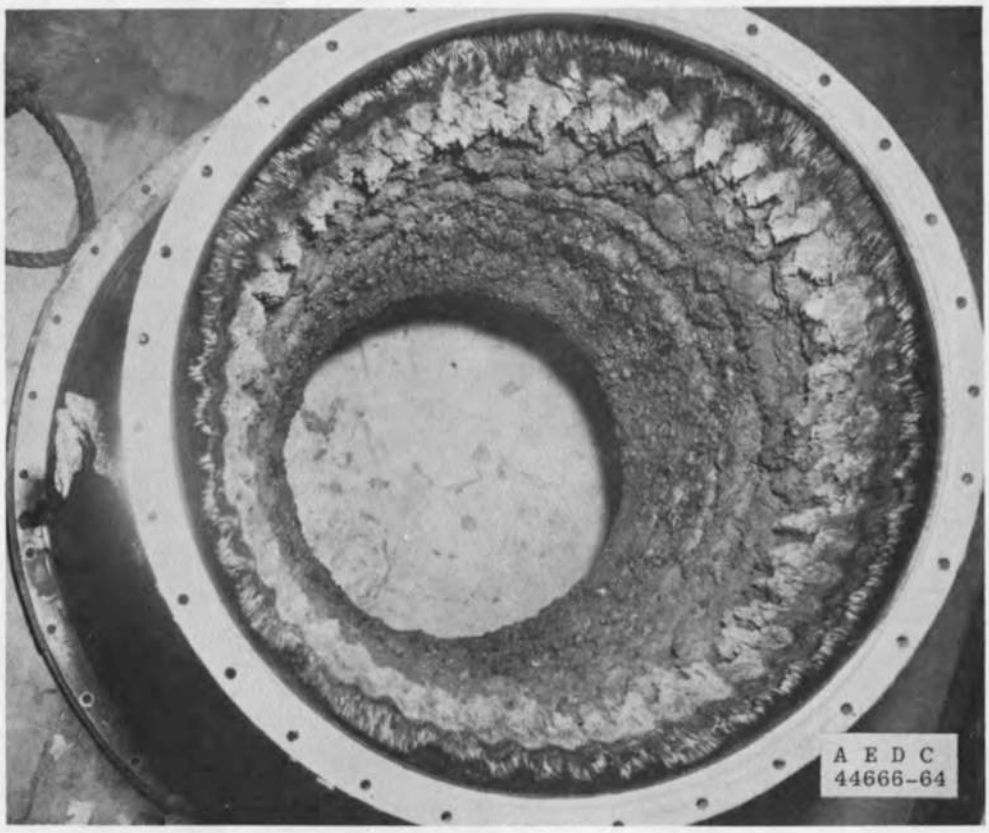

Fig. 33 Combustion Chamber Ablation and Melting

The last unbaffled doublet injector tested in Phase I was S/N AFF-23. At the completion of test C-01-1, an inspection showed that the injector was in good condition but that the chamber was severely eroded as shown in Fig. 34. This condition indicated an abnormal mixing pattern because this type of erosion was not present with the other injectors of this configuration. However, when this injector was tested again during tests C-03 (firings 1-21) and C-04 (firing 1-8), there was no evidence of chamber erosion; included was one firing of 635 sec (C-04-6). There was one CSM shutdown, 0.6 sec after ignition during firing C-04-4. No other difficulties were encountered.

The last injector tested in Phase I was the baffled doublet configuration, S/N BF-18 (Fig. 31). This injector was tested for a total of 379 sec in test series A-06 (7 firings), which included one firing of 260 sec. The injector performed satisfactorily with no CSM shutdowns. Postfire inspection revealed no abnormalities of the injector, but three longitudinal "streaks" occurred on the chamber wall, two of which extended to the throat (Fig. 35). These streaks were not in line with the baffles and were not attributed to the wake from the baffles.

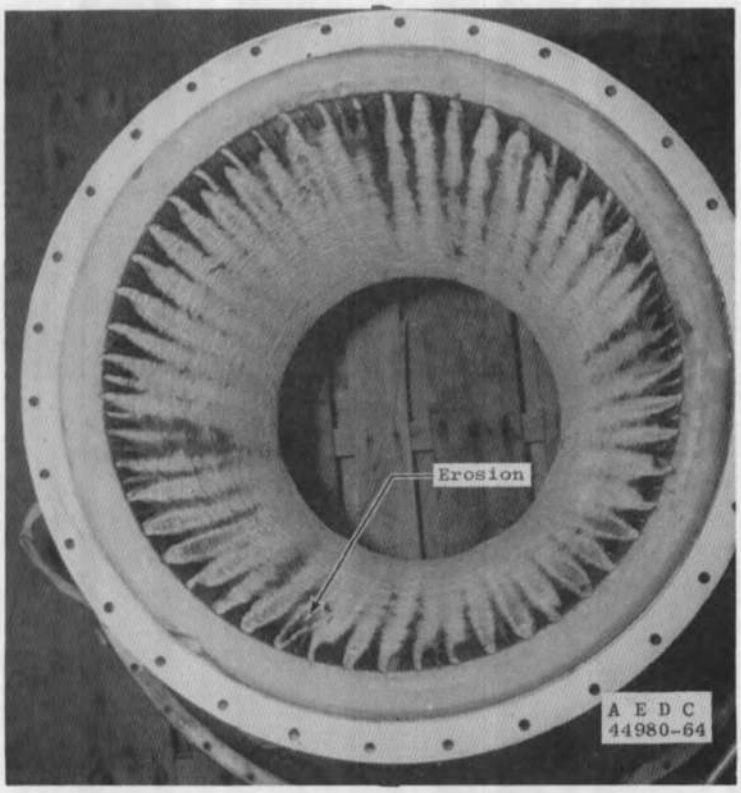

Fig. 34 Combustion Chomber Domage on Engine Assembly No. 2

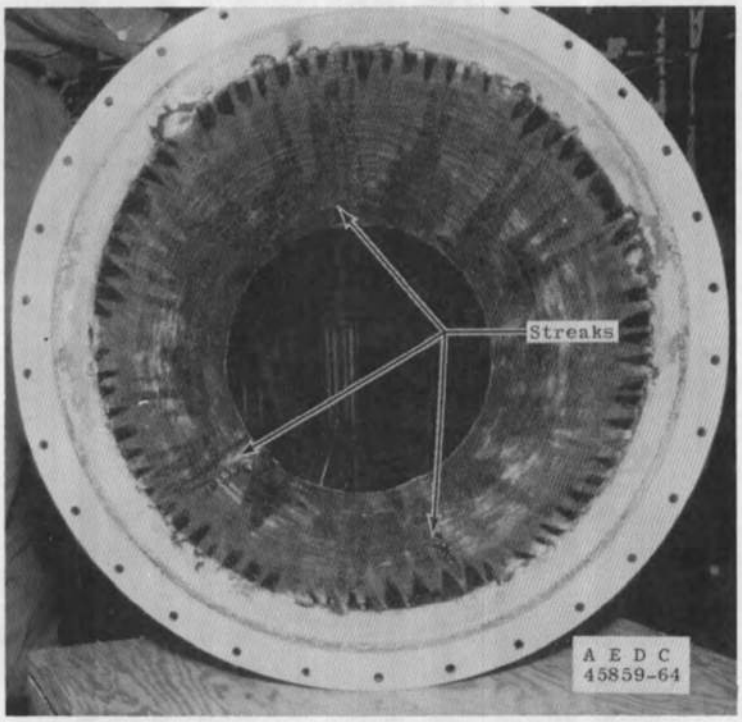

Fig. 35 Postfiring View of Combustion Chomber Used during Series A-06, S/N A-1

2.3.2 Phase II

During Phase II, five different injectors were used; all were the doublet impingement type; one was unbaffled, and the other four were baffled. The unbaffled injector was similar to those of Phase I, but the baffled type had five radial baffles instead of six, as used previously (Fig. 36).

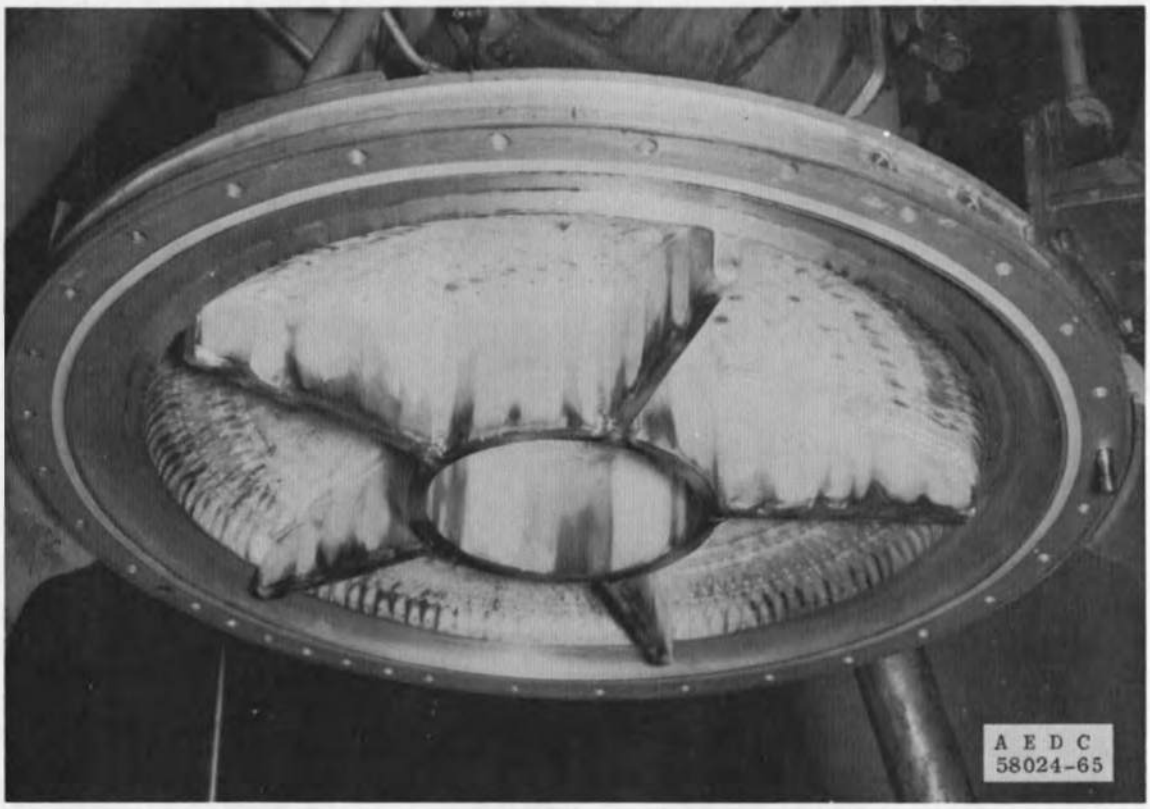

Fig. 36 Baffled Injector

The unbaffled injector (S/N AFF-78) was used in test periods A through F and performed satisfactorily with the exception of three tests which were terminated by the CSM. To eliminate the combustion instability problem, baffled injectors were introduced and were used for the remaining tests in Phases II, III, IV, and V. The baffles on these injectors were regeneratively cooled, using fuel as the coolant; the fuel was routed back to the injection ring passages and was not discharged directly from the baffles, except for the baffle tip weep holes. The baffled injector S/N's, the test numbers, and the total accumulated firing times were:

Injector, S/N	Test Period	Accumulated Firing Time, sec
AF-46	G, H, I, J, K, R, S	888
-47	L, P, Q	1011
-91	M, N	756
-64	T, U, V, W	1267

These injectors performed satisfactorily with the exception of S/N 91 which developed a crack in a weld adjacent to the cylindrical baffle (Fig. 37). This condition had been anticipated by AGC, and corrective measures were taken with the welding process. The baffled injectors caused no CSM shutdown during this phase. To induce combustion instability and document the suppression ability of the injector, a pulse charge (bomb) was placed on the injector face prior to each test period. The pulse charge was a No. 8 blasting cap plus 2.46 gm of C-4-type explosive in a Teflon® holder, which was screwed into the center of the injector face (Fig. 38). The pulse charge was located about 6 in. downstream of the injector face, and charge ignition was by combustion heat. A typical firing thrust/time history, showing the detonation and recovery of the thrust to normal, is shown in Fig. 39.

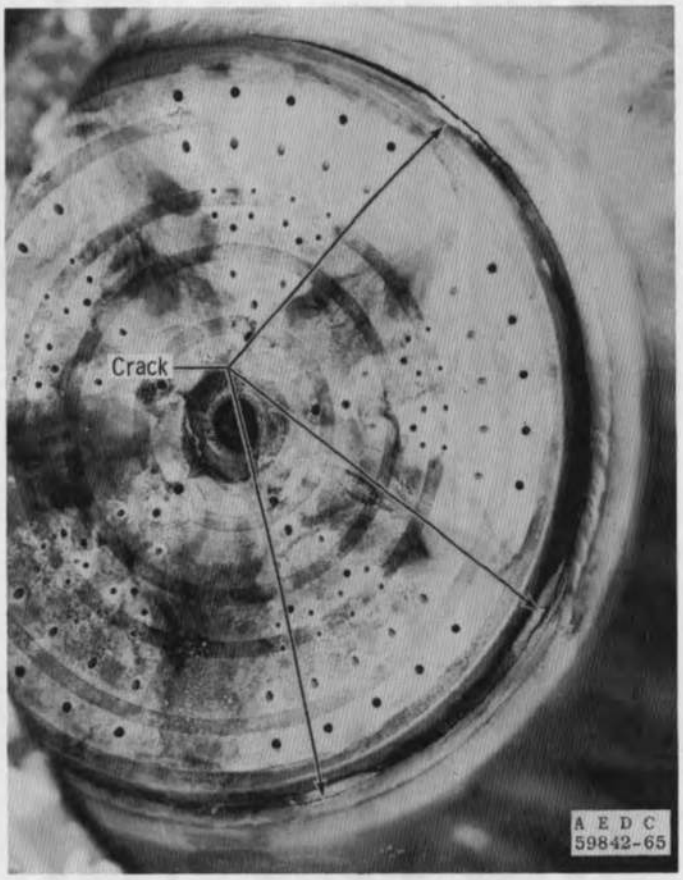

Fig. 37 Engine S/N 11A Injector, Postfire

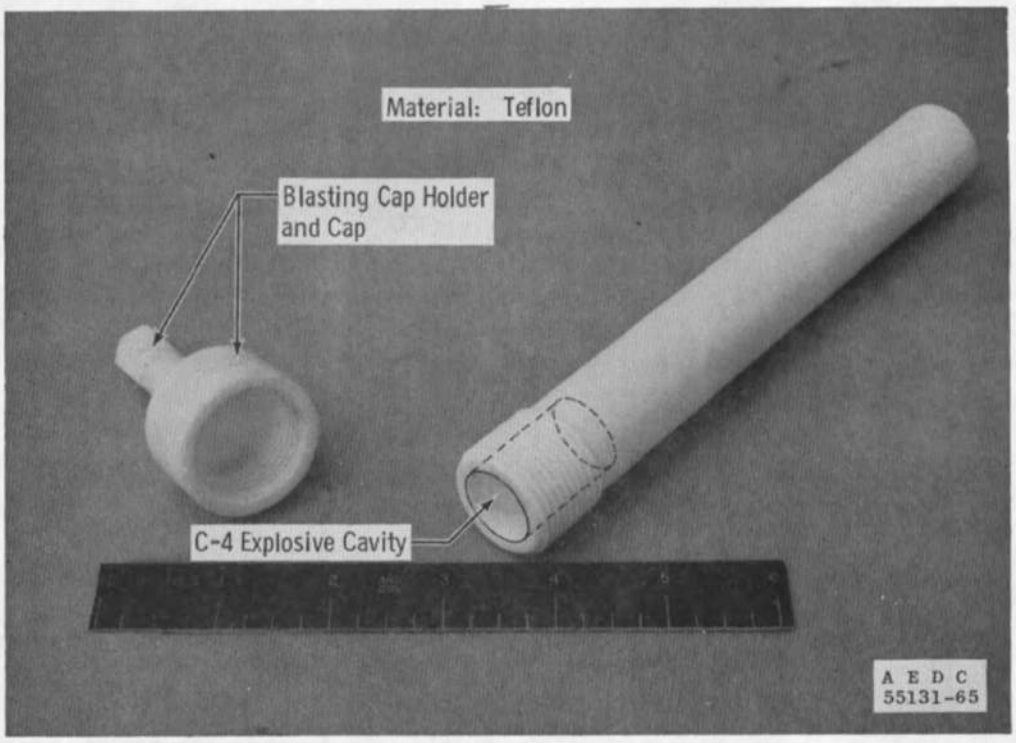

a. Holder Disassembled

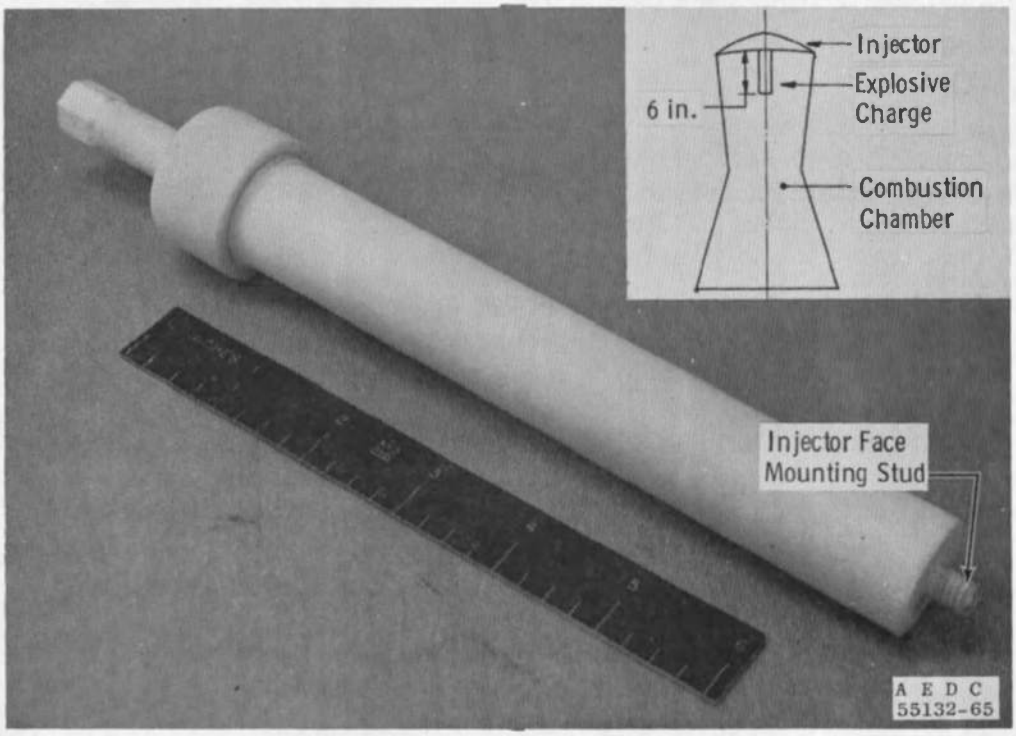

b. Holder Assembled

Fig. 38 Pulse Charge Container

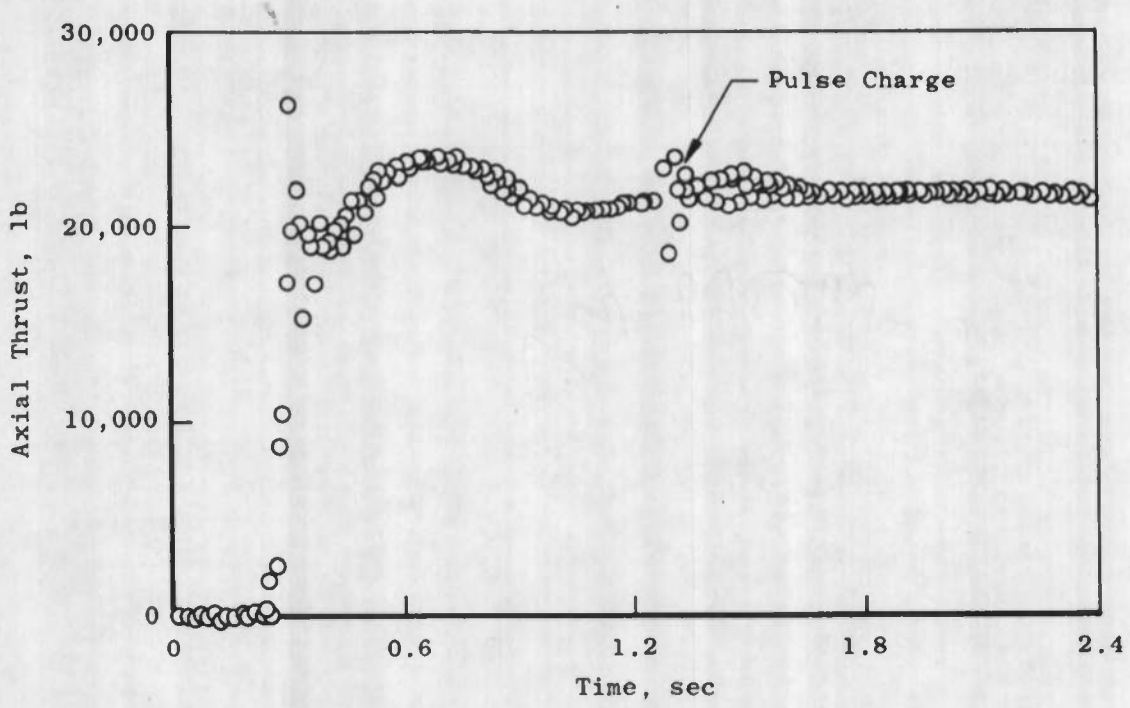

Fig. 39 Typical Pulse Charge Detonation and Recovery (Phase II, M-16)

2.2.3 Phase III

Four injectors were tested during nine Phase III test periods. The injector S/N's, test periods, the total accumulated firing time, and the termination criteria or "kill limits" for the CSM were:

Injector S/N	Test Period	Total Accumulated Firing Time, sec	CSM Limits: Peak-to-Peak Acceleration, g	CSM Limits: Frequency, Hz	CSM Limits: Time Interval, sec
65	CA	507	120	600 to 7000	0.040
65	CB	505	↓	↓	↓
82	CC	509	↓	↓	↓
82	CD	505	180	↓	0.060
82	CE	602	↓	↓	0.080
82	CF	150	↓	↓	↓
94	CG	604	↓	↓	↓
94	CH	152	↓	↓	↓
71	CI	690	↓	↓	↓

All injectors performed satisfactorily with only two engine shutdowns by the CSM (CC-13, CC-15). Engine vibration data showed that the combustion irregularity, which was commonly characteristic of the ignition transient, was satisfactorily dissipating at the instant of CSM triggering during these tests. In each case, combustion had returned to normal shortly after CSM triggering and before bipropellant valve activation. Therefore, the acceleration level and duration criteria for shutdown were extended to preclude further unnecessary terminations.

2.3.4 Phase IV

Block II development testing was initiated with Phase IV for the primary purpose of increasing performance. The mixture ratio was changed from 2.0 to 1.6, but the configuration of the injector remained the same. Five injectors were tested before the design of the Block II injector was finalized. The test numbers and the firing durations were:

Injector S/N	Test	Firing Duration, sec
97	DA 1-24	808
73	DB 1-28	748
	DC 1-4	602
110	DD 1-17	755
	DE 1-15	757
93	DF 1-15	760
	DG 1-14	752
105	DH 1-11	758
	DI 1-14	755

The initial injectors (S/N 97 and 73) showed evidence of a severe chamber compatibility (erosion) problem at the higher performance levels. Prior testing at AGC had indicated the existence of a chamber erosion problem at the injector baffle areas, which this altitude testing confirmed. The erosion in the injector baffle area was attributed to a low pressure area in the corners, between the baffle tips and the chamber wall. Resulting combustion cross-flow disrupted the fuel coolant film. Figure 40 indicates an apparent change in flow direction. To prevent this change in direction of fuel coolant flow, three propellant orifices were added to the next injector (S/N 73) on each side of the radial baffles (one additional doublet and one fuel cooling orifice) for a total of 30 holes. The test of this configuration revealed that the erosion problem still existed (see Fig. 41) but that the fuel coolant flow was not disrupted as before because the temperatures were lower at the injector/chamber interface. For the second test period with this injector (period DC,

injector S/N 73), a chamber with a modified fabrication process was used. With the exception of two blisters, the chamber condition after testing was quite good. The next injector tested (S/N 110), although of similar construction, did exhibit some spontaneous combustion irregularities (called "pops"). Injector S/N 93 was the same as those previously tested except the injector baffle chord was lengthened at the outer radius from 2 to 4 in. (see Fig. 42). This injector also produced combustion pops and developed a cracked weld at the juncture of the radial baffle and the cylindrical hub. The final injector of this phase (S/N 105) had all the oxidizer orifices and selected fuel orifices counterbored (Fig. 42c) to reduce the orifice L/D ratio and to stabilize the injected streams. No combustion pops were observed with this injector configuration (long baffles and counterbored orifices), which became the Block II design and was used for the Phase V and VI qualification testing.

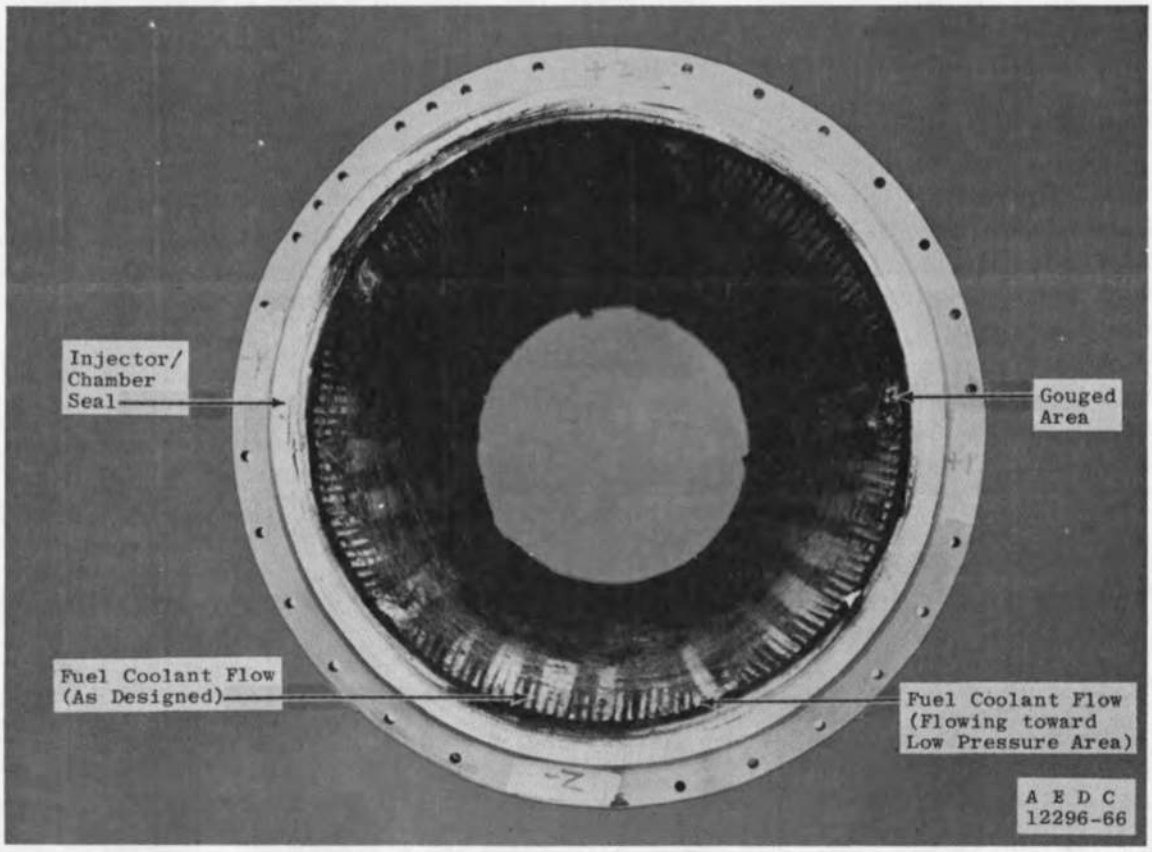

Fig. 40 Postfire Chamber S/N 260

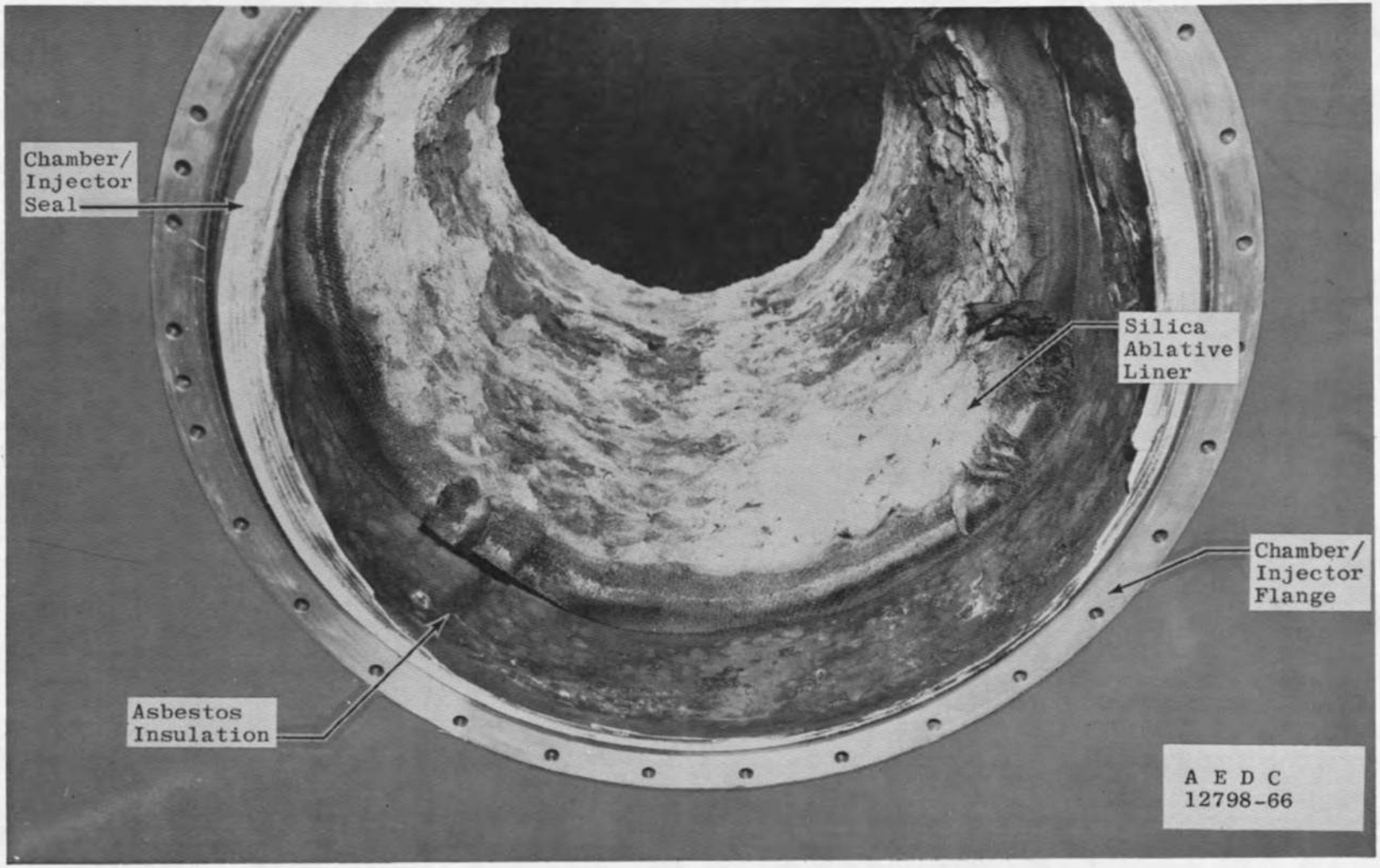

Fig. 41 Postfire Chamber S/N 261

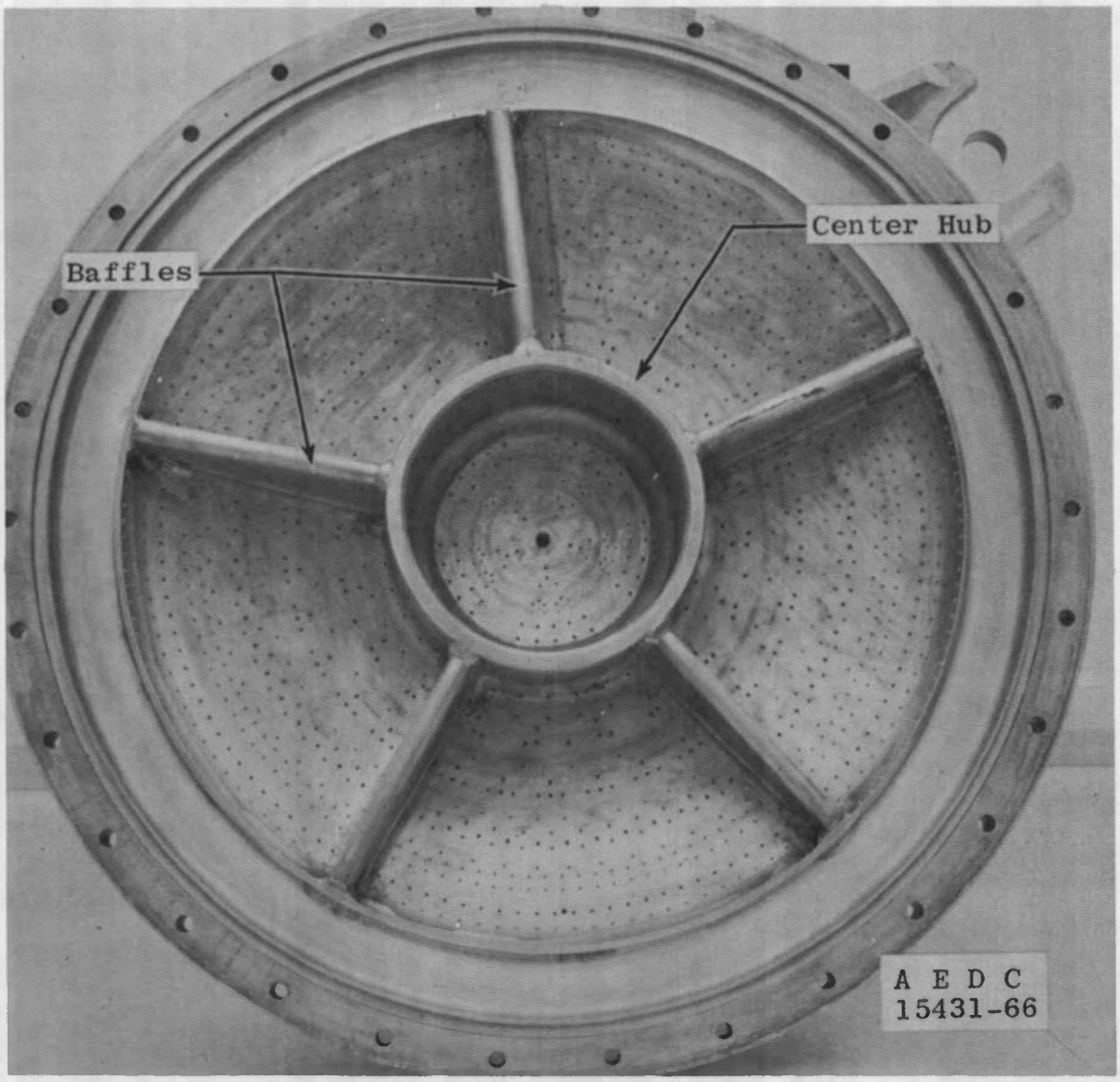

a. Injector Face

Fig. 42 Baffled Injector

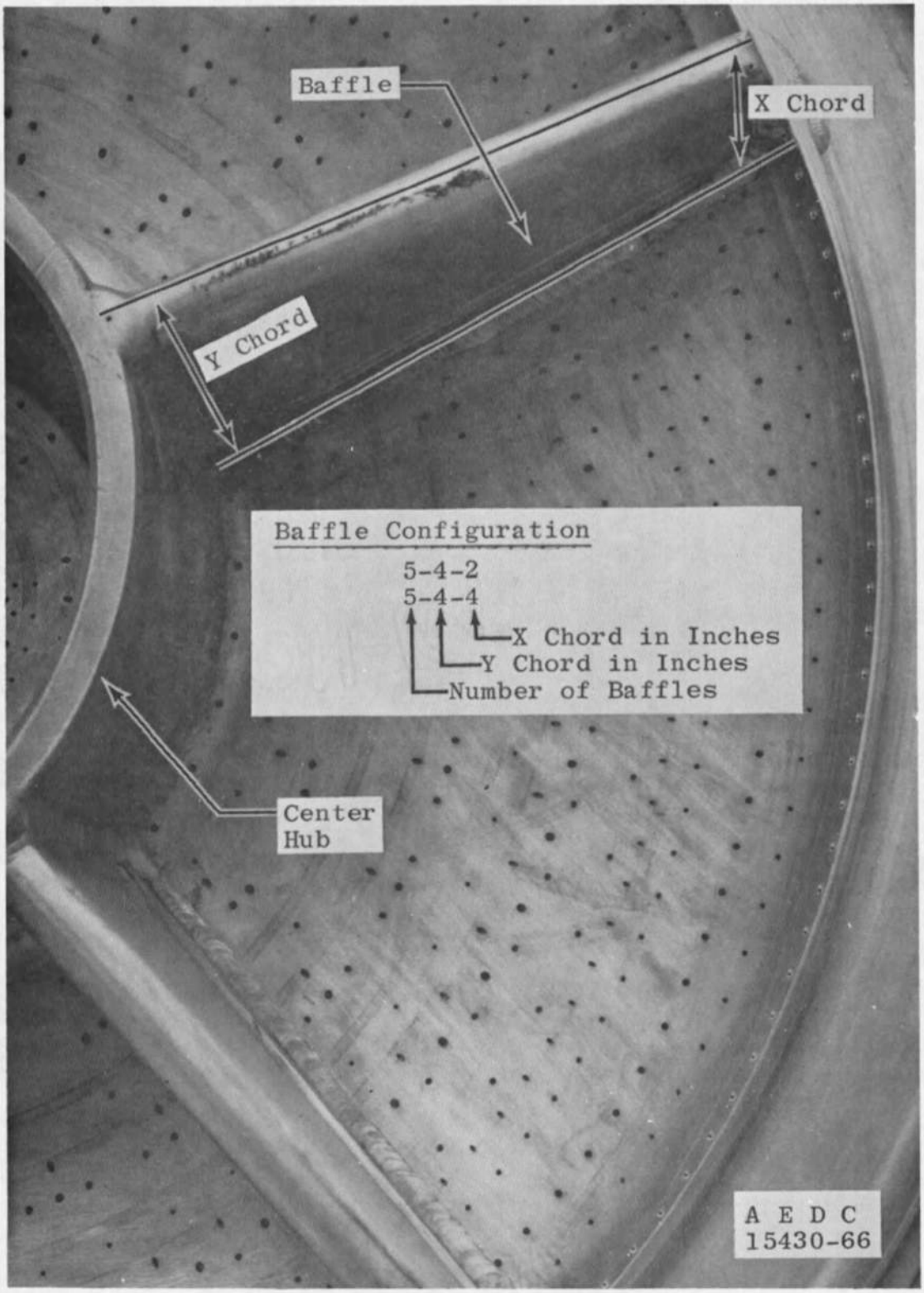

b. Baffle Configuration

Fig. 42 Continued

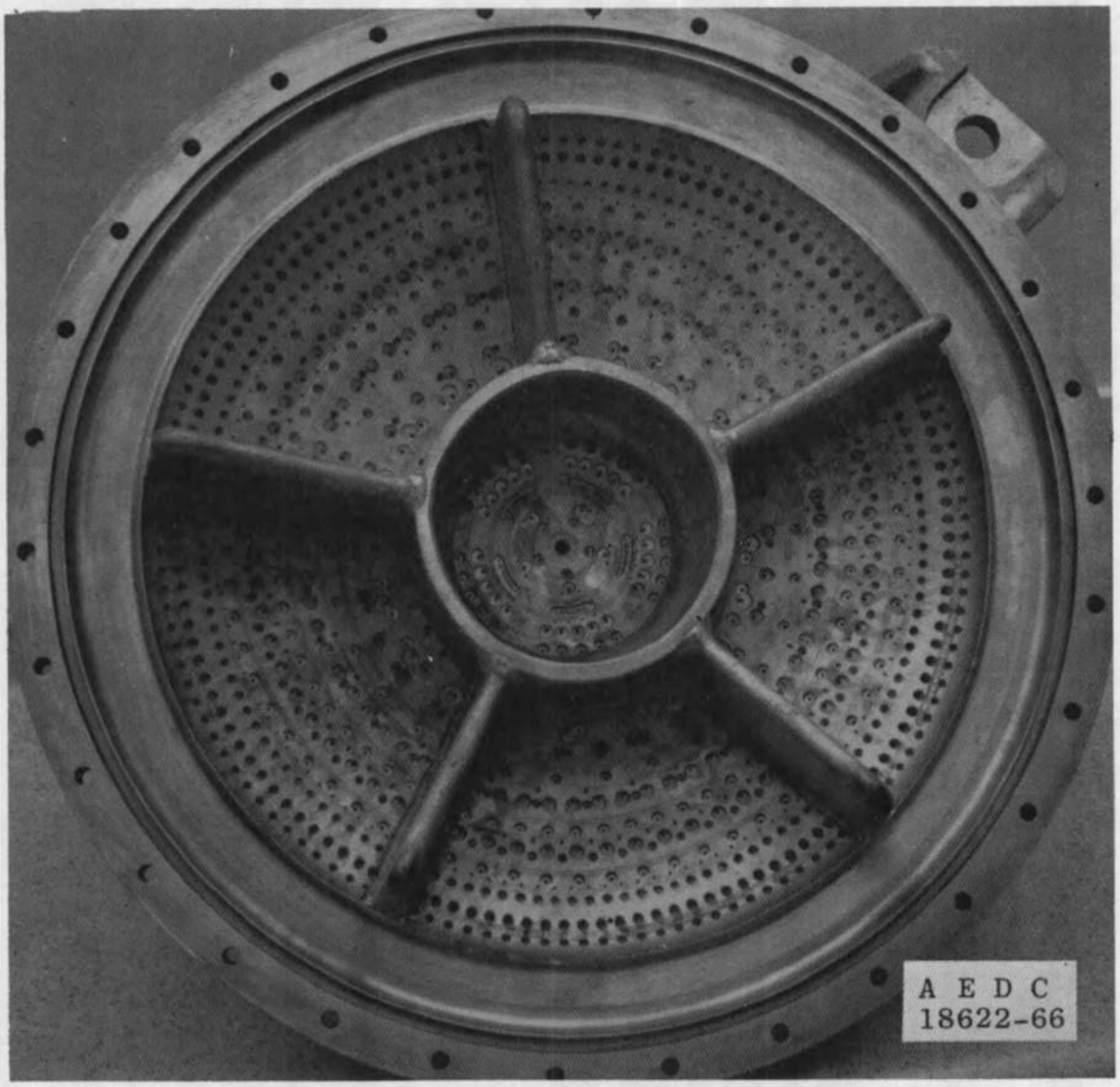

c. Counterbored Injector S/N 105
Fig. 42 Concluded

2.3.5 Phase V

During qualification testing, three injectors were used:

Injector S/N	Test	Total Firing Duration, sec
104	EA 1-12	754
	EB 1-12	753
115	EC 1-12	754
	ED 1-12	754
103	EE 1-12	754
	EF 1-12	754

All injectors performed satisfactorily. There was no evidence of combustion pops, the chamber compatibility was good, and there was little ablation evident when comparing prefire and postfire conditions of the chamber interiors (Fig. 43).

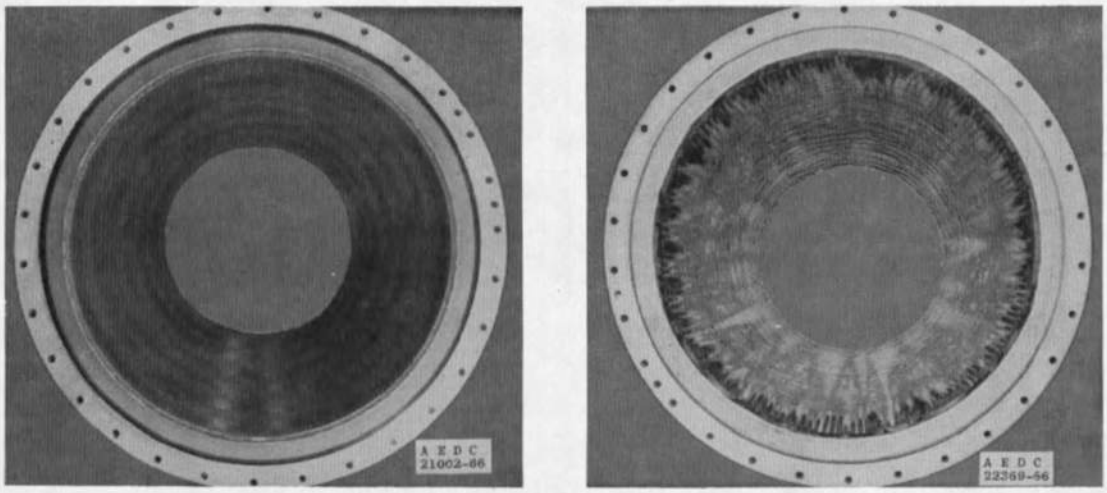

a. Prefire b. Postfire

Fig. 43 Typical Combustion Chamber

2.3.6 Phase VI

During qualification and research testing, three injectors were used:

Injector S/N	Test Periods	Total Firing Duration, sec
104	FA to FD	827
94	FE to FL, FP to FQ	959
98	FM to FO	62

Injector operation, performance, and chamber compatibility were satisfactory. During the research testing of the ignition characteristics of injector S/N 98, some of the oxidizer injection ports were damaged in the center hub section as shown in Fig. 44. The cause of the damage was not identified; a careful survey of the data did not reveal any unusual occurrences which would have caused such damage. The orifice deformation had no noticeable effect on engine performance and operation.

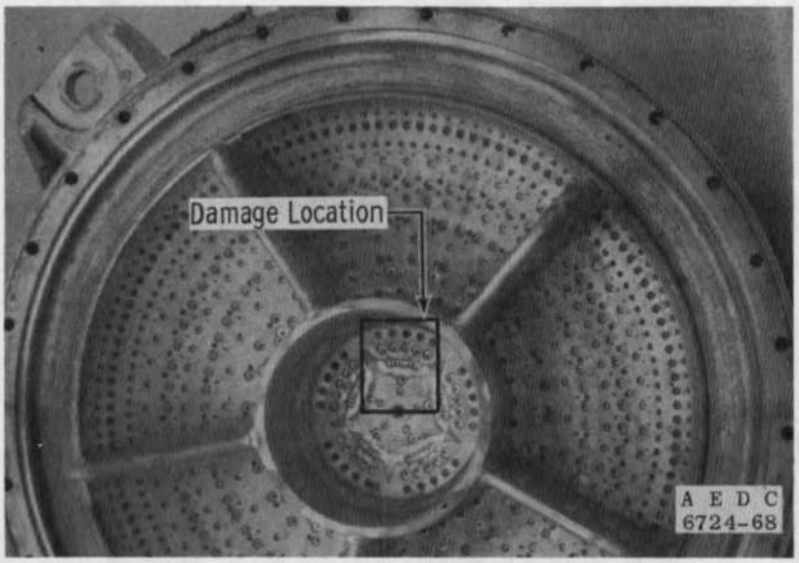

a. Area of Damage

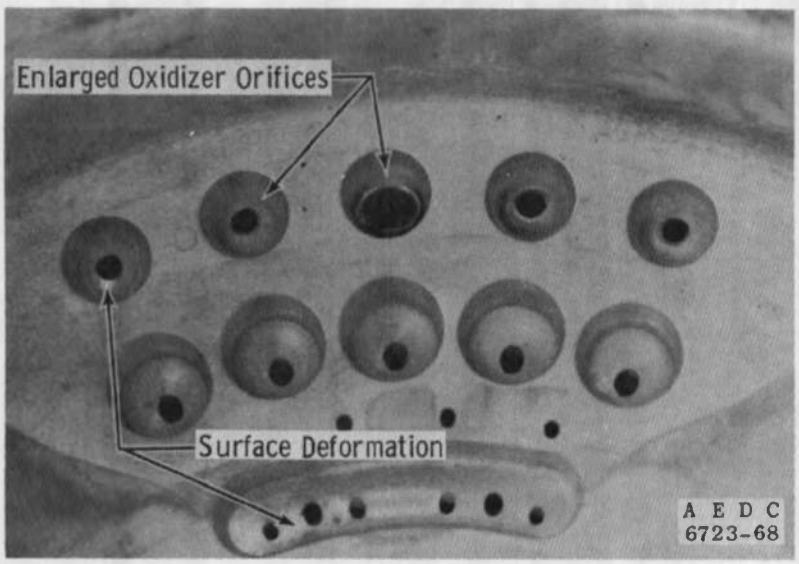

b. Close-Up View

Fig. 44 Injector Damage after Ignition Testing, Phase VI

2.4 BIPROPELLANT VALVE

During testing of the Apollo Service Module engine at AEDC, two different flight-type bipropellant thrust chamber valve (TCV) configurations were used. The only difference was in the method of actuation; the first configuration used was actuated by fuel pressure, and the second was actuated by pneumatic pressure. Each of the two configurations consisted of a dual-passage arrangement for both the oxidizer and the fuel flow valves (Fig. 45). Each of these propellant valve assemblies contained eight ball valves, four each in the fuel and the oxidizer sides arranged in a parallel-series configuration. Each of four pressure-driven actuators operated one fuel and one oxidizer ball valve. Each of two electrical solenoid pilot valves operated a pair of actuators. Half of the operating components comprised a bank which consisted of one pilot valve, two actuators, and the associated four ball valves. The banks were identified as A and B. Either bank A or B or both could be used to fire or shut down the engine. This redundancy was to provide control of engine operation in the event of a failure of either bank.

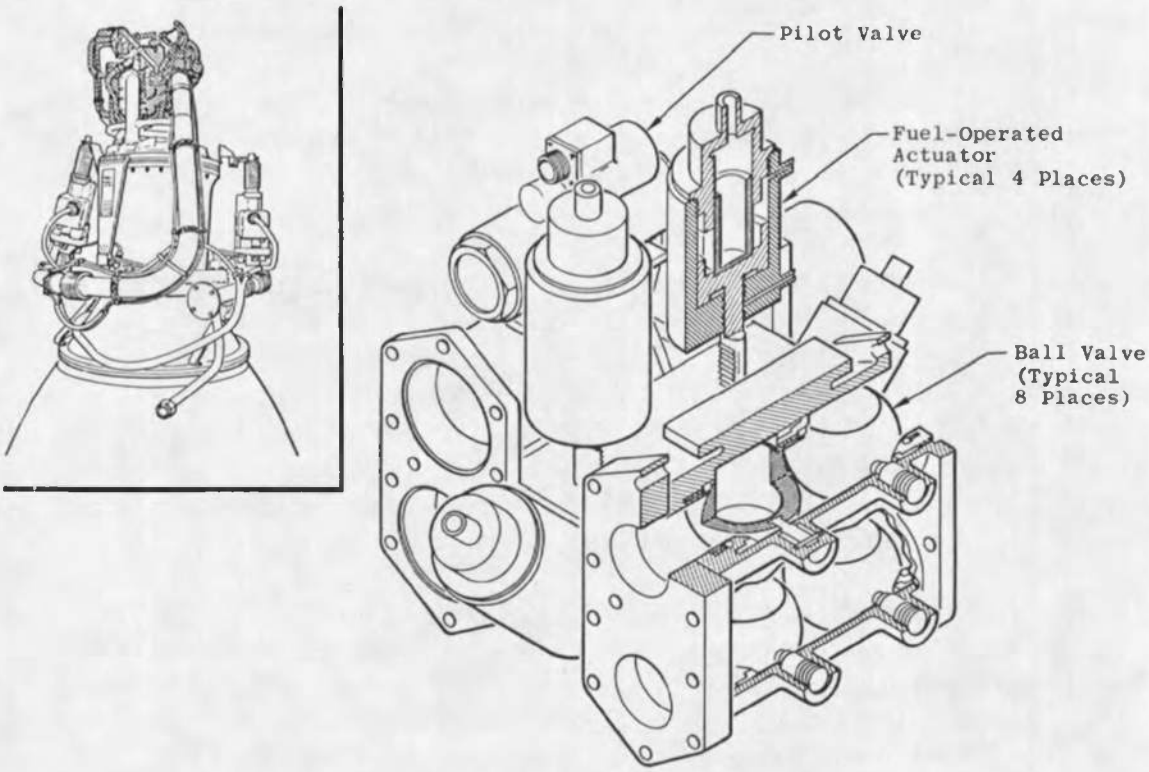

Fig. 45 Thrust Chamber Valve Cutaway

The first TCV valve configuration, which was used throughout Phase I and through the N test period of Phase II, was the fuel pressure actuation type (Fig. 46).

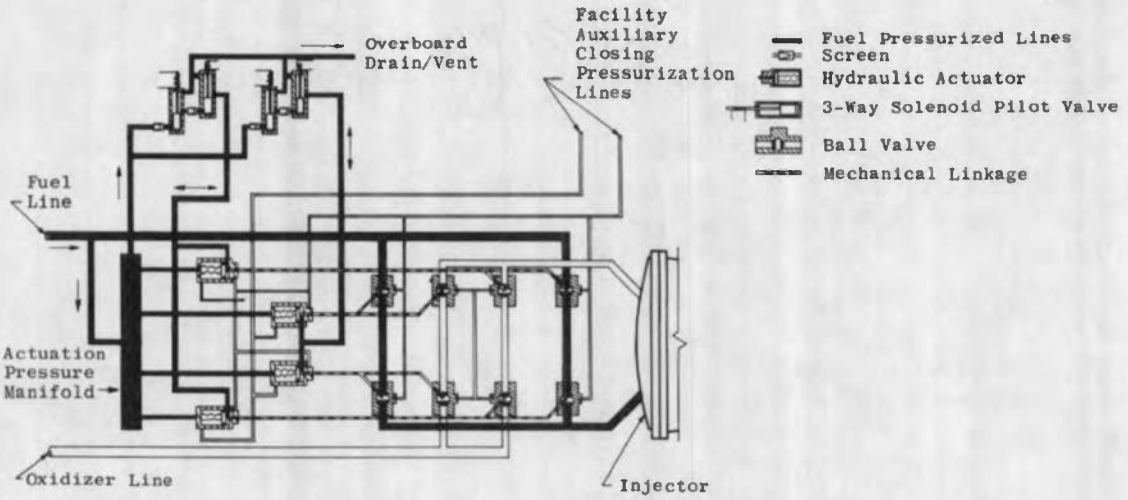

Fig. 46 Fuel Pressure Actuated Thrust Chamber Valve Schematic

Because occasional difficulties were encountered with the valve closing, an auxiliary gas-operated valve closing system was installed for ground tests at AEDC. Problems with this valve configuration were primarily with the pilot valves which stuck in intermediate positions.

The second TCV configuration, used from the beginning of test period P of Phase II through Phase VI, was opened by pneumatic pressure supplied from engine-mounted gaseous nitrogen storage spheres. The spheres were charged to 2500 psia, and the pressure to the actuators was regulated to approximately 220 psia (Fig. 47). For Phases IV and V, the actuator spring force and the regulated nitrogen pressure were increased to shorten actuation time for improved repeatability of starting and shutdown transient impulse (see Section 3.2).

Difficulties were experienced intermittently with these TCV's. The main problem was leakage past the ball valve seals in excess of the maximum specification value of 400 standard cc/hr. During the first half of Phase V (Tests EA through EC), ball seals of white Teflon (TFE) were used; during the later half, Teflon Floura Blue® (BF-1) seals were installed. Neither type of seal was completely satisfactory.

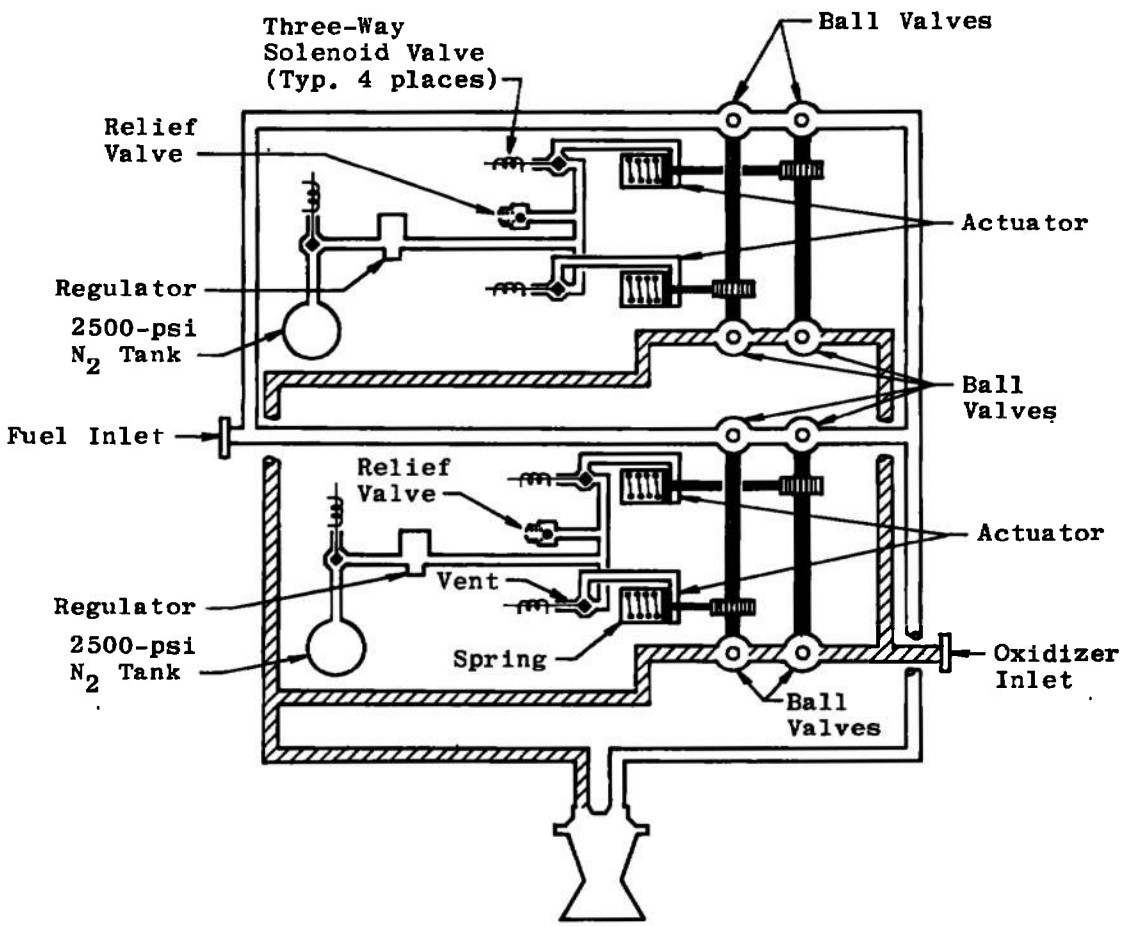

Fig. 47 Pneumatically Actuated Thrust Chamber Valve

Phase VI was instituted as a penalty qualification for the TCV, and three TCV assemblies with design variations (as shown below) were tested.

TCV Model	Test Period	Primary Design Changes
Mod I-C	FA-FD	Upstream ball seals added; seal material changed to glass-filled TFE; seal spring cartridge changed to greater number of springs with lower individual spring constant; one-piece ball shafts replaced two-piece stub shafts.
Mod I-D	FK-FL	Seal material changed to glass-filled BF-1; spring cartridge changed; oxidizer ball shaft seals and shaft drain manifolds changed; actuator shaft roller changed from Delrin® to CRES; gearbox tie bolts made hollow for vents.
Mod I-E	FP-FQ	Actuator piston changed from Delrin to aluminum; actuator O-ring design changed; fuel ball shaft seals and drain manifold seals changed.

The Mod-IC design was more durable than the Phase V TCV had been, but still developed excessive ball seal leaks and shaft seal leaks (Ref. 14). The Mod-ID glass-filled BF-1 ball seals and oxidizer ball shaft seals were fairly satisfactory; this valve revealed a differential thermal expansion problem in the actuator which produced excessive GN_2 leakage. The Mod I-E valve had some further shaft seal changes which remedied the shaft seal leakage tendency. This valve developed only one ball seal leak which exceeded the specification limit (Ref. 16). The one leak was caused by a peculiarly damaged seal which could not be related to valve operation or malfunction; therefore, the Mod I-E TCV was determined to be qualified satisfactorily. The pretest and posttest ball seal and shaft seal leakage rates for the Mod I-C, Mod I-D, and Mod I-E TCV qualification tests are presented in Tables II through IV.

TABLE II
MOD I-C BIPROPELLANT VALVE (S/N 128) LEAKAGE RATES

Seal Identification	Specified Leakage Limit, cc/hr	Pretest Leakage, cc/hr				Posttest Leakage, cc/hr			
		2-5 psig	100-105 psig	200-205 psig	2-5 psig	2-5 psig	100-105 psig	200-205 psig	2-5 psig
Downstream Seals									
Fuel Ball 1	150	0	0	0	0	0	0	0	0
Fuel Ball 2	150	0	0	0	0	0	0	0	0
Fuel Ball 3	150	10	50	0	0	0	0	0	0
Fuel Ball 4	150	0	0	0	0	0	0	0	0
Oxidizer Ball 1	150	0	0	0	0	0	7,200	32,400	0
Oxidizer Ball 2	150	0	0	0	0	0	0	0	0
Oxidizer Ball 3	150	5	0	0	0	0	0	0	0
Oxidizer Ball 4	150	0	0	0	0	0	0	0	0
Upstream Seals									
Fuel Ball 1	150	0	0	0	0	0	0	5	0
Fuel Ball 2	150	5	0	2.5	0	5	0	0	3
Fuel Ball 3	150	0	5	12.5	0	7.5	0	2.5	2.5
Fuel Ball 4	150	1	25	50	2.5	5	0	5	0
Oxidizer Ball 1	150	0	0	0	0	0	0	510	0
Oxidizer Ball 2	150	0	37.5	60	0	0	28	500	0
Oxidizer Ball 3	150	0	0	0	0	0	0	0	0
Oxidizer Ball 4	150	0	240	140	5	0	45	900	0
Shaft Seals (valve closed)									
Fuel Balls 1 + 4	20	0	0	0	0	0	0	0	0
Fuel Balls 2 + 3	40	0	0	0	0	0	0	0	0
Oxidizer Balls 1 + 4	40	0	0	22.5	0	14,200	10,800	4,800	450
Oxidizer Balls 2 + 3	20	0	0	0	0	0	0	0	0
(valve open)		2-5 psig	70-72 psig		2-5 psig	2-5 psig	70-72 psig		2-5 psig
Fuel, all	40	0	0		0	0	0		0
Oxidizer, all	40	2.5	0		0	17,280	34,200		17,960

Leakage determined with GN_2

TABLE III
MOD I-D BIPROPELLANT VALVE (S/N 122) LEAKAGE RATES

Ball Seals	Specification Leakage Limit (Ref. 16), cc/hr	Pretest Leakage, cc/hr Differential Pressure, psi				Posttest Leakage, cc/hr Differential Pressure, psi			
		2 to 5	100 to 105	200 to 205	2 to 5	2 to 5	100 to 105	200 to 205	2 to 5
Upper Fuel Bore	Prefire - For the two seals on each ball, one may leak up to 300 cc/hr and the other up to 5000 cc/hr. Postfire - For the two seals on each ball, one may leak up to 400 cc/hr and the other up to 10,000 cc/hr.								
1		0	0	0	0	0	342	600	0
2		0	15	10	5	0	0	0	0
3		0	0	0	0	0	0	0	0
4		0	7.5	4.0	0	0	0	0	0
Lower Fuel Bore									
1		0	0	4.0	0	0	600	389	0
2		0	0	0	0	0	0	0	0
3		0	5.0	0	0	0	0	0	0
4		0	0	0	0	0	0	0	0
Upper Oxidizer Bore									
1		0	0	2.0	0	5	45	10	25
2		0	5.0	10.0	0	25	200	600	80
3		0	0	0	0	0	62.5	212	0
4		0	5.0	2.5	0	0	50	42.5	2.5
Lower Oxidizer Bore									
1		11.0	30.0	5.0	5.0	5	243	330	0
2		0	0	0	0	5	130	130	15
3		0	5.0	5.0	0	0	3	2.5	0
4		0	0	0	0	12.5	5148	9000	21.5
Shaft Seals (Valve Closed)									
Fuel 1 and 4	20	0	0	0	0	0	0	0	0
2 and 3	40	0	0	0	0	0	0	0	0
Oxidizer 1 and 4	40	0	0	0	0	0	0	2.5	0
2 and 3	20	0	0	0	0	0	0	5.0	0
(Valve Open)			(10 psig)				(70 ± 2 psig)		
Fuel, All	40	0	0	-	0	0	0	-	0
Oxidizer, All	40	0	0	-	0	0	0	-	0

TABLE IV
MOD I-E BIPROPELLANT VALVE (S/N 126) LEAKAGE RATES

Ball Seals	Specification Leakage Limit (Ref. 16), cc/hr	Pretest Leakage, cc/hr				Posttest Leakage, cc/hr			
		Differential Pressure, psi				Differential Pressure, psi			
		2 to 5	100 to 105	200 to 205	2 to 5	2 to 5	100 to 105	200 to 205	2 to 5
Upper Fuel Bore	Prefire - For the two seals on each ball, one may leak up to 300 cc/hr and the other up to 5000 cc/hr. Postfire - For the two seals on each ball, one may leak up to 400 cc/hr and the other up to 10,000 cc/hr.								
1		0	0	0	0	4	8	5	1
2		0	0	0	0	9	263	450	9
3		0	0	0	0	0	18	8	0
4		0	0	0	0	0	1	3	0
Lower Fuel Bore									
1		8	5	2	1	0	11	23	0
2		0	0	0	0	10	368	960	10
3		6	23	15	8	5	45	44	5
4		0	0	5	0	0	9	14	0
Upper Oxidizer Bore									
1		3	5	0	0	11	400	1390	134
2		0	20	35	1	0	0	0	0
3		2	23	35	1	1500	26,400	48,900	1320
4		0	25	41	0	0	0	0	0
Lower Oxidizer Bore									
1		0	0	0	0	100	2400	2250	93
2		0	26	50	0	9	16	49	4
3		0	0	0	0	3	5	1	5
4		0	20	25	0	42	720	1680	25
Shaft Seals (Valve Closed)									
Fuel - 1 and 4	20	0	0	0	0	0	0	0	0
2 and 3	40	0	0	0	0	0	0	0	0
Oxidizer -									
1 and 4	40	0	0	0	0	0	0	0	0
2 and 3	20	0	0	0	0	0	0	0	0
(Valve Open)									
Fuel - All	40	0	0	0	0	0	0	0	0
Oxidizer - All	40	0	0	8	3	0	0	5	0

SECTION III
BALLISTIC PERFORMANCE DEVELOPMENT

3.1 OVERALL ENGINE PERFORMANCE

The overall engine performance (vacuum specific impulse, $I_{sp_{vac}}$) data for the early Block I engine development testing of Phase I (reported in Refs. 1 through 6) were adjusted for this report as described below. Phase I testing was conducted prior to installation of the flowmeter calibration system in test cell J-3. Therefore, the propellant flowmeter constants used in reducing the original Phase I data were obtained from straight pipe laboratory calibrations using water. For the purpose of this report, the assumption was made that the difference between a water and a propellant calibration was the same in a straight pipe as in the propellant line configuration. This is not entirely correct; however, it improved the Phase I data sufficiently to permit comparison with later data. The magnitude of the change in flowmeter calibration constant, between that obtained with the flowmeters calibrated in propellant and a calibration using water, was determined after installation of the in-place flowmeter calibration system. These changes were +0.94 and +1.99 percent for fuel and oxidizer, respectively, when both calibrations were conducted in place with propellant. These corrections were applied to the available Phase I $I_{sp_{vac}}$ data from three test periods using unbaffled doublet injectors. Although the corrected $I_{sp_{vac}}$ data still show some scatter (Fig. 48), the average $I_{sp_{vac}}$ at a mixture ratio of 2.0 is approximately 308 lb_f-sec/lb_m which compares closely with the 308.8 lb_f-sec/lb_m obtained during the first Phase II testing using an injector of the same design and propellant flowmeter constants obtained with propellants (Ref. 17).

The baffled-type injector was adopted for later Phase II testing because of the better combustion stability which had been demonstrated in Phase I, and in sea-level firings by the engine manufacturer. The engine demonstrated improved combustion stability as evidenced by the absence of valid CSM shutdowns even when pressure pulse bombs were employed to excite injector flow and combustion oscillations. Also, the engine performance was somewhat improved with this injector as shown in Fig. 49a; an $I_{sp_{vac}}$ of about 311.3 lb_f/lb_m/sec was obtained at the design mixture ratio of 2.0. The engine was qualified in Phase III with an average specific impulse level of about 312 lb_f/lb_m/sec (Fig. 49b); this was still considered inadequate for flights beyond the earth orbiting missions.

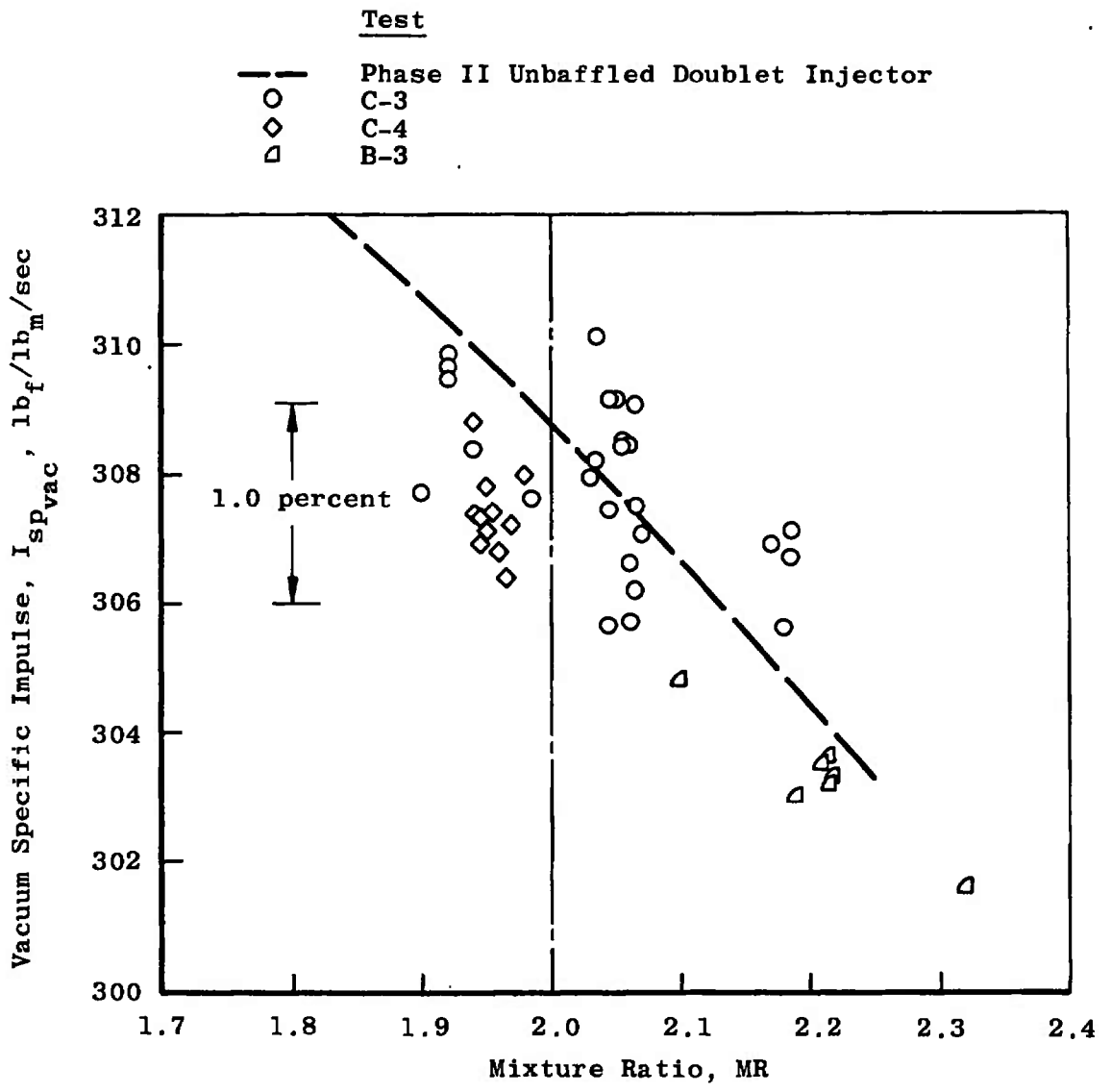

Fig. 48 Phase I Adjusted Engine Performance

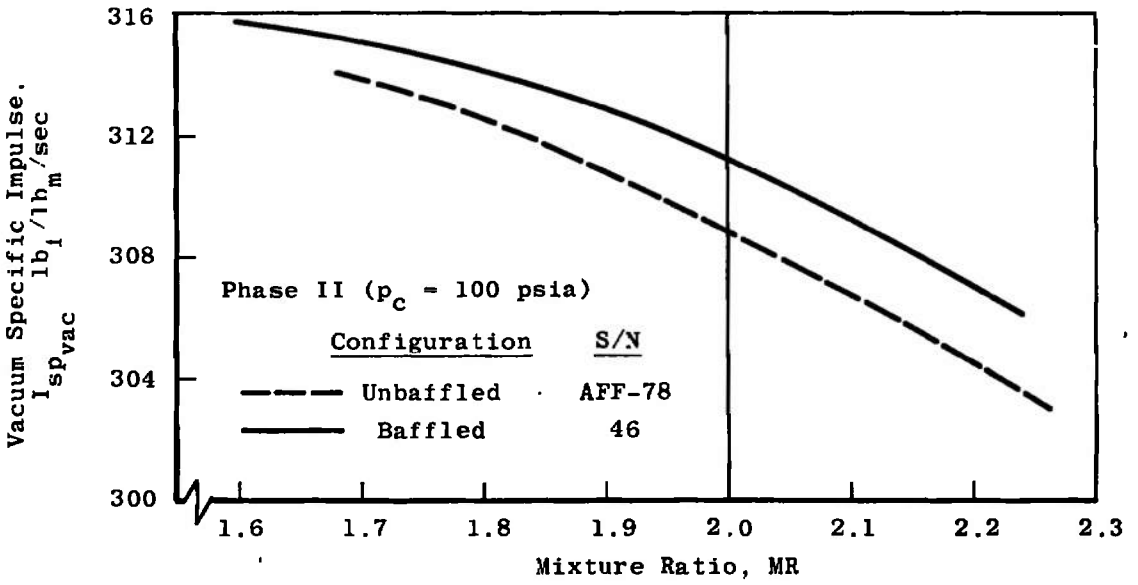

a. Unbaffled and Baffled Injector (PHASE II)

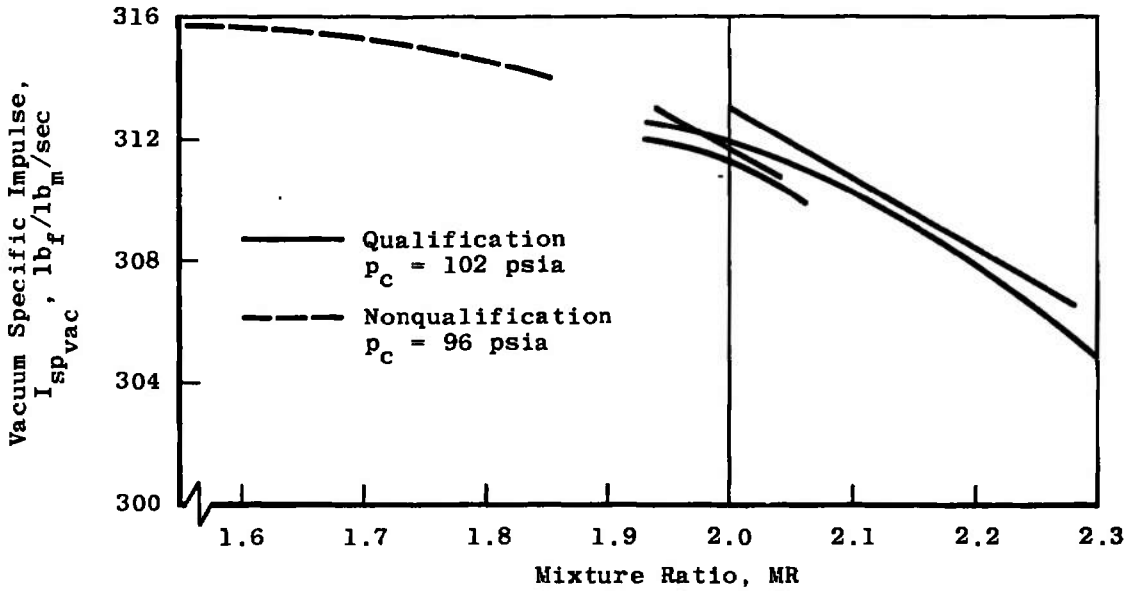

b. Qualification Testing (Phase III)

Fig. 49 Block I Engine Performance, $I_{sp_{vac}}$

Sufficient testing had been conducted in Phases II and III at lower than design mixture ratios to indicate that considerably higher performance might be derived at a mixture ratio of 1.6 (Fig. 49b). The selection of a different mixture ratio would normally necessitate a radical redesign of the propellant tankage for a Block II Service Module configuration. However, the specific mixture ratio of 1.6 results in equal volumetric flow rates of oxidizer and fuel. A rearrangement of plumbing interchanged one oxidizer tank and one fuel tank to produce a new tandem tank configuration with equal total volumes. Initial Phase IV Block II development testing verified the engine performance of Phase III and extended the testing range to various levels of combustion chamber pressure and propellant temperatures. The best engine performance averaged about 315 $lb_f/lb_m/sec$ $I_{sp_{vac}}$ at the new design mixture ratio of 1.6 for Block II (Fig. 50). However, this higher engine performance had a deleterious effect on the ablative combustion chamber durability, as described in Section 2.2; therefore, an injector modification involving additional doublets and fuel film cooling holes was instituted to regain injector-to-chamber compatibility. Engine performance with this injector was not changed greatly as shown in Fig. 50a, but a second injector with additional orifices (S/N 110) did produce somewhat lower performance.

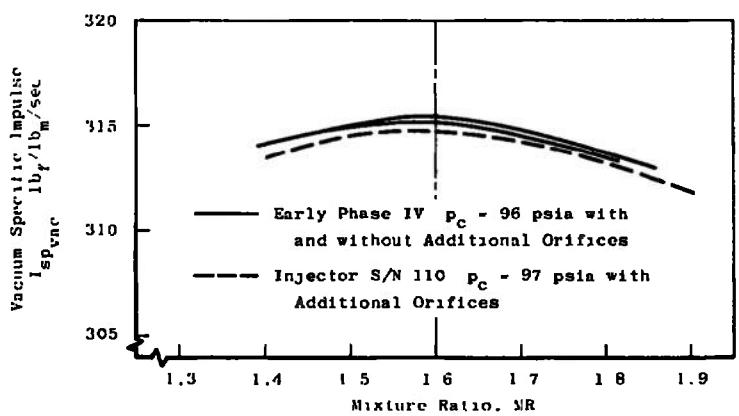

a. Effect of Additional Injector Orifices

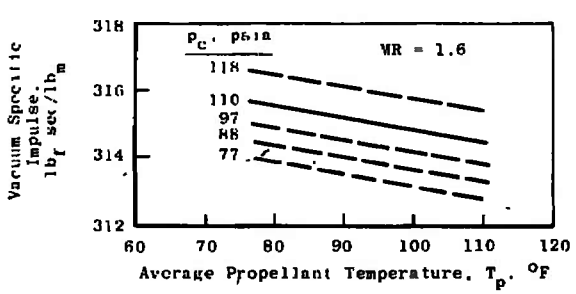

b. Propellant Temperature Effect on Performance with the Long Baffled Injector S/N 93

Fig. 50 Engine Performance with Injector S/N 110, $I_{sp_{vac}}$

Development attention was then turned to elimination of the disconcerting sporadic combustion irregularities termed "pops." Injector baffle chord length was increased at the outer tips of the radial baffles, but this failed to reduce the pops noticeably. Although engine performance at design operating conditions was unchanged by the longer baffles, this particular injector did show a new sensitivity to propellant temperature (T_p) as shown in Fig. 50b. Highly discerning analyses by the engine manufacturer produced the deduction that the pops were caused by hydraulic instability of propellant streams out of the injector. Injector hole configuration changes were made (counterbored orifices, Section 2.3.4), the pop frequency and intensity were reduced to insignificance, and the Phase IV Block II engine development was finished; however, the engine performance at design operating conditions was now reduced to about 313.5 $lb_f/lb_m/sec$ $I_{sp_{vac}}$, as shown in Fig. 51. The oxidizer type was changed between tests DC and DD of Phase IV from MIL-P-26539, nitrogen tetroxide, to MSC-PPD-2A, nitrogen tetroxide, which contained about 0.6 percent of nitric oxide (NO) inhibiting agent. The oxidizer change did not produce any noticeable change in engine performance or operating characteristics.

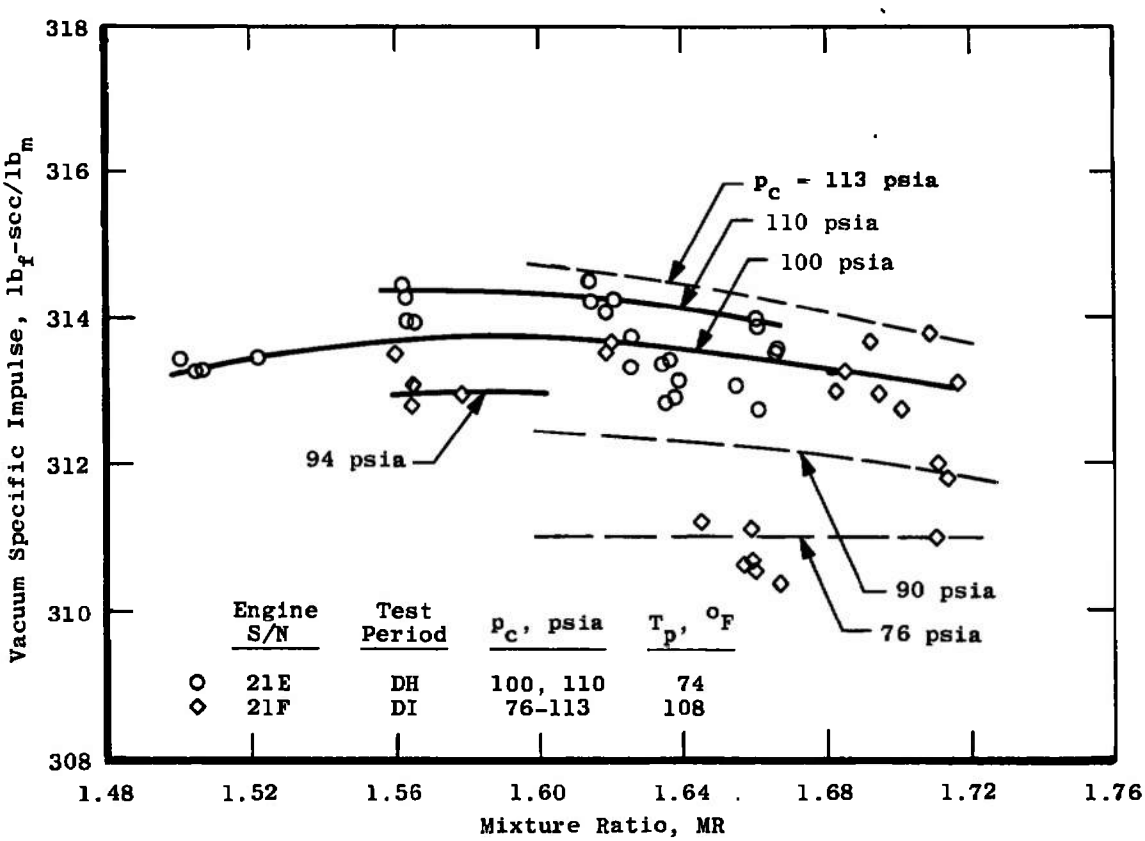

Fig. 51 Vacuum Performance with Long Baffled, Counterbored Orifices Injector, Phase IV

Phase V, Block II engine qualification performance is summarized in Fig. 52. The performance of the three Block II engine injectors tested varied from 311.3 to 314.8 $lb_f/lb_m/sec$ at design operating conditions. Considerable analysis effort was expended to determine why the performance of each injector was different, but no data irregularities could be identified. Since each injector was tested with two different engine buildups in two different test periods with separate instrument calibrations and since the data repeatability was quite good, the conclusion was made that the different performance levels were characteristic of the individual injectors.

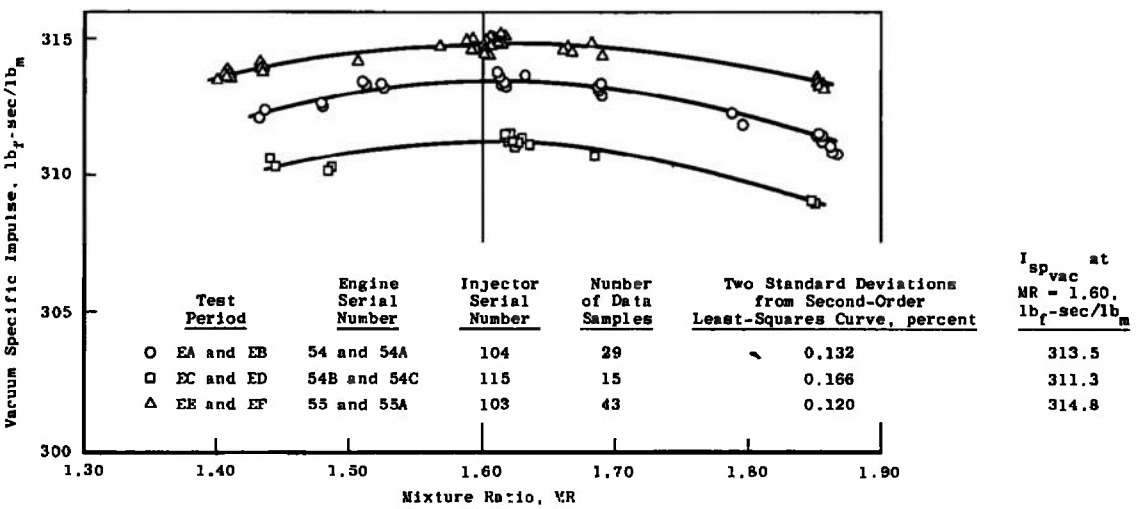

Fig. 52 Block II Engine Performance at Design Chamber Pressure, Phase V

Phase VI engine performance data approximated previous performance at nominal operating conditions as shown in Fig. 53.

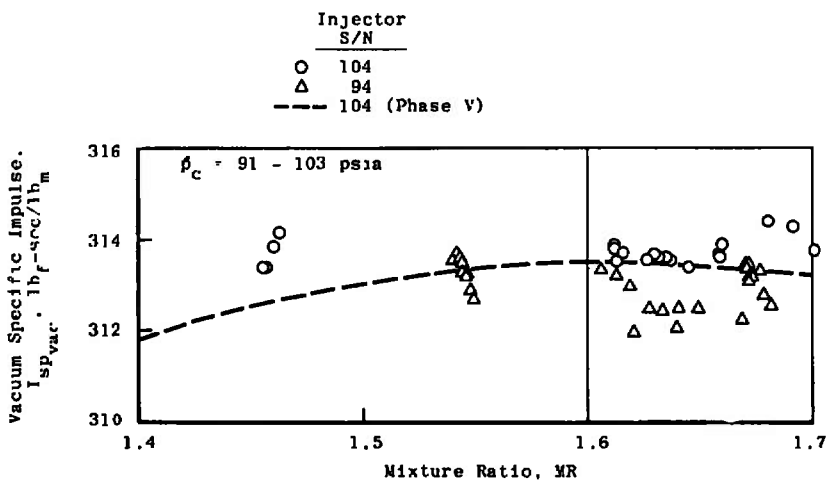

Fig. 53 Phase VI Engine Performance Compared with Previous Test

Engine performance was markedly influenced by combustion chamber pressure. Figure 54 shows the effect of chamber pressure which was experienced by the Phase V Block II qualification engines. The same general trend was typical of all the Apollo engine testing. Improved performance, which might have been obtained by simply operating at higher chamber pressure, was always precluded by the marginal durability of the ablative combustion chamber with the more severe (high pressure) operation.

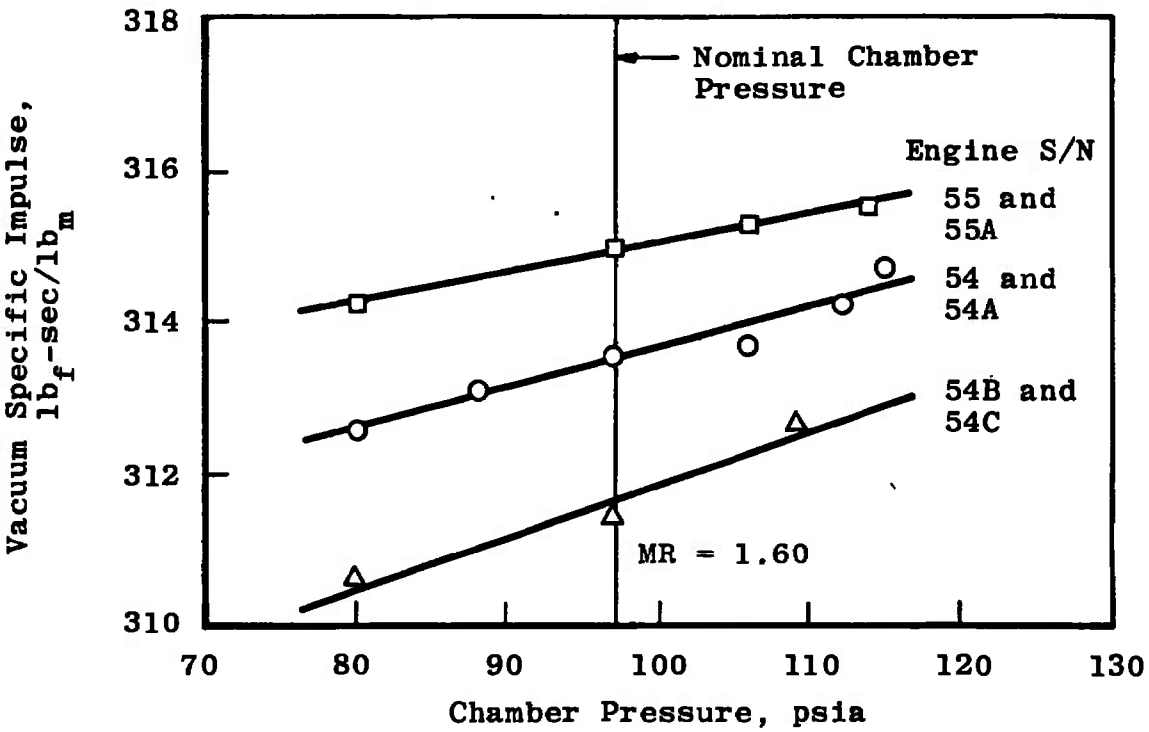

Fig. 54 Block II Engine Vacuum Specific Impulse-Chamber Pressure Relationship at Design Mixture Ratio, Phase V

The Block II engine produced characteristic velocities (c*) of about 5900 ft/sec and vacuum thrust coefficients ($C_{F_{vac}}$) of about 1.71, using the combustion chamber pressure measured near the outer edge of the injector face (Fig. 14e).

Estimates of the accuracy of the engine performance data obtained in these tests are described in the Appendix.

3.2 IMPULSE OF IGNITION AND SHUTDOWN TRANSIENTS

The impulse (lb_f-sec) of starting and shutdown transients was calculated for all test phases, except Phase I, to determine the

magnitude and repeatability of the impulse associated with the transient portion of engine firings.

The total impulse of the start transients was calculated for the time period from ignition (initial chamber pressure rise, i. e., p_c = 1 psia) to 100 percent of steady-state thrust. The impulse was derived from calculated thrust based on measured chamber pressure:

$$I_t = C_{F_{vac}} A_t \int_{t_1}^{t_2} p_c \, dt$$

Intermediate impulse values were also derived at 10-percent intervals of chamber pressure up to the steady-state value.

The total impulse of the shutdown transient was calculated by a similar equation. For Phase II, the integral covered the time period from shutdown signal (FS2) to the 1-percent steady-state thrust level. For the later phases, the integral extended from FS2 to the time at which the nozzle throat became unchoked (i. e., when the chamber-to-cell pressure ratio (p_c/p_{cell}) declined to 1.135 for Phase III, to 1.2 for Phases IV and V, and when chamber pressure declined to 0.3 psia for Phase VI). Vacuum thrust computed from measured thrust was not used because at low chamber pressures the exhaust nozzle does not flow full and the thrust measurement system did not record transients accurately. Measured combustion chamber pressure data were reduced at 0.005-sec intervals (200 intervals/sec) from the continuous magnetic tape recording of a close-coupled transducer. Beginning with Phase III, the shutdown combustion chamber pressure was reduced at 0.02-sec intervals (50 intervals/sec), and a low-range combustion chamber pressure data channel (0 to 15 psia) was added to increase accuracy at low p_c values.

The combustion chamber pressure was used with calculated nozzle throat area and $C_{F_{vac}}$ which were obtained from the data of a preceding or succeeding steady-state firing nearest the transient of interest and were assumed to be constant throughout the transient.

3.2.1 Ignition Transient Characteristics

The impulse (lb_f-sec) developed during the engine ignition transients was determined beginning with Phase II. A partial summary of the impulse developed from ignition to 90-percent steady-state thrust is shown below:

Phase	TCV Type	TCV Bank	p_c Level, psia	From Ignition to 90-percent Steady-State Thrust: Impulse, lb_f-sec	1σ, lb-sec	Time, sec	1σ, sec
II	Block I Fuel Pressure Actuated	A	100	1680	±327	0.465	±0.037
II	Pneumatically Actuated	A and B	104	2049	±175	0.440	±0.002
II		A and B***	104	149		0.355	
III		A and B	105	266	± 91	0.468	±0.026
III		A or B	107	580	±140	0.552	±0.053
IV	(a)	A	97	558	± 83	0.586	±0.009
IV	(a)	A*	110	471	± 76	0.530	±0.004
V	(a)	A**	97	568	±119	0.559	±0.016

(a) TCV modified with additional actuator spring force and increased regulator pressure

* Using only firings where TCV temperature was below 100°F

** Using only firings with standard interface pressures (p_{oxid} = 160 ± 4 psia; p_{fuel} = 166 ± 4 psia)

*** Valve timing shortened

The magnitude of the ignition impulse was primarily dependent on (1) the TCV timing, (2) the steady-state chamber pressure level, (3) the TCV bank selected, and (4) the propellant temperature.

Typical ignition transients of the fuel pressure actuated and the pneumatic TCVs (Phase II) are compared in Fig. 55. The slower opening of the fuel-actuated TCV caused the chamber pressure to rise more slowly and generally resulted in larger ignition impulse as shown in Fig. 56. Also, the fuel-actuated valve produced unsatisfactorily large variations in ignition impulse.

The data from Phases III and V (Block I and Block II Qualification tests) are compared with the qualification specifications in Refs. 10 and 13; the pneumatic valve did not sufficiently improve impulse repeatability.

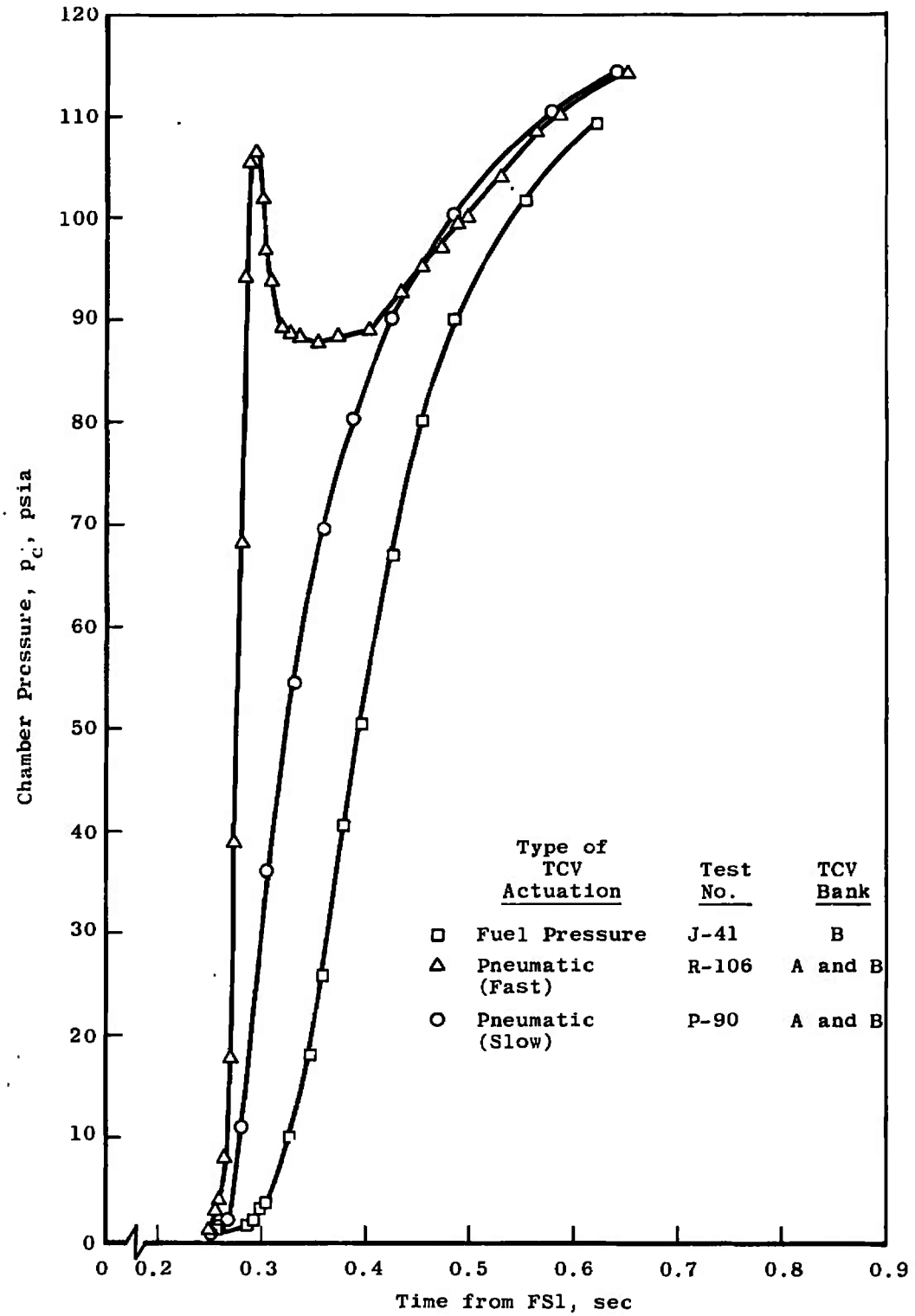

Fig. 55 Comparison of the Chamber Pressure Transients using Fuel Pressure Actuated and Pneumatically Actuated TCV

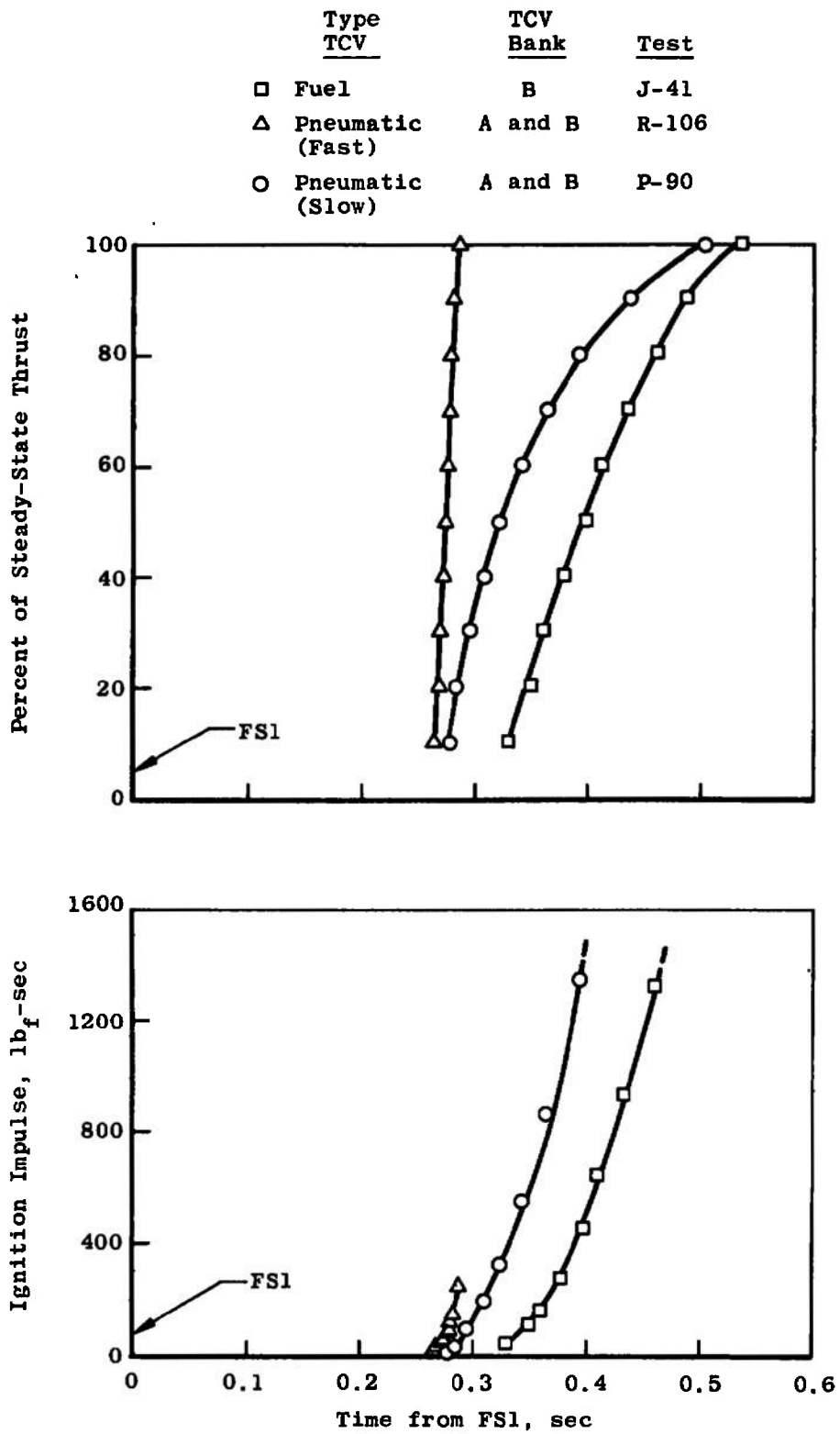

Fig. 56 Typical Ignition Transients

It was noted that the transient ignition impulse was affected by the prefire temperature of propellants in the TCV. High propellant temperature resulted in slower chamber pressure rise to 90 percent, which increased the ignition transient time and hence the ignition impulse. For the later part of Phase IV, the average ignition impulse was calculated using only those data obtained when the TCV temperature was below 100°F.

3.2.2 Shutdown Transient Characteristics

Impulse (lb_f-sec) developed during the engine shutdown transient was computed as described in Section 3.2; however, the shutdown transient was considered terminated at the 10-percent level, since the tailoff had a relatively small effect on the total impulse and its time duration was highly sensitive to cell pressure variations. The data obtained are summarized below:

			From FS2 to 10-percent Steady-State Thrust				
Phase	TCV Type	TCV Bank	P_c Level, psia	Impulse, lb_f-sec	1σ	Time, sec	1σ
II, Part 1	Fuel Pressure Actuated	A	100	13,731	± 543	0.856	±0.014
II, Part 1	Fuel Pressure Actuated	A*	100	6,368	± 390	0.641	±0.025
II, Part 2	Pneumatically Actuated	A and B	104	10,029	± 709	0.759	±0.025
III		A and B	105	10,710	± 343	0.802	±0.040
III		A or B	107	9,854	± 319	0.795	±0.049
IV, Part 1	(a)	A	97	9,702	± 366	0.868	±0.030
IV, Part 2	(a)	A	110	10,006	± 682	0.871	±0.062
	(a)	B	110	9,716	±1322	0.878	±0.105
	(a)	A	97	8,907	± 819	0.843	±0.074
	(a)	B	97	8,497	± 457	0.812	±0.027
V	(a)	A	97	10,190	± 430	1.008	±0.030

(a) TCV modified with additional actuation spring and increased regulator pressure

* Valve timing shortened

The magnitude of the shutdown total impulse was influenced by (1) propellant supply pressures (firing p_c), (2) TCV bank selected, (3) propellant temperature, and (4) TCV closing time.

During the initial part of Phase II, when the fuel pressure actuated TCV was used, there were two distinct levels of TCV closing times with corresponding different levels of shutdown impulse because of different valve actuation timing.

The timing was being adjusted by the engine manufacturer to improve the repeatability of the transient total impulse. Beginning with

the later part of Phase II, summarized data indicate that, in general, the use of bank A of the pneumatic TCV resulted in larger total shutdown impulse than did bank B. Again, this was the result of the individual bank timing adjustments. Phase III average engine shutdown transient impulse and time (from FS2 to 10 percent of steady-state thrust level) were beyond target values regardless of TCV bank selection. In the nine Phase V testing firings (6 with bank A; 3 with bank B) that were conducted with standard interface pressure conditions, the data showed that (1) the time from FS2 to 10 percent of steady-state thrust exceeded the target limit by 12 percent, and (2) the corresponding impulse was considered satisfactory although the run-to-run variation exceeded the target repeatability limits of ±300 lb_f-sec.

Typical shutdown transients for the two different types of TCV are presented in Fig. 57.

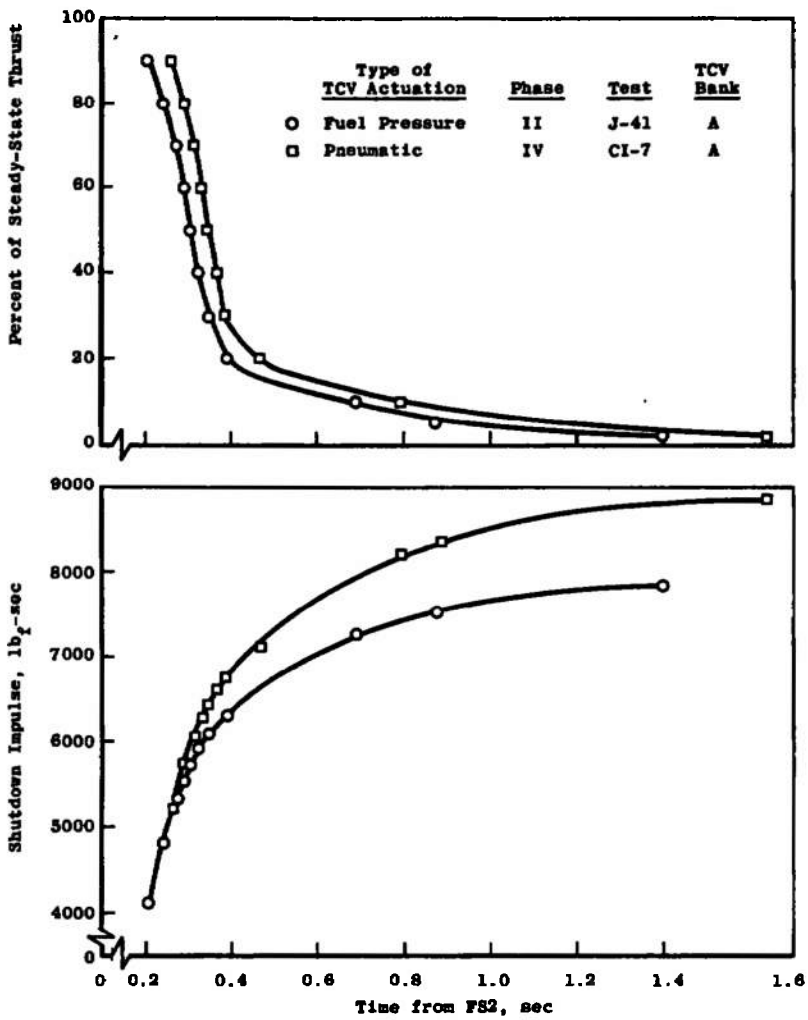

Fig. 57 Typical Shutdown Transients

3.3 IMPULSE BIT FIRINGS

The total impulse (lb_f-sec) of the impulse bit firings (duration of 1 sec or less) was calculated by a method similar to that used for ignition and shutdown transients, except that the impulse was totaled for the entire firing from ignition through thrust decay to the unchoked p_c/p_{cd} ratio (as described in Section 3.2). Since the impulse bit firings were too short to establish steady-state engine performance, $C_{F_{vac}}$ and A_t were obtained from the nearest firing which produced steady-state data at the same operating conditions. The $C_{F_{vac}}$ and A_t were assumed to be constant throughout the impulse bit firing. Impulse versus firing signal duration, using TCV bank A or bank B, for the various phases is presented in Figs. 58 and 59. The total impulse,

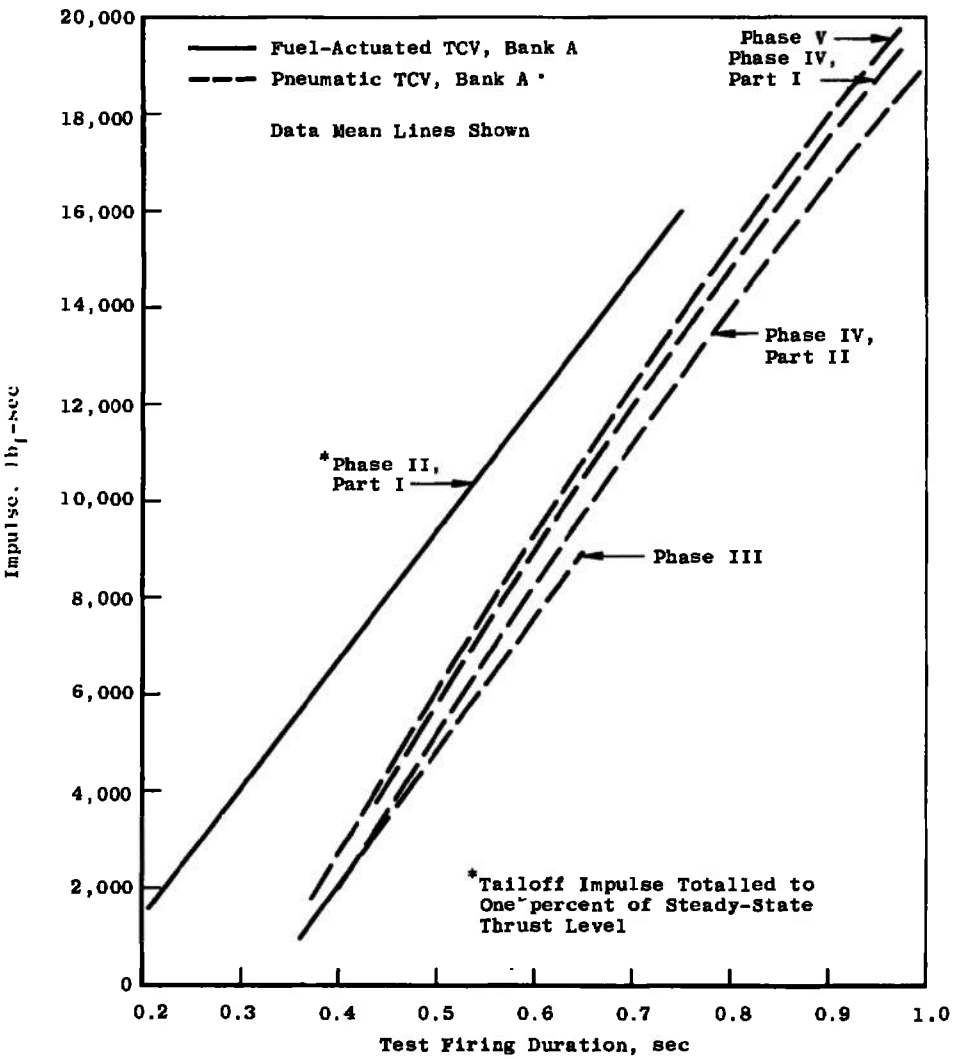

Fig. 58 Comparison of Impulse Bit Operation Using Different Types of TCV's

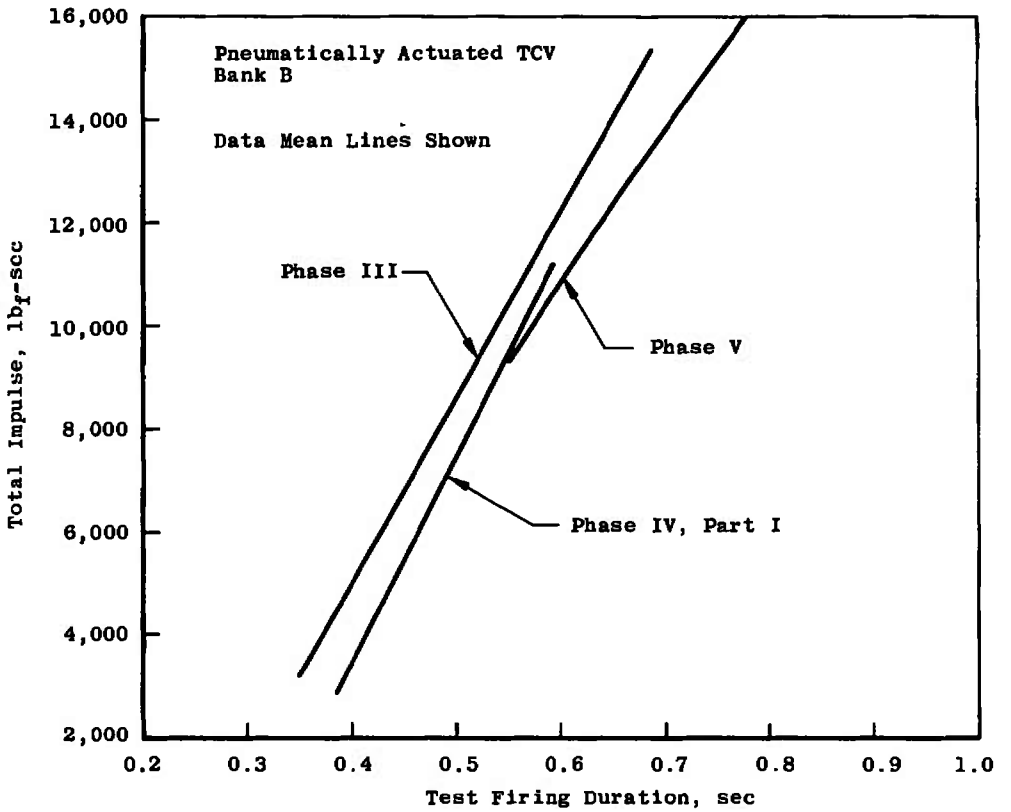

Fig. 59 Impulse Bit Operation

developed during the impulse bit firings, was almost directly proportional to the firing signal duration. The magnitude of the total impulse to a lesser degree was also a function of (1) propellant supply pressures, (2) the TCV type and bank selected, (3) the TCV opening and closing times, and (4) the temperature of the TCV. Figure 58 indicates that the fuel-operated TCV produced considerably higher total impulses than did the pneumatically actuated TCV. In addition to slower operation, the fuel-operated TCV opened earlier, and ignition occurred earlier, thus producing a slightly longer burning time and consequently a larger total impulse. The effect of this earlier opening, which produced larger impulse, is clearly indicated by the chamber pressure transients shown in Fig. 60.

Figures 58 and 59 also indicate that, with the exception of the later part of Phase IV, bank B of the pneumatically actuated TCV produced higher total impulses for the same firing signal duration than did bank A. This was a consequence of the intentional difference in timing of the two valve banks. By extrapolation, the minimum firing signal duration to obtain any impulse was approximately 0.19 sec for the fuel-operated TCV compared with about 0.30 sec for the pneumatically actuated TCV.

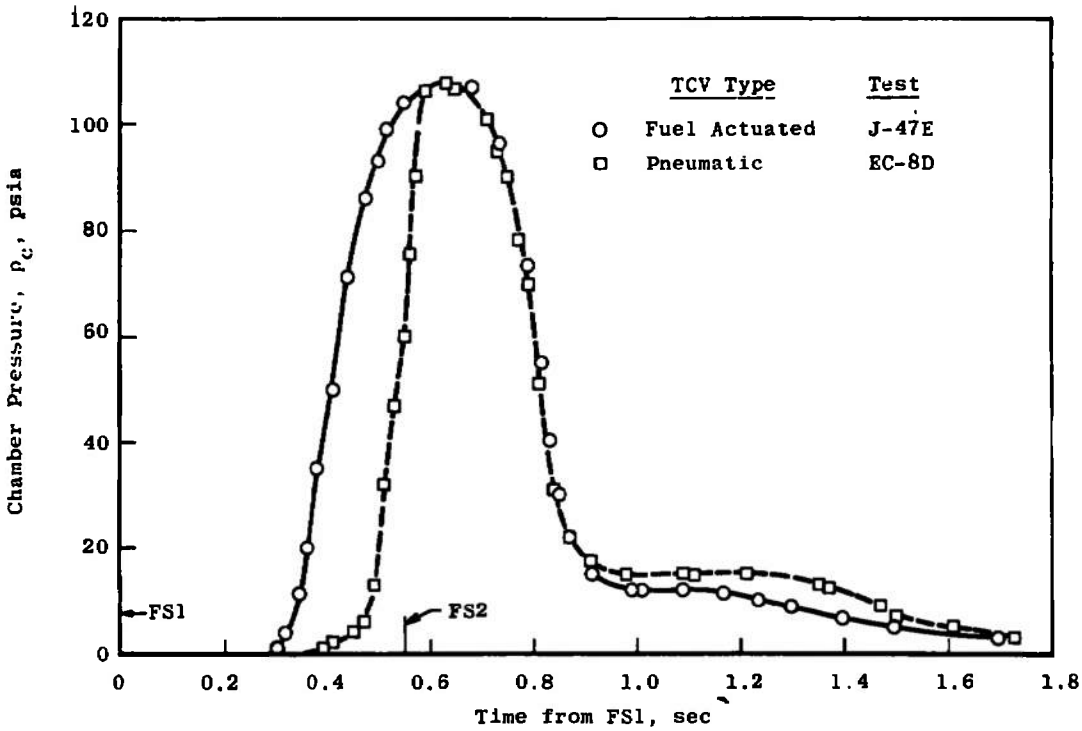

Fig. 60 Comparison of Chamber Pressure Transients Using Different TCV Actuation Systems

SECTION IV
RESEARCH AND DEVELOPMENT TESTING

4.1 PROPELLANT EVAPORATIVE COOLING EFFECTS

The cooling effect of propellants evaporating in the injector after engine shutdown was investigated during Phase VI test periods FE to FJ (Ref. 15). The injector temperature was depressed as much as 9°F in certain locations within 2.5 min after short firings which induced minimum heating (Fig. 61). The cooling effect was demonstrated to be cumulative with a series of short firings at short intervals as shown in Fig. 62. Although insufficient testing was done to establish what "optimum" conditions of firing and coast durations would produce the lowest temperatures or cause propellant freezing, a local temperature low of 17°F was reached in one instance, as shown in Fig. 62b.

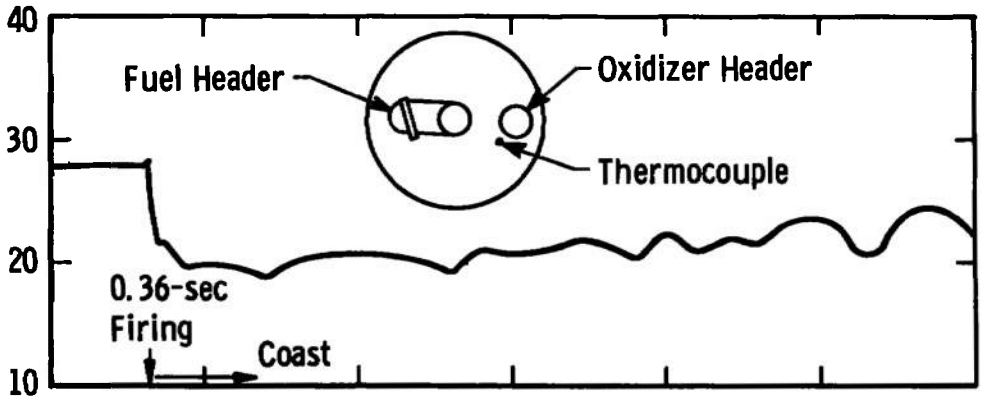

a. Temperature near Oxidizer Header

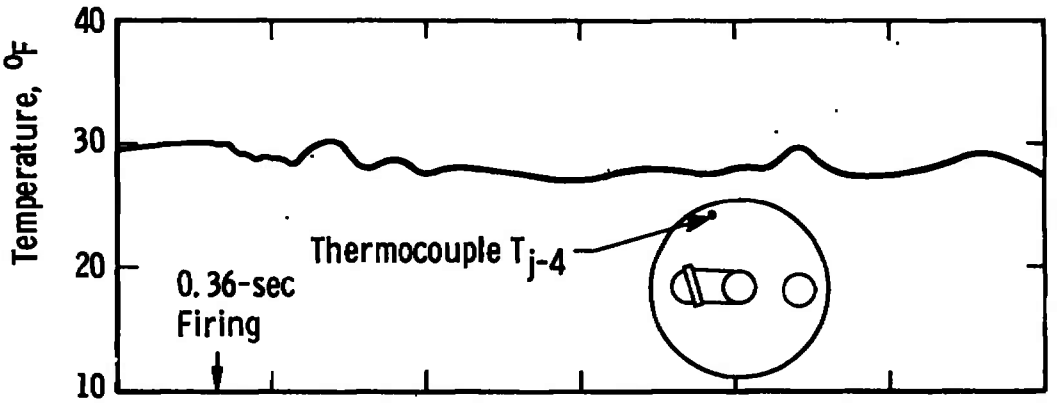

b. Temperature at Outer Rim

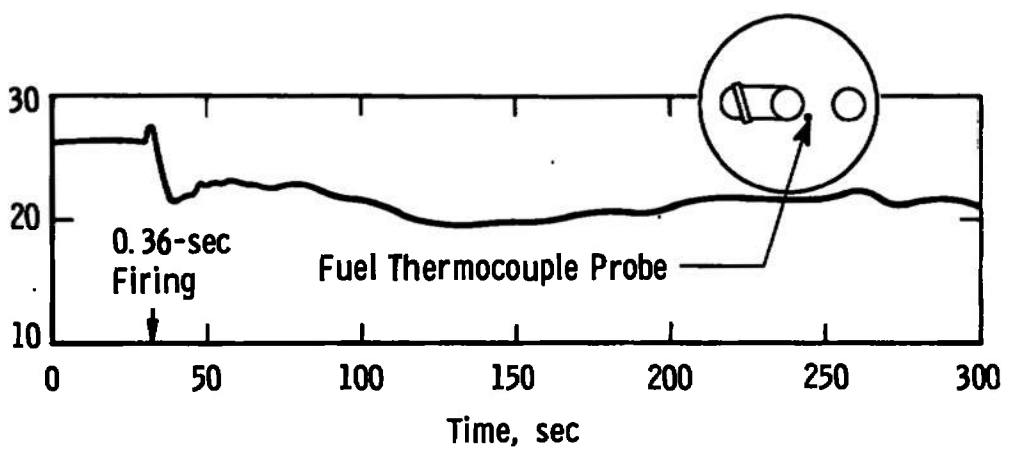

c. Fuel Temperature near Fuel Header

Fig. 61 Injector Temperature History after Short Firing FJ-33

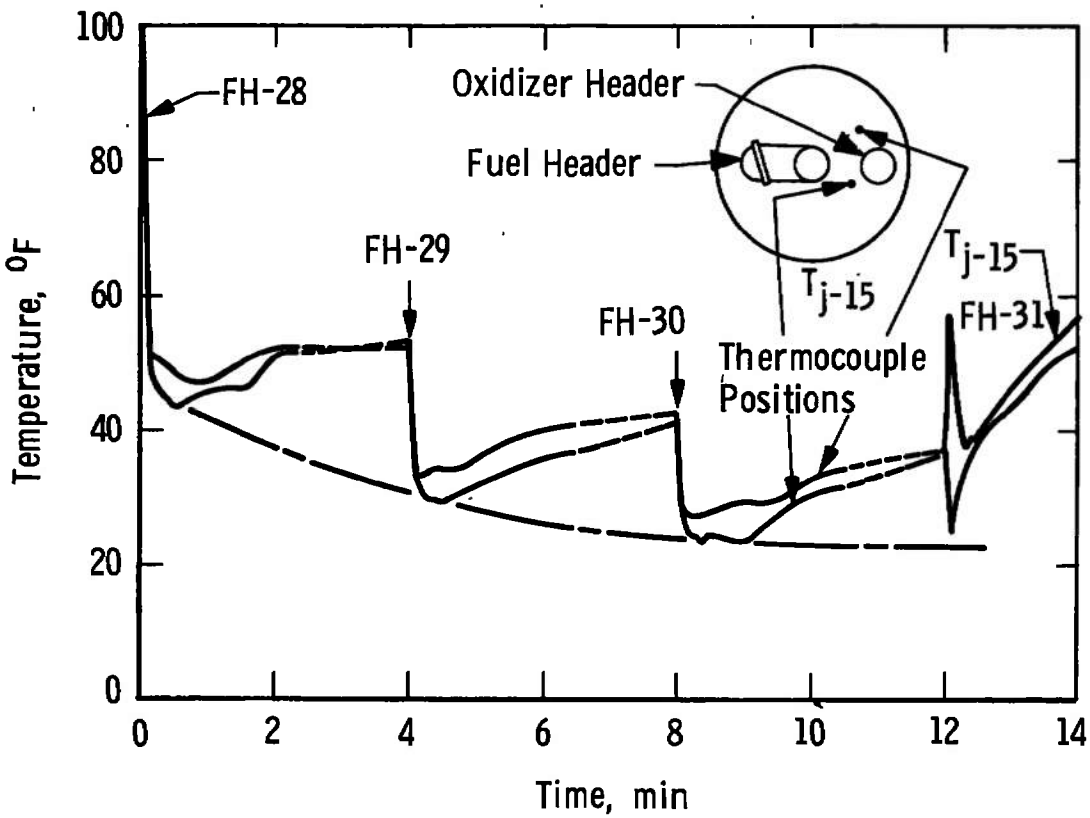

a. Multiple Firings with 4-Min Interval

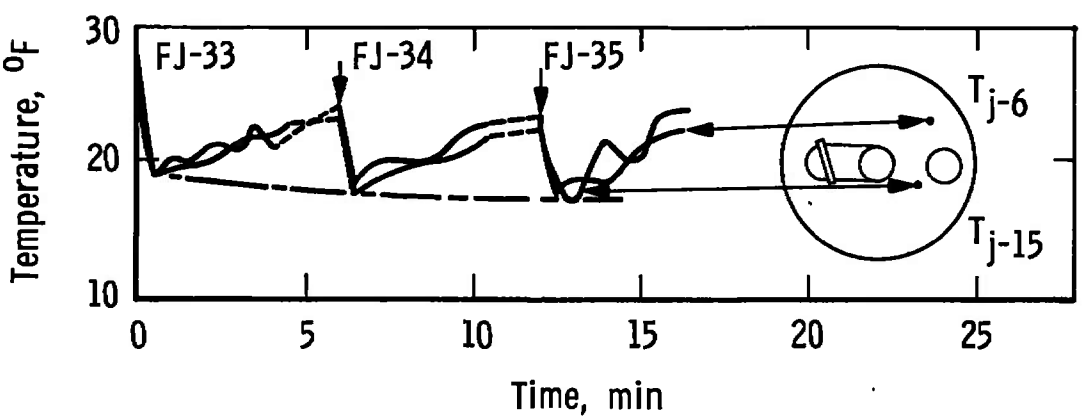

b. Multiple Firings with 6-Min Interval

Fig. 62 Effect of Multiple Firings on Injector Temperatures

4.2 IGNITION CHARACTERISTICS (PHASE VI)

The combustion chamber pressure data obtained from Apollo Spacecraft flights 17 and 20 indicated that a momentary combustion overpressure had occurred during the engine ignition transient of the Service Module primary propulsion system. The indicated magnitude and duration of the overpressure were considered detrimental to the Command Module/Lunar Module interstage structure of the Apollo vehicle. Phase VI test periods FM, FN, and FO were conducted to investigate the magnitude and duration of combustion overpressure at ignition as influenced by various starting conditions, and concurrently, to evaluate the standard flight-type chamber pressure transducer (Ref. 15). The testing was conducted with a steel combustion chamber which permitted installation of multiple high-response chamber pressure transducers in addition to the flight-type transducer (Fig. 63). The various starting conditions of temperatures and modes of TCV operation are listed in Table V ("dry" TCV indicates the absence of propellants trapped in the cavities between the valve balls, as would be the condition prior to the first engine firing of a space mission).

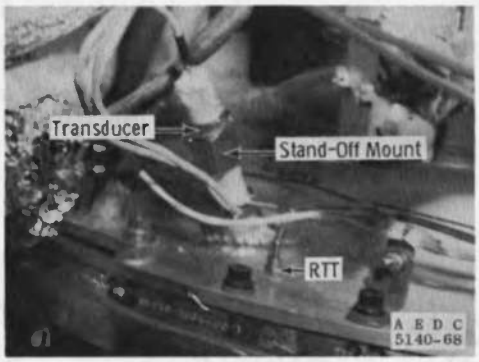

a. Flight-Type Transducer Installation

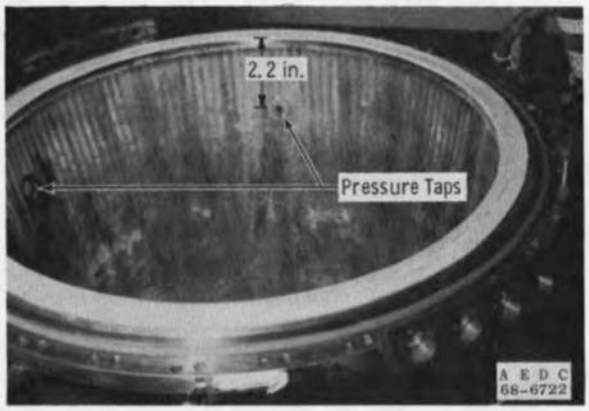

b. Steel Chamber Pressure Taps

Fig. 63 Combustion Chamber Pressure Measurement Locations

TABLE V
TEST CONDITIONS FOR IGNITION CHARACTERISTICS

Firing No.	Chamber Pressure, Pcg, psia	TCV Temperature, °F	Propellant Temperature, °F	Injector Temperature, °F	TCV Bank Selection	TCV Starting Condition	TCV Actuator Temperature, °F	TCV Opening Time, sec	
								Controlling Valve	
								Bank A Valve Set 1	Bank B Valve Set 4
Test Period FM									
01	95 2	35	32	39	A	Dry	33	0.580	
02*	95.2	31	31	33	B		30		0 860
03	95.2	30	32	35	AB*		25	0.620	0 910
04	96.5	28	31	35	A	Wet	27	0 010	
05	95.2	26	31	38	A		26	0.620	
06	95.2	28	31	39	A		26	0 620	
07	100.3	25	30	39	AB*		25	0.610	0 850
08	98.0	24	31	38	AB*		25	0.630	0 910
09	100.4	25	31	40	AB*		25	0 610	0 880
10	99.1	26	32	38	AB*	Dry	26	0 590	0.850
11	99.1	27	31	39	AB*		25	0.610	0 910
12	96.5	28	31	33	AB*		25	0.590	0.910
13	111.9	29	35	34	A	Wet	25	0 610	
14	111.9	30	35	31	A		30	0 610	
15	111.9	30	34	37	A		24	0 580	
16	109.3	26	31	38	B		25		0.930
17	117.0	26	31	37	AB*		25	0.630	0 965
18	117.0	26	30	38	AB*		25	0.630	0.965
19	117 0	26	30	35	AB*		25	0 620	0 960
Test Period FN									
01	112.6	84	70	80	A	Dry	--	0.590	
02	115.2	59	87	85	A	Wet	--	0 605	
03	113 9	62	66	87	A	Wet	--	0 600	
04	113.9	55	66	90	B	Dry	--		0 640
05	113.9	58	65	96	B	Wet	--		0 640
06	115.2	52	64	94	B		--		0 650
07	119.1	55	65	95	AB		--	0.565	0 650
08	119.1	58	65	100	AB		--	0 590	0.640
09	117 8	57	65	87	AB		--	0 570	0.625
Test Period FO									
01	99 7	38	30	26	AB*	Dry	43	0.540	0.960
02	97.8	28	32	27	AB*	Dry	41	0 540	0 925
03	97.8	35	25	40	AB*	Wet	43	0.560	0 960
04	97 8	34	28	38	AB*		46	0.575	0.920
05	97.8	30	28	40	AB*		44	0 570	0.850
06	95.9	55	32	50	B*		62		0.675
07	97 8	67	62	58	AB	Dry	59	0 475	0.521
08	95.9	69	61	78	AB	Wet	60	0.490	0.543
09	103 0	63	52	47	AB	Dry	78	0 495	0.560
10	103.0	61	48	87	AB	Dry	65	0.473	0.532
11	101.0	62	50	78	AB	Wet	70	0.473	0.539
12	101.0	66	52	95	AB		73	0.520	0.540
13	103 0	67	52	98	AB		71	0 525	0.570
14	117.3	70	54	95	AB		72	0.540	0 575
15	119.7	59	54	99	AB		73	0 505	0.560
16	118.1	83	53	82	AB		68	0.520	0.595
17	118.1	67	54	48	AB	Dry	65	0 520	0.590
18	116.9	68	--	--	AB		65	0 473	0.528
19	109.3	88	54	160	B		65		0 567
20	109.3	74	60	140	A		65	0 494	
21	111 2	73	62	--	B	Wet	64		0.570
22	92.0	72	64	121	A		65	0.500	
23	94.0	72	62	120	B		65		0.575
24	95.1	72	64	113	A		65	0 490	
25	93 2	71	64	113	B		65		0 543
26	116 9	70	64	114	AB		85	0.455	0.546

*Improper TCV Operation

The combustion overpressure (peak) ranged from 0 to 48 percent above the steady-state chamber pressure level, as shown in Table VI (Fig. 64 depicts typical start transients). The combustion overpressure duration displayed no apparent trend based on the various starting conditions (Fig. 65).

Overpressure Duration, msec	Proportion of All Starts, percent
Less than 20	10
20 to 30	75
30 to 40	18

TABLE VI
AVERAGE COMBUSTION OVERPRESSURES

Firing No.	Average Chamber Pressure Value, psia	Average Duration, sec	Average Combustion Overpressure, percent	Firing No.	Average Chamber Pressure Value, psia	Average Duration, sec	Average Combustion Overpressure, percent
FM-01	95.4	30.3	25.5	FO-01	99.9	25.0	26.3
02	94.4	15.0	7.1	02	102.0	25.0	31.4
03	97.8	32.3	27.7	03	100.6	29.7	18.0
04	97.1	25.0	11.0	04	101.9	26.7	16.6
05	96.2	22.5	8.6	05	100.1	30.7	23.4
06	95.8	21.3	14.2	06	98.0	20.0	12.9
07	99.8	25.8	23.3	07	100.9	39.5	36.1
08	99.5	27.8	23.2	08	98.1	32.7	35.6
09	99.8	25.8	20.0	09	103.5	27.3	34.5
10	99.3	25.0	19.4	10	100.6	25.3	47.9
11	98.9	23.5	23.7	11	102.4	33.0	30.4
12	99.9	24.5	19.4	12	101.2	30.0	36.0
13	114.3	25.0	3.6	13	102.6	29.3	30.5
14	114.3	24.5	2.8	14	117.2	39.3	10.4
15	114.3	20.3	3.6	15	121.7	26.7	22.5
16	112.1	No Over-pressure	---	16	118.3	28.3	22.2
				17	117.5	22.3	40.0
17	119.4	28.0	11.6	18	119.2	25.5	36.4
18	118.3	28.0	10.7	19	111.6	---	8.9
19	117.9	28.5	6.2	20	112.2	31.0	10.9
				21	113.7	21.5	6.0
FN-01	111.3	22.3	14.2	22	94.6	37.7	15.9
02	112.6	23.0	1.7	23	97.3	23.3	
03	112.2	23.5	2.9	24	95.9	25.7	18.1
04	112.2	20.0	7.5	25	95.7	21.3	14.7
05	112.7	19.5	5.2	26	117.4	21.3	24.3
06	113.1	20.0	2.4				
07	117.2	29.3	17.3				
08	116.7	28.0	17.4				
09	115.9	29.5	19.0				

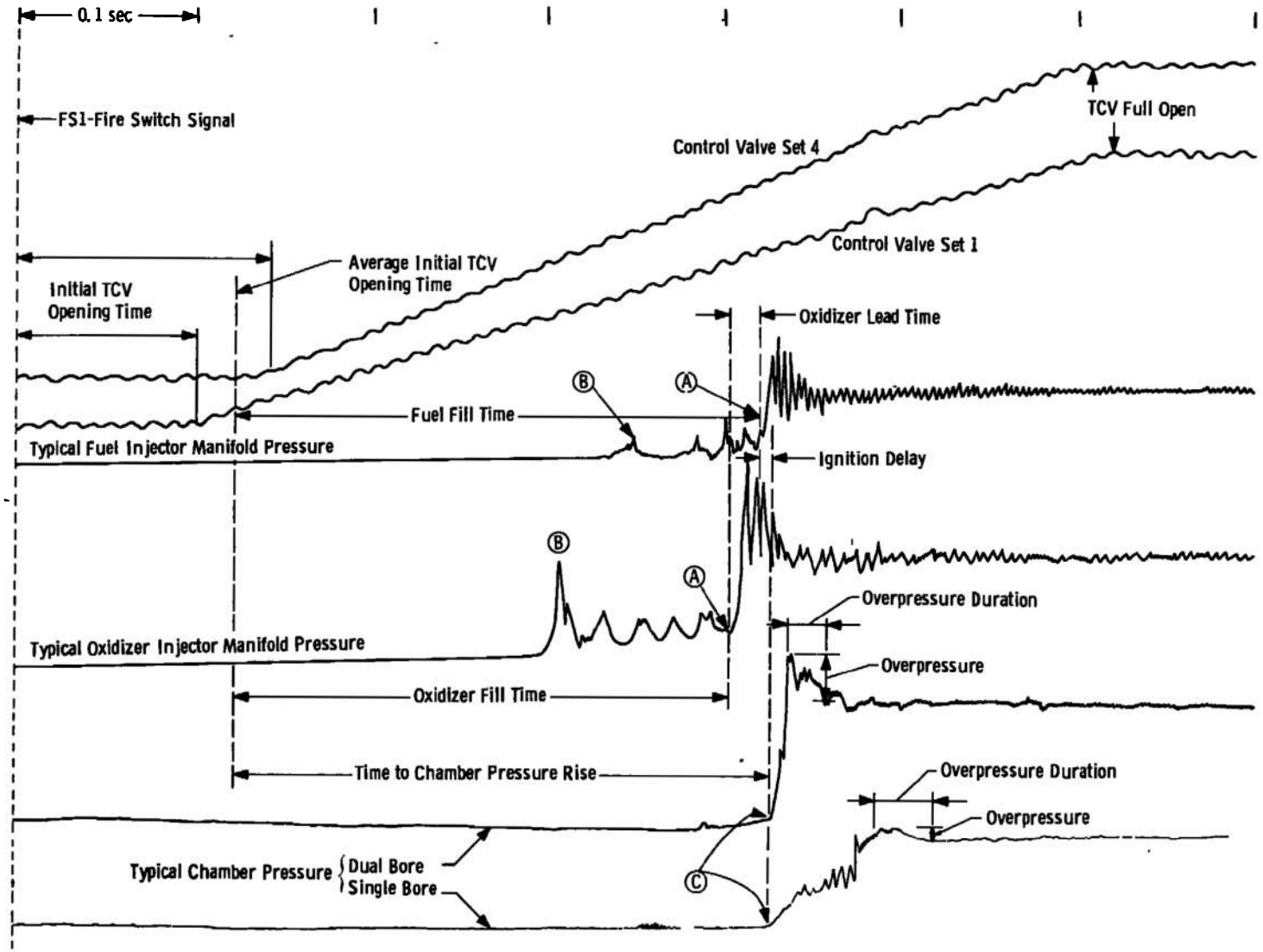

Fig. 64 Typical Start Transient Oscillograms

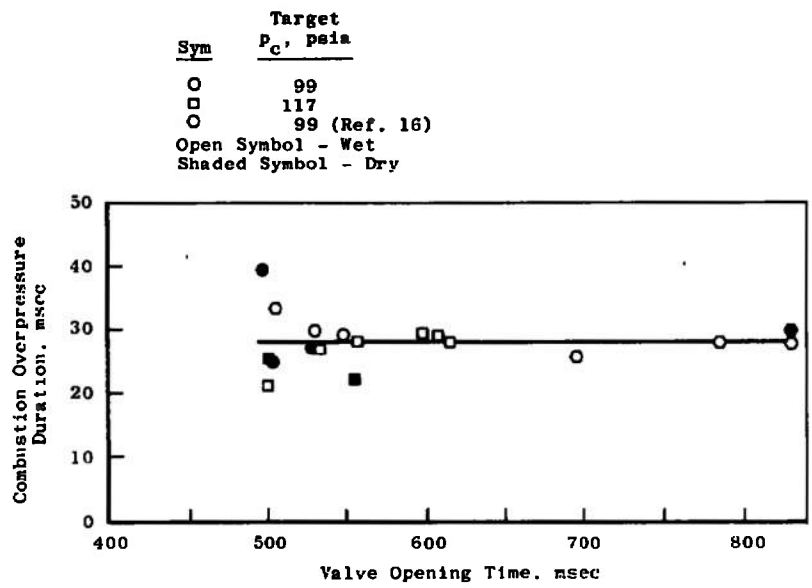

a. Dual-Bore Starts

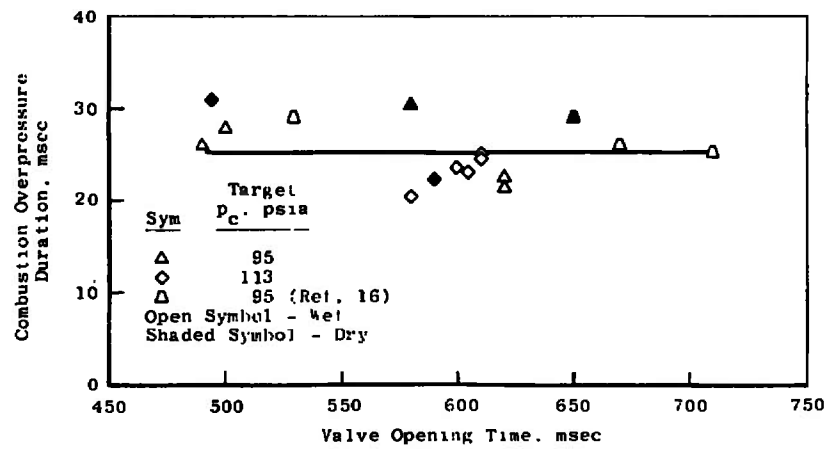

b. Single-Bore, Bank A

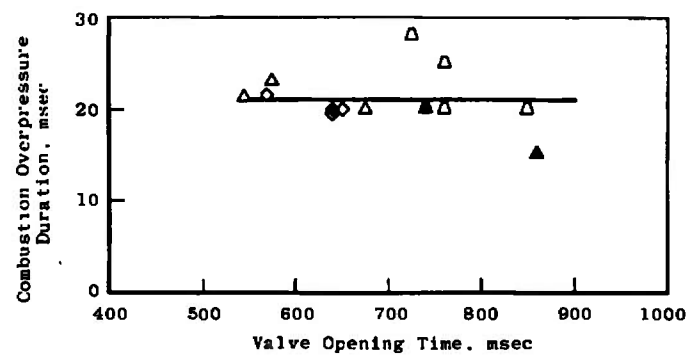

c. Single-Bore, Bank B

Fig. 65 Combustion Overpressure Duration as a Function of TCV Opening Time

Propellant and injector temperatures from 30 to 70°F did not have any pronounced influence on combustion overpressure (Fig. 66).

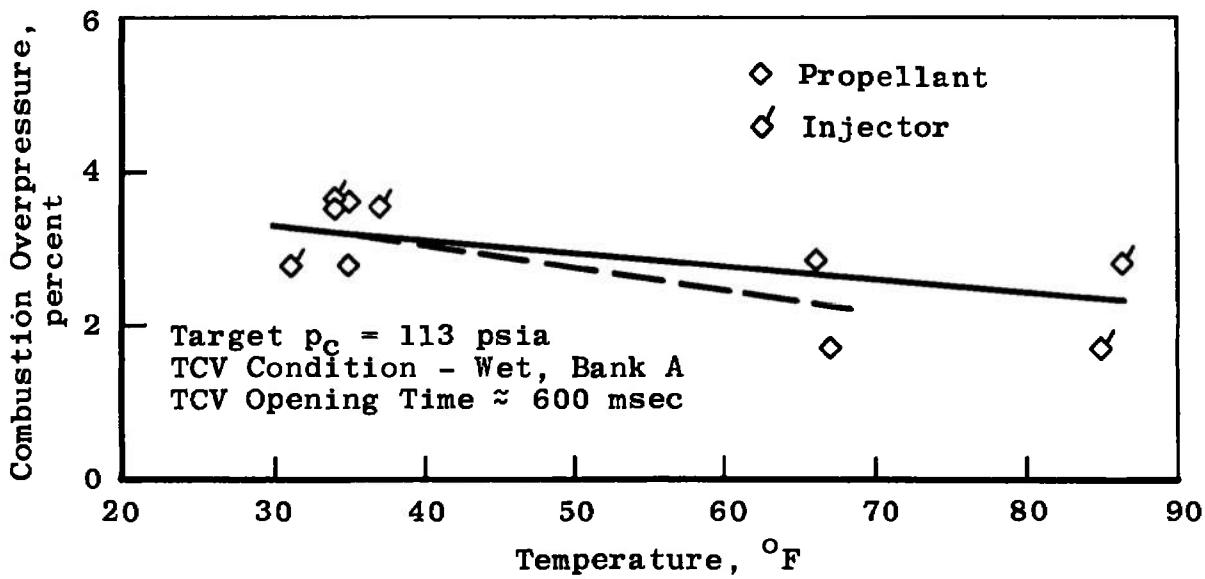

Fig. 66 Combustion Overpressure as a Function of Propellant and Injector Temperatures

The most influential factor in producing and aggravating the combustion overpressure appeared to be the injector filling characteristic, which was contingent on the operation of the TCV and the prestart propellant pressures. Combustion overpressure was generally less severe when the TCV opened slowly or the start was made with single-bore TCV operation, as shown in Fig. 67 (see also Fig. 55). Also, combustion overpressure tended to be less severe with the wet bore starts (i. e., propellant trapped in the inter-ball cavities) or with higher prestart propellant pressures (higher target chamber pressure). Any combination of starting conditions which resulted in the injector being filled before ignition occurred produced the more severe combustion overpressures, and the overpressure increased with increased ignition delay as shown in Fig. 68. The flight-type transducer chamber pressure data did not agree with the data obtained from the other transducers either for the peak pressures or for steady-state pressure, as shown in Figs. 69 and 70.

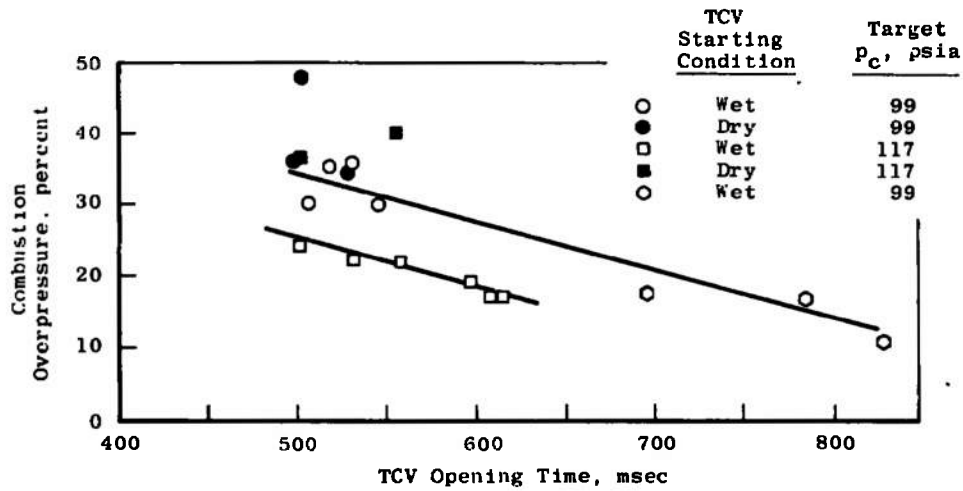

a. Dual-Bore Mode

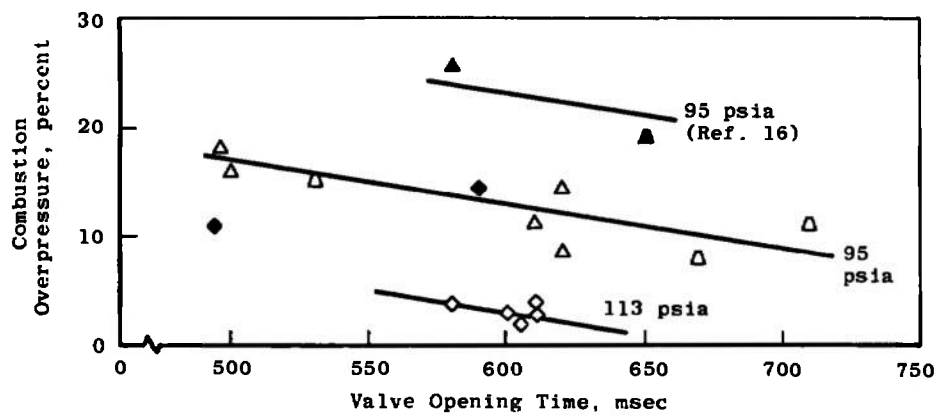

b. Single-Bore, Bank A

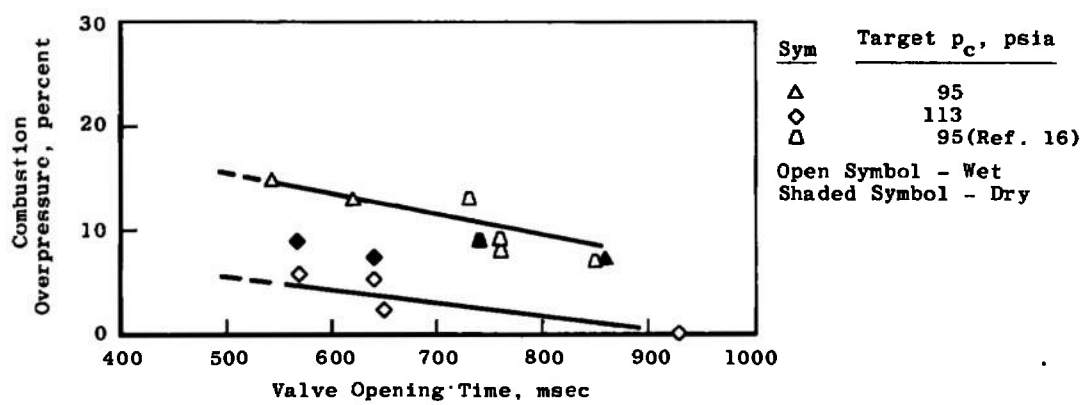

c. Single-Bore, Bank B

Fig. 67 Combustion Overpressure as a Function of TCV Opening Time

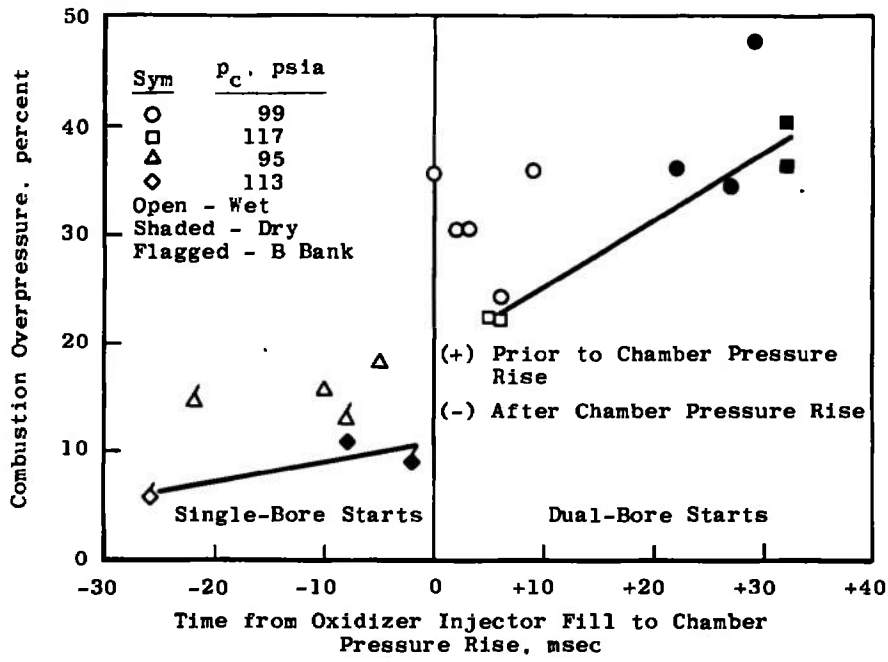

Fig. 68 Combustion Overpressure as a Function of the Time from Oxidizer Injector Fill to Chamber Pressure Rise

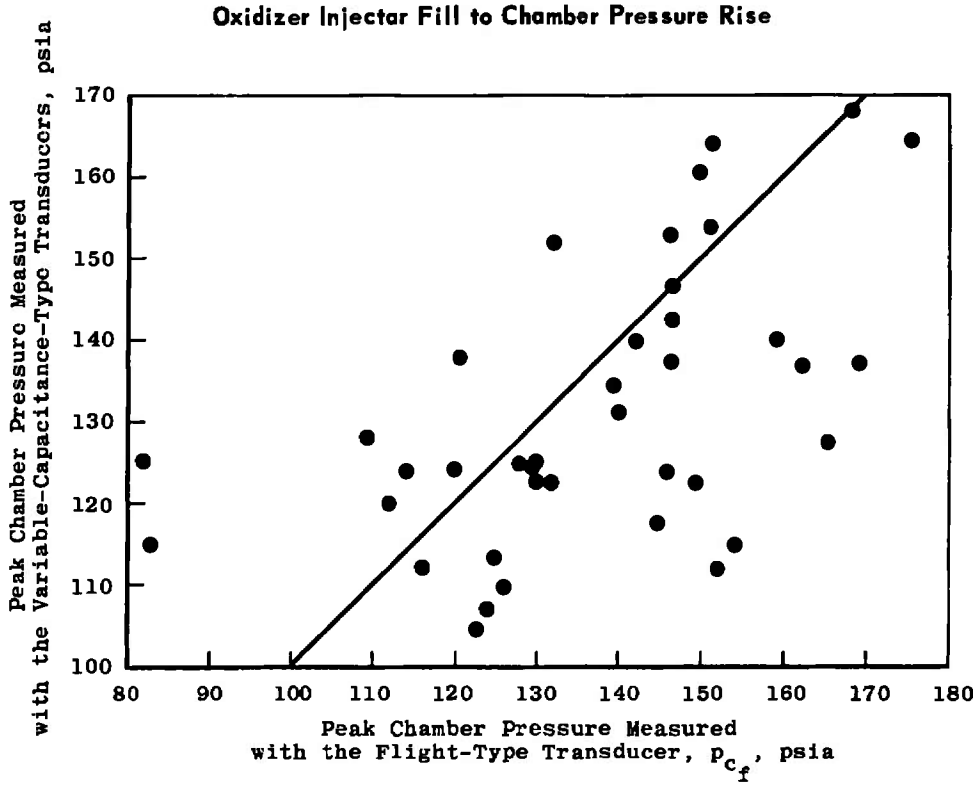

Fig. 69 Comparison of Peak Chamber Pressure Measured with Variable-Capacitance-Type Transducers and Flight-Type Transducer

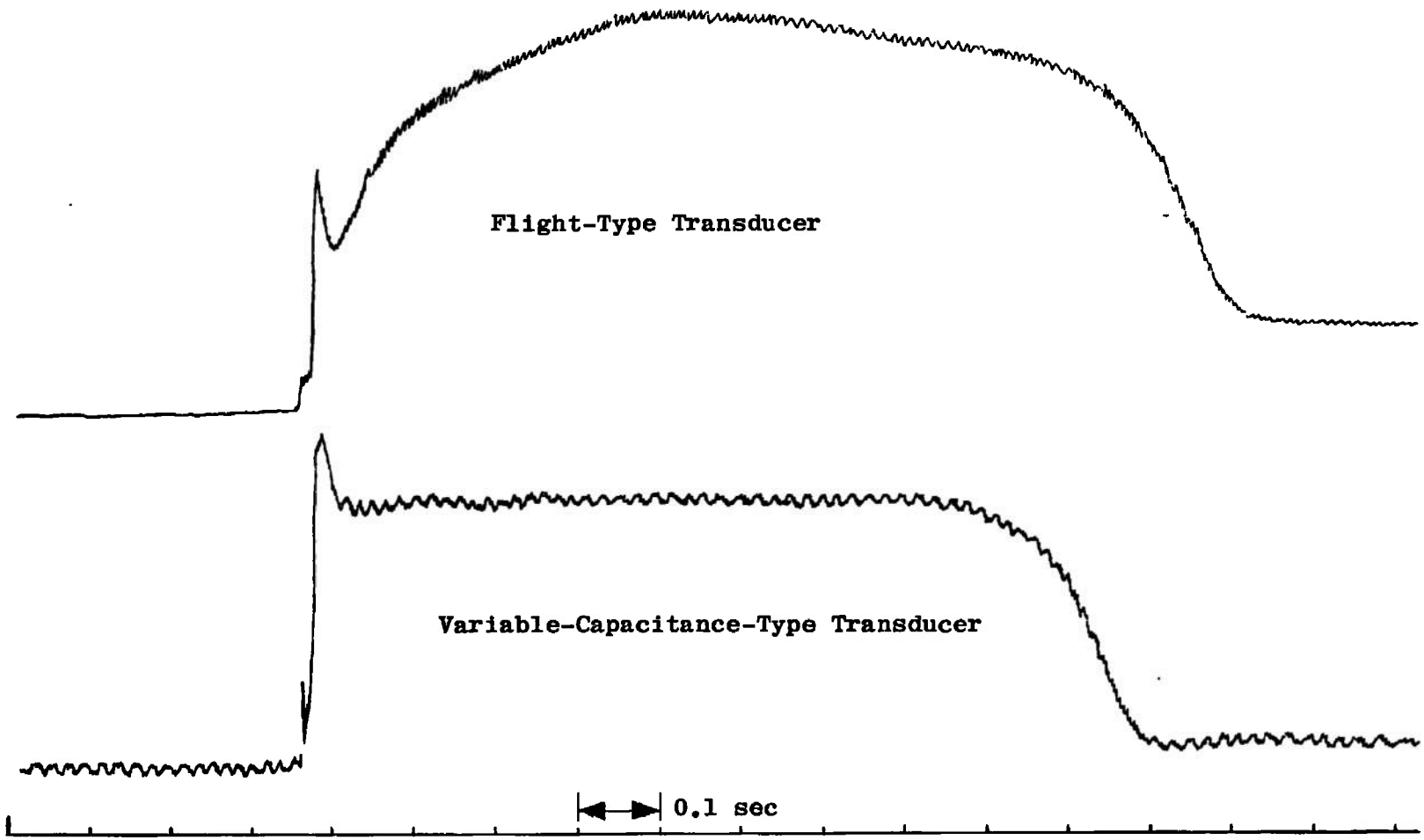

Fig. 70 Comparison of Flight-Type and Variable-Capacitance-Type Transducer Chamber Pressure Data

REFERENCES

1. DeFord, J. F. "Simulated Altitude Testing of the Aerojet-General Corporation AJ10-137 Rocket Engine (Report I - Phase I Development Test)." AEDC-TDR-64-81 (AD350408), May 1964.
2. McIlveen, M. W. "Simulated Altitude Testing of the Aerojet-General Corporation AJ10-137 Rocket Engine (Report II - Phase I Development Test)." AEDC-TDR-64-82 (AD350407), May 1964.
3. Vetter, N. R. and DeFord, J. F. "Simulated Altitude Testing of the Aerojet-General Corporation AJ10-137 Rocket Engine (Report III - Phase I Development Test)." AEDC-TDR-64-146 (AD352141), July 1964.
4. McIlveen, M. W. "Simulated Altitude Testing of the Aerojet-General Corporation AJ10-137 Rocket Engine (Report IV - Phase I Development Test)." AEDC-TDR-64-147 (AD352327), August 1964.
5. Vetter, N. R. and DeFord, J. F. "Simulated Altitude Testing of the Aerojet-General Corporation AJ10-137 Rocket Engine (Report V - Phase I Development Test)." AEDC-TDR-64-158 (AD352700), August 1964.
6. Vetter, N. R. and McIlveen, M. W. "Simulated Altitude Testing of the Aerojet-General Corporation AJ10-137 Rocket Engine (Report VI - Phase I Development Test)." AEDC-TDR-64-171, September 1964.
7. Schulz, G. H. and DeFord, J. F. "Simulated Altitude Testing of the Apollo Service Module Propulsion System (Report I - Phase II Development Test)." AEDC-TR-65-233 (AD368743), January 1966.
8. Robinson, C. E. and Runyan, R. B. "Thrust Vector Determination for the Apollo Service Module Propulsion Engine using a Six-Component Force Balance." AEDC-TR-65-250 (AD475564), December 1965.
9. Schulz, G. H. and DeFord, J. F. "Simulated Altitude Testing of the Apollo Service Module Propulsion System (Report II - Development Test)." AEDC-TR-66-17 (AD369807), February 1966.
10. Gall, E. S., McIlveen, M. W., and Berg, A. L. "Qualification Testing of the Block I Apollo AJ10-137 Service Module Engine." AEDC-TR-66-129, August 1966.

11. Pelton, J. M. and McIlveen, M. W. "Block II AJ10-137 Apollo Service Module Engine Test at Simulated High Altitude (Report I - Phase IV Development)." AEDC-TR-66-169, November 1966.

12. DeFord, J. F., McIlveen, M. W., and Berg, A. L. "Block II AJ10-137 Apollo Service Module Engine Testing at Simulated High Altitude (Report II - Phase IV Development)." AEDC-TR-67-47, April 1967.

13. Gall, E. S., McIlveen, M. W., and Berg, A. L. "Qualification Tests of the Apollo Block II Service Module Engine (AJ10-137)." AEDC-TR-67-63, May 1967.

14. Schulz, G. H., Berg, A. L., and Robinson, C. E. "Apollo Block II SPS Engine (AJ10-137) Environmental Tests and Mod I-C Bipropellant Valve Qualification Tests (Phase VI, Part I)." AEDC-TR-68-178, October 1968.

15. Barebo, R. L. and Ansley, R. C. "Investigation of Combustion Overpressure during Ignition of the Apollo Block II SPS Engine (AJ10-137) (Phase VI, Part II)." AEDC-TR-68-273, November 1968.

16. Farrow, K. L., Berg, A. L., and Robinson, C. E. "Apollo Block II SPS Engine (AJ10-137) Mod I-D and Mod I-E Bipropellant Valves Qualification Tests (Phase VI, Part III)." AEDC-TR-69-7 (AD850062), April 1969.

17. Berg, A. L. "Rocket Propellant Inplace Flowmeter Calibration System-Propulsion Engine Test Cell (J-3)." AEDC-TR-68-41, May 1968.

APPENDIX
DATA ACQUISITION AND REDUCTION ACCURACIES

All engine ballistic performance parameters were recorded on magnetic tape in continuous modulated frequency form throughout Phases II through V.

Digital computers were used to recover data from the magnetic tape records, produce data printouts in engineering units, and calculate engine ballistic performance information.

The equations used for determining engine performance were in accord with general industry practice, except for special adaptations which were incorporated to account for throat area changes of the ablative combustion chamber. Chamber pressure (p_c) was measured at the injector face with an in-place calibrated pressure transducer. Vacuum specific impulse ($I_{sp_{vac}}$) was calculated from measured thrust (F_a) obtained from in-place calibrated load cells and measured flow rates ($\dot{w}$) obtained from turbine-type flowmeters calibrated in place with propellants. Steady-state performance calculations were made from measured data which were averaged over 2-sec time intervals.

The estimated uncertainty (two standard deviations) of the measured parameters required for engine performance was as follows:

Parameter	Estimated Uncertainty, 2σ, percent					
	Phase II Part I	Phase II Part II	Phase III	Phase IV Part I	Phase IV Part II	Phase V
F_a	0.30	0.30	0.30	0.30	0.30	0.30
p_c	0.50	0.50	0.50	0.50	0.50	0.50
$\dot{w}_{fuel}$	0.40	0.44	0.44	0.42	0.44	0.34
$\dot{w}_{oxid}$	0.36	0.36	0.30	0.42	0.42	0.28
p_{cell}	3.70	3.70	3.70	3.70	3.70	3.70

The estimated uncertainty (two standard deviations, 2σ) in calculated total propellant flow rate ($\dot{w}_t$), vacuum thrust (F_{vac}), and vacuum specific impulse ($I_{sp_{vac}}$) was:

Parameter	Estimated Uncertainty, 2σ, percent					
	Phase II Part I	Phase II Part II	Phase III	Phase IV Part I	Phase IV Part II	Phase V
$\dot{w}_t$	0.28	0.28	0.24	0.30	0.30	0.22
F_{vac}	0.32	0.32	0.32	0.32	0.32	0.32
$I_{sp_{vac}}$	0.42	0.42	0.40	0.44	0.44	0.38

UNCLASSIFIED

Security Classification

DOCUMENT CONTROL DATA - R & D

(Security classification of title, body of abstract and indexing annotation must be entered when the overall report is classified)

1. ORIGINATING ACTIVITY *(Corporate author)*
Arnold Engineering Development Center
ARO, Inc., Operating Contractor
Arnold Air Force Station, Tennessee 37389

2a. REPORT SECURITY CLASSIFICATION
UNCLASSIFIED

2b. GROUP
N/A

3. REPORT TITLE
SUMMARY OF FIVE YEARS OF ALTITUDE TESTING OF THE APOLLO SERVICE MODULE ENGINE IN ALTITUDE TEST CELL (J-3)

4. DESCRIPTIVE NOTES *(Type of report and inclusive dates)*
Final Report: May 1963 through August 1968

5. AUTHOR(S) *(First name, middle initial, last name)*
G. H. Schulz, ARO, Inc.

This document has been approved for public release its distribution is unlimited. per AF Ltr dated 27 June 1973.

6. REPORT DATE	7a. TOTAL NO. OF PAGES	7b. NO. OF REFS
October 1969	96	17

8a. CONTRACT OR GRANT NO
F40600-69-C-0001

b. PROJECT NO. 9281

c. Program Area 921E

d.

9a. ORIGINATOR'S REPORT NUMBER(S)
AEDC-TR-69-144

9b. OTHER REPORT NO(S) *(Any other numbers that may be assigned this report)*
N/A

10. DISTRIBUTION STATEMENT This document is subject to special export controls and each transmittal to foreign governments or foreign nationals may be made only with prior approval of NASA-MSC (EP-2), Houston, Texas 77058.

11. SUPPLEMENTARY NOTES
Available in DDC.

12. SPONSORING MILITARY ACTIVITY
NASA-MSC (EP-2)
Houston, Texas 77058

13 ABSTRACT

The primary results of the development and qualification testing of the Aerojet-General Corporation AJ10-137 rocket engine for the Apollo Service Module conducted at the Arnold Engineering Development Center (AEDC) are summarized. Testing of the AJ10-137, a 20,000-lb_f nominal thrust liquid-propellant engine, was conducted at combustion chamber pressures of from 77 to 133 psia and at mixture ratios of the two hypergolic propellants, nitrogen tetroxide and Aerozine-50 , from 1.4 to 2.4. Both Block I and Block II engines were tested to determine engine performance and to establish durability and reliability of the basic engine design and subsequent modifications. As a result of these tests, the Block II engine performance was established, and the engine was qualified for the lunar mission. This testing indicated and permitted solution of inadequate durability of the ablative combustion chamber at low-pressure/altitude conditions. The chamber had appeared reliable in sea-level testing conditions.

This document is subject to special export controls and each transmittal to foreign governments or foreign nationals may be made only with prior approval of NASA-MSC (EP-2), Houston, Texas 77058.

DD FORM 1 NOV 65 1473

UNCLASSIFIED

Security Classification

14. KEY WORDS	LINK A		LINK B		LINK C	
	ROLE	WT	ROLE	WT	ROLE	WT
Apollo Service Module						
rocket engines						
liquid propellants						
altitude simulation						
performance evaluation						
summarizing						
spacecraft propulsion						
lunar spacecraft						
manned space flight						
Apollo Service Propulsion System						
AJ10-137 rocket engine						

AFSC
Arnold AFS Tenn